REFRACTORIES IN VACUUM INDUCTION MELTING

by

André Luiz V. da Costa e Silva
Eng. Met., Instituto Militar de Engenharia, Brasil, 1976

A THESIS SUBMITTED IN PARTIAL FULFILLMENT OF
THE REQUIREMENTS FOR THE DEGREE OF
MASTER OF APPLIED SCIENCE

in

THE FACULTY OF GRADUATE STUDIES
Department of Metallurgical Engineering

We accept this thesis as conforming
to the required standard

THE UNIVERSITY OF BRITISH COLUMBIA

March, 1979

In presenting this thesis in partial fulfilment of the requirements for an advanced degree at the University of British Columbia, I agree that the Library shall make it freely available for reference and study. I further agree that permission for extensive copying of this thesis for scholarly purposes may be granted by the Head of my Department or by his representatives. It is understood that copying or publication of this thesis for financial gain shall not be allowed without my written permission.

Department of **Metallurgical Engineering**

The University of British Columbia
2075 Wesbrook Place
Vancouver, Canada
V6T 1W5

Date **March 20, 1979**

ABSTRACT

The literature in Vacuum Induction Melting is briefly reviewed, with especial emphasis on refractory practices and refractory-metal interactions. Since it was determined that in both steel and superalloy vacuum melting in large furnaces lining failures are associated with attack on the cement joints, tests were performed to characterize this attack and determine the most suitable cements from this standpoint.

The presence of low-stability oxides (SiO_2, P_2O_5,...) was shown to be the main reason for the cement's low resistance to metal attack. It is suggested that in the case of steels, diffusion of the less stable oxides may be the rate controlling step in the corrosion process. In the case of superalloys, the high interaction between oxygen and the elements present in the alloy (Ti, Al, Cr) causes an extreme depression of the oxygen activity in the melt, hence enhancing the dissolution of all refractory oxides. In order to produce cements with a very small content of the low-stability oxides, the use of fluorides as fluxes was attempted. The cements so produced performed well, as far as resistance to attack, adherence to bricks and technological properties were concerned.

To verify the validity (on a large scale) of the mechanisms observed and proposed in the tests, samples from industrial Vacuum Furnaces were examined. It was concluded

that the processes occurring in a large furnace can be rationalized based on the test observations. Also comments were made on the need for improved pouring facilities, if the products of the metal-refractory interaction are to be kept out of the final material produced. This is because in the present state of the refractory technology and practice, these interactions cannot be avoided.

TABLE OF CONTENTS

LIST OF TABLES

LIST OF FIGURES

ACKNOWLEDGEMENTS

The author would like to express his gratitude to Dr. Alec Mitchell, for his help and guidance throughout the course of this work. The cooperation of several of his colleagues in the industry has been extremely gratifying. Much appreciation is given for the many helpful discussions with fellow students and other faculty members. The author would also like to thank Dr. A.C.D. Chacklader and Dr. A.S. Ballantyne, for their helpful criticism of the draft manuscript.

The support of the Canadian International Development Agency and of the Ministerio da Industria e Comércio, Brasil, are gratefully acknowledged.

Special thanks are due to Electrometal Aços finos S.A., for their support during this project.

CHAPTER 1

INTRODUCTION

1.1 Introduction

With the increasing demand for high quality materials for the aerospace, nuclear and other highly sophisticated industries, Vacuum Induction Melting (VIM) has reached a very important position as an alloy-making process. Due to its now well understood and controlled technological advantages it is very likely that it will keep its position as a primary process for some considerable time into the future.

The idea of removing the atmosphere as a source of contamination is not a new one and even a mediocre vacuum is much less contaminating than a very pure gas. One must be aware, however, of the effects of the various pressure sensitive reactions occurring in steel or high-temperature alloy-making.

Induction heating is, without question, one of the cleanest and easiest to control heating methods available, offering "contactless" heating with a high degree of temperature control and little or no problem in operating under reduced pressures.

Since we are dealing with a primary melting process for very expensive alloys, it is clear that a continuous

process is not feasible. Batch operation is then necessary, bringing into the situation the need for a container. This container should be able to resist the temperatures of the molten metals and, at the same time, keep the heat losses within a reasonable level. It is also clear that the container should interact to the minimum extent possible with the metal. Although the two first demands are fulfilled by a series of conventional refractory materials, the last one poses the biggest difficulty, reducing the number of possible aternatives to a handful of materials which are usually expensive and hard to utilize.

Even though non-oxide materials have been used as refractories for VIM furnaces, most of the potential candidates amongst these materials find severe economic limitation. What is then seen is the extensive use of oxides or mixtures of oxides in the form of prefired, or rammed in place, or brick/cement lining as containers for steels and high temperature Nickel-based alloys.

To aggravate the chemical interaction problem, most of the alloys made by VIM contain relatively large amounts of reactive alloying additives such as Ti, Al, etc., or, in the case of steel, carbon, the latter becoming much more reactive at lower pressures due to the effect of reaction

$$\underline{C} + \underline{O} = CO\ (g).$$

In addition, high quality materials require high heat-to-heat reproducibility in properties, maximum hot-workability (since they are, per se, hard to work) and, in the

case of heat-resisting alloys, excellent creep properties. All these characteristics are influenced greatly by trace element contamination and inclusions, both likely products from refractory interaction.

In VIM, one then sees chemical stability (no reaction-no dissolution) as one of the paramount properties desired in a refractory. Recognition that the refractories are one of the components taking part in the refining process becomes then essential if the best vacuum melting practice is to be achieved. Refractories should be attacked to a minimum extent by the alloys being processed and the product of any unavoidable reaction thoroughly defined in order to achieve the best refractory/alloy combinations.

1.2 Literature Survey

1.2.1 Metal-Refractory Interactions Under Vacuum

1.2.1.1 Vaporization

Although vaporization of refractory oxides is a definite possibility (1), this problem will not be dealt with extensively in the present study since it is likely to be of secondary importance, compared to direct chemical attack by the melt.

1.2.1.2 Dissolution of Refractories

The simplest process that can occur when a piece of refractory oxide XO is brought in contact with a metal Y, in which both X and oxygen are soluble to a certain extent, is the dissolution

$$XO = \underline{X}_{inY} + \underline{O}_{inY} \qquad \Delta G_1 \qquad (1)$$

This reaction will occur at the metal-oxide interface and, given sufficient time, achieve the solubility limit given by the product

$$h_X h_O = a_{XO} e^{-\Delta G_1/RT} \qquad (2)$$

When h_X and h_O and a_{XO} are the activities of $\underline{X}$, $\underline{O}$ and XO, respectively.

Table 1 presents the solubility products for a series of oxides in iron at 1600^{o}C and atmospheric pressure. Since most of the dissolution processes listed in Table 1 are not pressure sensitive, one can use them a guidelines for the thermodynamics of the dissolution process.

Should X be highly volatile and insoluble (or almost), such as Mg or Ca in iron, the dissolution will proceed to saturation of the bath with oxygen (5). This will lead to the formation of a FeO slag, due to the evaporation of Mg (or Ca) at the metal/vacuum interface, displacing the reaction

$$MgO = \underline{Mg} + \underline{O}$$

by the constant removal of one of the products. This may not be observed, however, when the process kinetics are very sluggish.

All these processes are obviously undesirable since they will introduce an unaccounted alloying element and oxidize the bath, most probably compromising the properties of the resulting alloy.

1.2.1.3 Reaction With Alloying Elements

1.2.1.3.1 Carbon

The above picture changes, however, when alloying elements are present. In the case of steels, carbon is the most important element in VIM and the one over which most confusion has been generated. Although all authors observe a steady decrease in carbon content of the alloy, as the reaction

$$XO + \underline{C} = CO + \underline{X}$$

proceeds, a great deal of misunderstanding has been brought about by failing to acknowledge the kinetic aspects of the process and trying to compare results from steels with widely different initial carbon contents. The experiments by Bennett

et al. (6), who started his tests with a 0.2%C steel in a MgO crucible and observed reaction times of up to 85 minutes, showed the achievement of a clear minimum oxygen level, of about 8 ppm. This is in obvious conflict as the authors point out, with the previous results of Moore (7), who started with a 0.1%C steel and observed a peaked minimum in the oxygen content, somewhere above 10 ppm. Although Öberg et al.(8) point out that "no work covering a wider range of carbon concentration has been found", the kinetic study of Machlin (9) has shown what should be expected in such a case. If one starts with a high carbon activity melt, the dissolution step

$$MgO = \underline{Mg} + \underline{O}$$

and the deoxidation step

$$\underline{C} + \underline{O} = CO$$

will define a kinetic equilibrium fixing a steady-state oxygen level in the bath. As the carbon content goes down during this period, the steep ascendent side of the C/O equilibrium hyperbole will be reached and what Öberg called the "free oxygen uptake" will prevail. This whole process can be described by a curve as Fig.1, where one observes an initial deoxidation, then a steady-state and finally a fast oxygen content increase, due to the lack of sufficient CO flushing. It is easy to understand that what Moore observed, actually, was just an overlapping of both unsteady-state processes, due to an injudicious selection of carbon content.

The understanding of this process is clearly of paramount importance for the operation of VIM furnaces, since it will permit the best deoxidation and the minimum inclusion content to be reached.

Since the minimum oxygen content attained at steady-state and the carbon consumption rate are both direct functions of the dissociation reaction

$$XO = \underline{X} + \underline{O}$$

it is evident that those two conditions will be adequate criteria for assessment of refractory stability and adequacy in VIM.

Schaffer (10) and others have calculated the thermodynamics of the various melt-refractory reactions possible. With extensive simplifications he found that, for an iron bath, containing 0.4%C the equilibrium pressures of CO for the reaction

$$XO + \underline{C} = CO + \underline{X}$$

would be as given in Table 2. As they are all well over the usual operating pressures of VIM furnaces (80μ), one should expect the reduction of the refractories to be highly favourable from a thermodynamic viewpoint. However one should also take in account the fact that these relationships should prevail only for the metal-crucible-vacuum interface, where there is no nucleation barrier for CO formation. As one goes deeper in the melt-crucible interface, the C/O supersaturation must be sufficient to overcome the ferrostatic head and the surface forces (CO nucleating then as bubbles) otherwise

the attack has to proceed as dissolution of the oxide, (enhanced by the low O content of a C rich bath), transport of O through the bath and CO formation and desorption at the surface.

Turillon (11) and others have studied the deoxidation of iron melts under Vacuum Induction Melting conditions and recognized the importance of the refractory decomposition reaction. He observed the behaviour predicted by Machlin, in Fig. 2. Turillon also noticed that, in his MgO/spinel crucibles, at the point of minimum C and O concentration preceding the "free oxygen uptake", the deoxidation and the refractory decomposition rates, determined independently, were equal, with a value of approximately 1.5 ppm O/min.

A considerable number of studies have also been made taking in account the carbon boil conditions, i.e., critical crevice sizes for nucleation of bubbles, supersaturation needed, etc. Besides the conventional treatment of Darken (12), Kraus (13) has calculated the characteristics of CO bubbles in vacuum carbon deoxidation. He presented bubble characteristics graphics, showing the maximum active depth of bubbling, the minimum supersaturation needed for bubble nucleation, and the effect of several other variables on the degassing processes. He pointed out that, if the nucleation frequency as a function of pressure and concentration was known, the rate of degassing during the boil could be determined. Unfortunately, as Kinsman et al. (14) point out, this knowledge is not available and should depend on several hard

characterize factors such as agitation of the bath, surface characteristics of the crucible, presence of heterogeneous nuclei, etc.

It is important to keep in mind, that, although the boil is the major CO elimination process, once it subsides, substantial oxygen removal still happens by surface desorption.

1.2.1.3.2 Other Alloying Elements

Precipitation hardening nickel-based alloys rely basically on aluminium-, and titanium-rich precipitates to achieve their high temperature strength (15). It is not uncommon to find alloys with up to 4-5% Ti+Al (Table 3). A brief look at an oxide stability diagram will show that both Al_2O_3 and TiO_2 are among the most stable oxides. These elements will present then, reactivity problems with crucibles. Although vacuum will not likely play any role in these reactions, it is still important to study them since one of the main driving forces for the use of VIM is the possibility of producing alloys rich in reactive elements.

Various authors (16, 17, 18) have studied the wettability of ceramics by Nickel alloys. Sutton (19) observed rapid wetting of refractories by alloys containing Zr, Al, Ti and C, and found that wetting increased with the content of the alloying addition. Snape (20) observed that the wettability order of various alloys is the same in different refractories substrates. He also noticed the increased wetting of alumina crucibles by reactive alloying elements in

a large number of commercial high temperature alloys and nickel-carbon alloys.

The process in question, for a Ni-Ti alloy in a pure Alumina crucible, would be described by

$$\frac{3}{2}\underline{Ti} + Al_2O_3 = \frac{3}{2}TiO_{2\,in\,Al_2O_3} + 2\underline{Al}$$

It is clear that the aluminum content of the bath will play a role in the equilibrium. Sutton found strong variations in wettability depending on the Ti/Al ratio in the alloy. The dissolution of the TiO_2 formed in the crucible and its final activity will be important in this process--a large solubility in the crucible increasing the erosion. An extensive study of those reactions was made by Snape, Gupta et al.(21) and Kamamura et al. (22) who noted the alteration suffered by the refractory subsurface layers and enrichments in Cr, Ti and other alloying elements.

1.2.1.4 Effect of Minor Components

The use of pure silica refractories under vacuum in contact with either steel or nickel-alloys should be clearly ruled out due to the low stability of SiO_2 in presence of C at low pressures, or of Al, Ti alloying elements. But, the vast number of commercial refractories in which silica plays an important role as a binding agent--such as mullite, silico-aluminous and high-alumina--has precluded its complete elimination from the vacuum induction melting scene. The abundance of silica and its presence in most ores pose economical

problems in making refractories with very low-silica content. Fe_2O_3 is also often present as impurity (23), its removal being economically unfeasible.

The work of Graham et al.(24) shows clearly the increased interaction to be expected as the silica content of silico-aluminous refractories is increased. Machlin estimated a 10 fold increase in the steady-state oxygen content of a steel melted in a 1% SiO_2-MgO crucible, used by Fisher and Hoffmann. Although some suggest that a wash heat should be able to consume the silica in the working face, causing the silica reduction to be controlled by diffusion in the refractory, one must consider the increase in porosity and the possible decrease in strength associated with the corrosion of the intergranular silico-aluminates. Most likely, this wetted altered layer will spall when the residual metal, after teeming, solidifies (23) and/or be dissolved in the next heat, as the binding phase is absent. A much better explanation for the favorable effects of a "wash-heat" in reducing the "pollution" potential of the crucibles is given by Hunter & Tarby (25) who observed that a crucible which was air dried at 225°C and then vacuum dried produced the same carbon consumption in the molten steel as a crucible after one wash-heat. This would indicate that absorbed water and gases in refractories can be major sources of oxidation in alloys. They therefore recommended an air drying at 1250°C for 24 h. for research purposes (crucibles of 206 cm^3).

Snape also reported increased wettability due to increased silica content (although some increase in porosity

was also experimented).

As boron oxide is a powerful flux to MgO and several other oxides, it has been used--in the form of boric acid additions--as chemical bonds for various applications. However as Decker et al.(26) showed, alloys produced in MgO refractories containing 1.2% B_2O_3 contained some boron, which accounted for variations in creep and hot workability properties. In the case of high quality materials in which reproducibility is mandatory, the different levels of contaminations during the life of the crucible reported by Decker et al. cannot be tolerated. As Winkler (23) observes, wetting and erosion of the crucible are promoted if binders of lower chemical stability are used during the manufacture of the crucible, as they are preferentially decomposed.

1.2.1.5 Kinetic Aspects

Although the thermodynamic predictions suggest extensive and violent corrosion, that is not what is usually observed. In addition, discrepancy is found between experimental results from different authors which cannot be accounted for simply by different experimental techniques.

It is important to keep in mind that factors such as open and closed porosity, mechanical resistance, grain size and size distribution, temperature of the test, degree of agitation (frequency of current, size of furnace, etc.) will play a definite role in determining the reaction kinetics for the various refractories.

Turillon (27) noticed sharp differences in the minimum oxygen content attainable when using rammed MgO or fused MgO crucibles, the latter giving the better results, although they have, unfortunately, lower thermal shock and mechanical resistance. Machlin assumed the reaction to be transport controlled at the crucible/metal and metal/vacuum interfaces, i.e., the reaction itself proceeded fast enough not to pose limitations to the process. Although this may be so for crucibles in which the corroded phase is the main one, i.e., depletion at the interface will hardly occur, it can certainly be expected not to be true when there is differential reaction of phases of various stabilities. It is clear that for the purpose of modelling, most variations in crucible parameters will appear as effects on the mass transfer coefficient at the metal/crucible interface. Besides, as Snape observed, much of the oxygen intake by the metal takes place by discrete pieces of refractory falling into the bath.

The effect of temperature, apart from its obvious influence in increasing the rate of transport phenomena, will also be one of bond softening, again helping the loosening of refractory grains. The higher the frequency, the lower the agitation of the melt and hence, less erosion is to be expected. Once a piece of refractory has been eroded it is very likely that it will be dissolved at a fast rate due to its much increased area.

1.2.2 Refractory Practice in VIM

Besides the clear importance of the thermodynamic stability of the lining material, we have seen that the actual structure of the refractory will play a definite role in the kinetics of the attack process. It is then instructive to study the different refractory practices applied in VIM, comparing their advantages and drawbacks.

Table 4 presents various practices quoted in the literature and the following can be observed.

Laboratory furnaces and small furnaces up to about 25kg capacity usually employ prefired crucibles. Although it would be possible to use rammed linings, the labour costs are prohibitive. As the furnace size increases the limit for prefired crucibles is reached at about 250kg, the rammed lining becoming more economical as this value is approached (51).

For iron and nickel melting purposes, one usually relies on high purity MgO (96%MgO, 2%SiO_2, 1%Fe_2O_3) or Al_2O_3 (96%Al_2O_3, 2%SiO_2) (51), although $MgO.Al_2O_3$ or stabilized zirconia crucibles can also be used.

As Child et al. (51) points out, however, prefired crucibles are not considered for industrial applications, due to the high price and short lifes. Besides, cracks are much more dangerous than in rammed crucibles, since they can open wide and cause leakage.

Ramming mixtures for Induction Furnaces are produced by a number of manufacturers. Care should be exercised, however, when extending their use to Vacuum Induction Melting.

High silica linings for instance, quite common in Air Induction furnaces, must be banned if the best refractory practice is to be achieved. The Fe_2O_3 content must also be kept low, although it is an excellent additive to promote MgO sintering, due to its fluxing ability. Although Child et al. (51) present a 1%Fe_2O_3, MgO crucible as a typical VIM material, Winkler (15) prefers to set the upper limit at 0.5%Fe_2O_3, if low oxygen levels are to be attained.

Ramming mixtures can be either wet or dry rammed, the ramming being made, in both cases, using a metal plate mould or a similar kind of core.

The ideal goal in producing a rammed lining is to have some 30% of the thickness fully sintered, with low porosity at the working face--the rest of the lining should be decreasingly sintered and hence more porous and more able to accommodate thermal and mechanical stresses. This less sintered layer acts as a cushion, holding the hard sintered "crucible" in place. To achieve this, several factors must be taken into account.

The grain size distribution should be so as to produce the desired porosity in the unsintered zone and achieve the dense structure necessary to the working face. Usually these distributions are very similar to the Fuller curve (5).

Regarding composition, the ramming mixture will always consist of main constituents and a binding agent. In the case of a MgO/MgO.Al_2O_3 spinel mixture, for instance, SiO_2 is added to promote sintering (in amounts up to 3% (5)). Care should

be exercised when selecting the amount and composition of the binding agent since it is usually less stable and, as far as attack resistance is concerned, deleterious to the lining. One should use the minimum amount necessary to achieve sintering at the desired firing temperature. Obviously, as the amount of binding agent is decreased, the firing temperature must be increased usually introducing technical difficulties.

Depending on the kind of core used for ramming the mixture, firing can be done in two ways. If a mild steel template was used in ramming this will usually be left in place during firing and will melt away in a first wash heat that will provide the correct firing temperature. In this case, the lining should be allowed to dry completely and then be fired under vacuum, to minimize iron oxidation and subsequent iron oxide pick-up by the lining. If a graphite or a wood core is used, firing can be done either by heating up a graphite core or by removing the core and melting an initial charge in the furnace. The use of the wood core is recommended since it can be removed and a graphite core with imprecise dimensions can be used to fire up the lining. Should a graphite core be used, the firing should not be made under vacuum, to minimize the reaction between the lining and the core (5).

The main problem experienced with monolithic linings, however, is cracking, since the lining is subjected to severe mechanical and thermal stresses. During firing it is not uncommon to produce a lining with cracks, particularly as the

lining dimensions, and hence the stresses, are increased. When a crack is found after firing, the crucible must be allowed to cool, and the crack filled with cement. This thermal cycle and the introduction of a different material can produce new cracks. This becomes a very difficult problem with large furnaces. As Schlatter and Simkovich(30) pointed out, "as the size of furnace is increased, all the problems concerning refractories performance (tightness or construction, volume stability, resistance to cracking and spalling) are escalated". To avoid this problem in a 60,000 lb VIM furnace, they used refractory brick/cement construction and reported excellent crucible lifes. They used Korundal XD (Alumina bonded with Mullite) as a backing lining, due to its good thermal stability and either this or Magnesia bonded with spinel (Magnel) as the working lining, the latter being the present industrial practice in large furnaces. Due to the high density of the XD brick, it showed better resistance to FeO slags than a 90% Alumina ramming mix (29). Simkovich (28) studied the chemical stability of Korundal XD as compared with zirconia and magnesite-chrome commercial refractories, in contact with different carbon activity alloys. He observed that the performance of the three compositions was essentially the same for the same alloy, as far as carbon consumption was concerned. As the authors found, the behaviour of the Zirconia crucible was indeed difficult to justify, since the higher porosity alone would be unlikely to override the higher thermodynamic stability. The comparable

behaviour of magnesite-chrome and alumina-silica should present no surprise, since the former contained 17.4%Cr_2O_3 and 10.5% Fe_2O_3 and the latter 10%SiO_2. The behaviour of the zirconia crucible has to find its explanation in a kinetic basis only (porosity, strength, abrasion resistance, etc.), since at the pressure used (5μ at the bath surface) all the oxides in question (including MgO,Al_2O_3 and ZrO_2) are less stable than CO for the carbon contents encountered. This is exactly the fact that gives validity to the test, especially since surface/volume effects are more detrimental than in practice. The MgO/Al_2O_3 (Magnel) brick was expected to give even better results. Although this point is not emphasized by Schlatter and Simkovich (30) or by Renkey et al. (29), "close size tolerances, good brick laying and improved mortars" are essential to obtain the best results from one of these linings since the joints are definitely the weak link in the system. This effect has been reported earlier by Chester (52) who observed, in air induction melting, a substantial increase in lining life when bricks were used instead of ramming mixtures; but recommended the use of the latter, due to the very difficult and dangerous situation caused by joint penetration in induction furnaces. In high frequency induction melting it is quite possible that the metal penetrating between the bricks will be progressively heated as it approaches the coils. In the case of lower frequency melting (larger furnaces) it is likely that this metal will not experience further heating, due to the large penetration depth of low frequency induced current.

Bonchack (47) reported severe erosion at joints in an industrial VIM furnace, using Korundal XD bricks and Coralbond cement (82%Al_2O_3/15% SiO_2/2% TiO_2/1% Fe_2O_3). He also observed that the joints with less mortar were less eroded and concluded that the mortar quality was inferior to the brick quality. The need for the development of a MgO/Al_2O_3 base cement to be used both with Korundal XD and Magnel bricks was then suggested.

It is interesting to note that the use of Korundal XD in the working lining is not industrial practice any more, since Schlatter (53) reported persistent boiling with certain steel compositions, due to the 8.5% SiO_2 present in Korundal XD.

The main difficulty with cements and mortars is the fact that they should bond to the brick and acquire strength at relatively low temperatures, since the whole furnace cannot be fired for the same time and at the same high temperature as were the bricks. This makes it then necessary to use larger amounts of fluxes than in the brick. Unfortunately, most of the fluxes used in commerical cements are rather unstable under VIM conditions (as silicates, phosphates and borides) and may lead to contamination of the melt, as pointed out earlier for boron. A 3000kg heat of steel in a VIM furnace for instance, with 5% area covered by a phosphate bonded commercial cement, will absorb as much as 1.1ppm per mm of cement eroded.

1.2.3 Other Reactions With the Lining

Apart from reactions involving oxygen (oxides) in the lining, most of the work done is related to desulphurization (de-S). Sulphur removal by vacuum is extremely ineffective, either as gas

$$2\underline{S} = S_2(g)$$

or as volatile compounds as

$$\underline{Si} + \underline{S} = SiS(g)$$

T.P. Floridis (54) reports 1.25h @ 6μ in C and Si rich melts--which increase S activity--are needed to reduce sulphur content to 50% of its initial value. Since de-S is an important reaction in steel and Ni-alloy making, three approaches have been used: the use of slags, the painting or coating of the refractories, and the use of Rare Earth Metals (REM).

Ward et al. (55) tried several different methods of adding lime to de-S a VIM steel heat. The use of calcined marble chips was of very little effect since the lime rapidly formed a ring around the crucible wall, reducing the contact area. The use of lime/water paste over the refractories presented the best results, with very good de-S. In the case of spinel refractories, however, the lime reacted with the refractory and swelled, decreasing the inner diameter of the crucible. Also, when using pure MgO refractory, the CaO coating and adherent metal was removed after each head and a fresh application was made. This process is only feasible under vacuum due to the high fluxing ability FeO has on lime. This would probably present problems with an industrial scrap

charge. Also, no observation is made with regard to the life of the crucible.

The use of slags in VIM is extremely cumbersome, due to the fact that the whole process occurs in a sealed chamber. Although very ingenious processes for slag handling can be proposed in principle (56) it is extremely unlikely that they will survive technical problems as the removal of the slag handling tool introduced through movable vacuum joints. Besides, since only electric conductors are heated by induction heating and the slag is constantly radiating to the freeboard, it is likely to solidify if it does not have a very low melting point. Although there are suggestions of using a plasma torch to keep the slag molten in the center (57), this is not a common industrial practice at present and will not be considered here. In order to guarantee a low melting point, fluxing additions such as CaF_2 must be introduced in large quantities, thereby having a fluxing effect on the refractories. Despite these difficulties, various trials were made with slag-desulphurization. Afanasyev et al. (58) tried slags in the system $CaO/SiO_2/Al_2O_3$ with low FeO contents, having melting points of ~1500°C or 2000°C. The slags were melted in graphite crucibles and poured either after or before the metal in the crucible and good de-S was observed. No reference is made to refractory wear apart from observations that when the slag was poured over the metal, considerable foaming happened causing severe incrustations in the walls of the crucibles. Although the slags were analysed after use the values are not given but one can anticipate silica reduction

with CO formation (especially in the higher carbon melts) as one of the main causes of foaming. The de-S results are improved for all C contents, as compared to atmospheric pressure de-S, but the most significant improvement is found in the low C (0.035%) steel, probably due to the much lower FeO content achievable under vacuum. Polyakov et al. (59) investigated the effect of various $CaF_2/CaO/Al_2O_3$ slags on sulphur content and concluded that the effect of CaF_2 is only one of fluxing, having no de-S power. Lincheviskii (60) investigated the use of both of CaO/CaF_2 mixtures and of CaO slurries painted to the walls and achieved good de-S in both cases. Volkov et al. (61) studied various mixtures of CaO/CaF_2, $CaO/Al_2O_3/CaF_2$, $CaO/CaF_2/SiO_2$, placed on the bottom of the crucible. The best results were achieved with a 90% CaO/10% CaF_2 mixture placed on the bottom of the crucible that would, after the melting process, sinter to the bottom of the crucible, being cleaned after the pouring. In this work the authors do admit that the use of slags may form accretions on the crucible walls, reducing its life.

Schlatter et al. (62) patented the use of mixtures of CaO/CaF_2 or other fluxes and a reducing agent, either C or REM, having lower melting point than the metal being produced. Their trials were performed in Magnesia/Spinel (possibly Magnel) crucibles. Although there is no reference to brick erosion in the patent, the control of the slag composition is critical (53) in this respect.

In a somewhat different approach Strushchenko (35) employed fused lime crucibles, achieving excellent de-S, deoxidation by silicon (due to the lowered activity of SiO_2 in the refractory) and resistance to more than 8 cycles of cooling and heating to room temperature. However the small crucible (20kg) was fired at 2000°C which is not feasible in larger scale operations. One has also to consider the hydration problems, should the furnace chamber need to be opened for repairs.

Several reports of de-S with REM in VIM are found in the literature (63, 64, 65). Small problems with unpredictable Rare Earth Metal recovery, carry-over to subsequent melts (56), formation of "oxide-like" slags (63), etc., still persist, but the main problem is one of acceptance by the costumers. This is because the exact effects of REM addition to superalloys are not well understood, except for the known formation of deleterious RE-Fe phase (64) when these additions exceed certain limits.

1.3 Objectives of the Research Project

Since it is well established that in VIM furnaces using brick-mortar linings the wear is localized on the mortar joints (50,66), it was decided that the attack of mortar (or cements) by steels and/or superalloys was the most important point to be studied. This study was to encompass both the attack mechanisms and some rough estimation of the reaction rates, although no attempt to derive the exact kinetics was to be made. In addition, attempts were to be made to develop a cement without low stability oxides, in order to improve the overall lining performance.

Finally, samples of used VIM refractories were to be analysed and correlations attempted between these observations and the test results, in order to verify the validity of the experimental findings.

CHAPTER 2

EXPERIMENTAL

In order to study the attack of mortar by metals, as we proposed, different techniques were considered. Although wetting studies (such as sessile drops) have been extended to predict the stability and reaction of metals with ceramic substrates (Sutton's (19), for instance) it was felt that they would not, in all cases, simulate exactly or closely enough the conditions of VIM. This arises because in some cases reaction products which limit the spreading of the droplet may be formed (67) and the chemical composition of the droplet may be substantially altered in a reasonably long experiment. This effect has been noticed particularly in cases where the reaction of carbon in the metal with the oxide refractories is concerned due to the very high interface/volume ratios (both metal/ceramic and metal/vacuum). In addition it was desired to acquire sufficient knowledge of the order of magnitude of the reaction rates so that alloying element losses and/or oxygen pick-up (if any) could be estimated in a real furnace based on the data generated. As a last factor it was felt that wettability tests would over-emphasize small variations in surface finish. Since the materials used were either commercial products used in real furnaces or experimental compositions, they would necessarily vary slightly in surface finish.

In order then to simulate the VIM process, small crucibles as shown in Fig. 3 were produced, and fixed amounts of metal were melted under vacuum, for a certain length of time. As a natural consequence of the size and the arrangement of the experimental set-up, each crucible was used only once, and no attempt was made to study the effect of subsequent heats in a crucible. It was realized that the surface/volume ratio in this crucible was obviously quite dissimilar to even a small VIM furnace; however, this ratio is, in the experimental case, larger than in the actual case. Consequently a magnification of the reaction effects is observed, hence improving the ability of the test to assess the stability of refractories in contact with melts under vacuum. Another effect present was possibility that wetting of the crucible by the metal, would cause variations in the vacuum/metal and in the metal/refractory interfaces, as shown in Fig.4. It was felt, however, that since these wetting characteristics were quite reproducible for each metal/refractory pair and did not cause a significant variation in interfacial area that they could be assumed not to alter the placement of the relative stabilities of the refractories under vacuum.

The apparatus employed is shown in Fig.5. The temperature measurements were made with a narrow-angle infrared pyrometer through a Pyrex glass, placed at a sufficient distance from the metal to minimize condensation on it. In order to calibrate for emissivities, pure Fe and Ni were used. The pyrometer directly controlled the power supply and a

variation within $\pm$ 5°C of the specified temperature was typical. The pressure was always kept below 30μ and the leak rate was verified before each run.

The compositions of the materials used for the tests are given in Tables 5 and 6 and except where noted, they are nominal compositions given by the suppliers.

The metallic samples weighed 10g $\pm$ 0.1g for the tests with steel or 13.5g $\pm$ 0.1g for the tests with superalloys.

A typical melt cycle would involve slow heating from ambient temperature for complete outgassing of the crucible, a short holding time at around 1000°C, melting the sample, superheating to 1520°C (in the case of 1095 steel) or to 1500°C (in the case of Nickelvac X-750), holding at that temperature for the desired period of time, turning off the power supply and cooling to ambient temperature under vacuum. This was done in order to minimize the chances of oxidation of the metallic sample.

The crucibles were produced in a paper mould with a paraffin wax core. After drying (or setting) at ambient temperature they were either fired at the required temperature (in a gas-fired furnace) or heated to a temperature in the range of 600°-700°C to burn the paper and the paraffin wax and thoroughly dry them.

Metal samples for chemical analysis were separated from the crucibles, carefully cleaned of refractory incrustations, filed to eliminate open porosity and then cut in small pieces for analysis. The carbon and oxygen analyses were made

by the conventional techniques in LECO analysers.

In order to observe the refractory-metal interfaces or other refractory samples it was necessary to cut and polish the specimens without separating the metal from the ceramic or removing grains of the ceramic. In order to accomplish this, the samples were impregnated with low-viscosity epoxy, under vacuum. After polishing by standard metallographic techniques, down to 1μ diamond paste, they were observed either in an Optical Microscope or in a Scanning Electron Microscope equipped with an X-Ray Energy Spectrometer. In some cases the microprobe was also used.

CHAPTER 3

RESULTS

Since the tests made with steels and with superalloys are analysed in different ways, as discussed below, this section will be divided according to the alloy used for the tests.

3.1 Tests Using AISI 1095 Steel

In order to avoid problems with variation of carbon and oxygen content and activity over a wide range, and to ensure reaching the steady state described by Machlin, a high-carbon steel was selected for these tests. Although carbon was the element to be studied, the interest was in steel interaction with refractories and so a plain carbon commercial steel was selected. The low initial oxygen content in this steel (due to the high C content) minimizes initial variations in carbon consumption under vacuum. The tests were conducted for various lengths of time, from 5 minutes to 2 hours, and the metal was analysed for carbon content.

3.1.1 Tasil X--(Mullite Based Cement)

Although this product is not designed to be used in contact with metal in a VIM furnace but rather as a mechanical support for the coils and the lining itself, its mullite composition makes it particularly interesting since it enables

one to analyse the behaviour corresponding to the minimum silica activity in the binary SiO_2/Al_2O_3, widely used in the refractory industry. Any cement with higher alumina than the mullite composition should be designed so as to have all its silica content in a mullite form, to minimize the silica activity.

Fig. 6 presents the variation of carbon content ($C_{initial} - C_{final}$) after melting in Tasil X crucibles, compared with melting in alumina crucibles (Alundum 1139). The very high consumption of carbon by the mullite refractory is readily apparent. The parabolic relationship indicates that the controlling step in the process is the diffusion of silicon and oxygen.

Observing the metal/refractory interface after a short time (5 mins.) Fig. 7, one can see how the mullite is depleted of silica at the interface and how the alumina particles remaining have a higher specific area, further enhancing the dissolution of the refractory.

If one calculates the activity of silica in mullite, in equilibrium with pure alumina, using the data from Rosenqvist (68) for the reaction

$$3Al_2O_3 + 2SiO_2 = 3Al_2O_3 \cdot 2SiO_2 \text{ (Mullite)}$$

$$\Delta G_{1600^oC} = -6000 Cal$$

a value of 0.45 is obtained. Calculating the pressure of CO in equilibrium with pure silica or with silica at this activity using the equilibrium

$$SiO_2 + \underline{2C} = 2CO + \underline{Si}$$

one finds

$$p_{CO}^{mullite} = 0.67\ p_{CO}^{SiO_2}$$

and hence in both cases silica will be extremely unstable in presence of carbon under vacuum, i.e., the lowering in the activity of silica caused by the mullite formation is not comparable to the increase in carbon activity caused by depressing the CO pressure.

3.1.2 Cements with 10% SiO_2 (Taylor 320, Alundum 1162)

Following the tests with the mullite based cement, lower silica cements were tested, in order to determine whether or not they would be more immune to attack by the steel. This could happen due to the lower exposed area of the low-stability phase (mullite or silica rich compound, since in some cases, other fluxes, such as Alkaline oxides were present).

In all cases extensive wetting of the crucible was observed. When Taylor 320 was used after drying at 600°C (since it is recommended that it be used without firing), a voilent boil occurred, throwing most of the metal out of the crucible. When these samples were analysed, they showed carbon consumption of up to 0.1% in 5 minutes. Since the crucibles were certainly well dried (not only due to the 600°C drying but also because of the slow heating under vacuum before melt-down), firing was attempted with the aim of making sure that the most stable silica containing phases would be formed. The metal did not boil in the fired crucibles, although the carbon consumptions were still high, being of the order of

0.2% in 30 min. X-Ray diffraction analyses on powder of both refractories revealed a low intensity set of quartz peaks in the unfired sample, while the fired sample presented a much lower intensity set of quartz peaks as well as peaks of sodium-potassium alumino-silicates. The most dramatic change, however, was in the physical appearance of the crucibles, with the firing bringing an extensive densification of the structure, particularly at the surface, as shown in Fig. 8. This would probably be responsible for the higher stability in the fired condition.

When one observes the altered layer of a 10% SiO_2 crucible (Fig. 9) one notices a reasonably thick layer depleted in silica caused by the diffusion and decomposition of this less stable component. It is also obvious from Fig. 9 that the high alumina layer depleted in silica has had the binding phase removed from the region between the grains which resulted in a much lower density than the bulk of the refractory. It is reasonable to suppose that this layer has a much inferior mechanical strength and will probably break off very early, maybe even during the shrinking or the cleaning of the skull, in an actual furnace.

3.1.3 Cements Produced Using Fluorides

Since the tests with silica bearing cements revealed the inadequacy of silica as a flux for use under vacuum in contact with carbon steel, it was decided to try different additions to alumina in order to promote its reaction with the spinel-bonded Magnesia brick (Magnel) used in VIM.

It is known that fluorides are very good fluxes for this system (and for that matter, for almost any oxide system) and they have been used in many cases to promote reaction in refractory production (69, 70). Although they are very effective in this they present some limitations such as excessive attack on the refractories (during the production of clinker) (69), a decrease in sintering ability (in pure alumina sintering) (70), the possibility of health hazards (since water soluble fluorides are hazardous) and possible flouride emissions during firing. However, the two first limitations are actually advantages in the case of their utilization in a cement, i.e., reaction with the refractories and controlled sintering, in order to achieve a relatively porous product with little dimensional change. The two other problems may indeed present difficulties if not dealt with carefully.

The selection of a non-water soluble fluoride, at a reasonable price, limits our choice essentially to Ca, Mg and Li fluorides. With respect to the fluoride emissions, if the percentage of fluoride in the cement is kept at a reasonable level, and the amount of cement minimized, as practiced in VIM operations, one should not expect a high concentration of fluoride emissions during the firing of the crucible.

Due to its ready availability, calcium fluoride was selected for the initial tests. In order to ensure the possibility of fluxing, some calcium oxide was also added, with the aim of reaching the ternary eutectic at approximately

4% CaO/72% CaF_2/24% Al_2O_3. Of course all the compositions tested were saturated with alumina, the final one used in the tests being 82% Al_2O_3/14% CaF_2/4% CaO where the alumina used was actually the high alumina castable cement Alundum 1139, in order to impart plasticity and formability to the mixture. All the samples were fired for two hours at 1300°C in a gas-fired furnace following which they were mainly composed of calcium aluminates and alumina, with the typical microstructure shown in Fig. 10.

No calcium fluoride peaks were present in the X-Ray spectrum. In all cases, the calcium aluminate peaks could be identified as C_3A_5 or CA_2 and, in some cases CA_6. Only in cases when the amount of calcium fluoride was increased to 28% and the calcium oxide to 8% could some low-melting $C_{12}A_7$ be observed. The production of the calcium aluminates is attributed to the conversion of the calcium fluoride into calcium oxide by one of the following reactions:

$$3CaF_2 + Al_2O_3 = 2AlF_3 + 3CaO$$

$$CaF_2 + H_2O = 2HF + CaO$$

In order to test the adequacy of this material adherence tests and stability tests were performed. Fig. 11 displays the results of the adherence tests. The reaction of the cement and the brick is evidenced not only by the physical observation of the interface but also by the chemical composition profile. One should also expect this behaviour with almost any brick, again due to the high fluxing ability of the fluoride employed.

The same series of stability tests was performed with alumina cement Alundum 1139. Comparing Figs. 12 and 13 one can see that there is no significant difference in carbon consumption with either of the cements, indicating that the cement does not have lower stability than the original alumina cement used to produce it.

To further investigate the possibilities of the fluoride-mineralized cements, it was decided to try MgF_2, with the aim of producing magnesia-alumina spinel, instead of calcium-aluminates.

Finely ground MgF_2 and MgO were mixed with Alundum 1139 in the proportions 85% Al_2O_3/14% MgF_2/1% MgO (SP2) and fired at 1300°C, i.e., slightly above the melting point of the fluoride. The mechanical properties obtained were much superior to those of Alundum 1139 and of the calcium-fluoride cement (CAF). Fig. 14 shows the microstructure of the material produced. The large grains are Al_2O_3 (from the original cement) while the intergranular material is a mixture of spinel and alumina. In the X-Ray powder diffraction, only alumina and spinel peaks were present.

Fig. 15 shows the results of carbon consumption tests in this material, which are as good as the values for pure alumina cement, within the experimental variations.

It is clear then that this composition would be highly favourable for use under VIM conditions (at least for steels).

In order to improve its plasticity and cold adherence, lignin sulphite was added as a 10% solution in water, mixed

with the cement powders. The cold adherence tests gave excellent results. In most tests the brick/mortar interface was stronger than the mortar itself, and the structure of the fired material was not altered by this addition.

Observing the fired interface, it was noticed that this cement reacts with the spinel phase and with the binding phase of the periclase grains in the Magnel brick, and reacts to a lesser extent with the MgO itself (Fig. 16). Analysing the results achieved previously (CaF_2 producing highly reactive CaO and calcium aluminates, MgF_2 producing highly reactive MgO and spinel with the excess alumina) it was decided that, in order to promote more reaction with the MgO particles, AlF_3 should be used to form spinel with the MgO grains from Magnel. This could be done in two ways: By adding AlF_3 to the $Al_2O_3/MgF_2/MgO$ mixture and reducing the initial Al_2O_3 percentage or, by designing an MgO based mixture, with AlF_3 and Al_2O_3 additions. The former was selected as being easier to do and a 70% Al_2O_3/16% AlF_3/13% MgF_2/1% MgO mixture was used, mixed with the 10% lignin sulphite solution and spread between Magnel bricks. Again, the cold strength and plasticity were very good, indicating that cements without silica can achieve these properties. The binding characteristics however, did not differ substantially from those of SP2, probably due to the short reaction time given to both samples (2 hrs.).

3.1.4 Low Silica Phosphate Bonded Cement

The other component extensively used in connection with alumina to produce cements is phosphoric acid with or

without silica. In order to investigate the behaviour of the phosphate bond, tests were performed with Taylor 341 cement.

It is believed that in a phosphate bonded alumina mixture, $AlH_3(PO_4)_2 \cdot 3H_2O$, the hydrated aluminum-phosphate phase is the major phase produced in the binder system and, upon firing, aluminum orthophosphate ($AlPO_4$), which in isostructural with silica, would be present. The orthophosphate is believed to decompose according to the reaction

$$2AlPO_4 = Al_2O_3 + P_2O_5$$

forming Al_2O_3 with the volatilization of P_2O_5. There is no agreement, however, concerning the exact temperature of the decomposition, Khoroshavin, et al (72) reporting its start at 1460-1480°C and O'Hara et al (71) stating that it is stable to, at least, 1760°C. It is clear however, that since P_2O_5 is an oxide even less stable than SiO_2 (ΔG_{1873K}= -55KCal/molO_2 for P_2O_5, as compared to -125KCal/molO_2 for SiO_2) and as the process in question is to occur under vacuum (and hence low partial pressure of P_2O_5) one should expect the decomposition of the bond to be enhanced under vacuum induction melting of steel.

Fig. 17 shows the carbon consumption in Taylor 341 crucibles. One can see that although they are higher than those in the Alumina cement Alundum 1139, the difference is not pronounced. The main reasons for the acceptable behavior of this cement are to be found in its relatively low P_2O_5 content, the absence of SiO_2 and its excellent grain sizing, surface quality and strength as compared to the corresponding

properties of Alundum 1139. Observing the metal/refractory interface for a 15 minute steel-test in this material (Fig. 18), one notices no alteration in the structure of the cement. Although some grains can be seen to be going into the melt and a depletion in phosphorous can be noticed close to the interface, this seems to have little or no effect on the strength of the material.

3.1.5 Silica Containing Phosphate Bonded Cement

The most widely used cement in VIM furnaces is Coralbond, a silica containing phosphate bonded cement. The addition of silica is probably made to improve plasticity, cold strength and to enhance its fluxing ability, since silica and P_2O_5 form an eutectic at 900°C, while the lowest melting eutectic in the high alumina side of the Al_2O_3/P_2O_5 binary is at 1200°C. Indeed, one observes that this cement is extremely plastic, adherent to almost any surface, and develops a very good cold strength. It is hence a very desirable cement, from the standpoint of its actual utilization by bricklayers on the shopfloor.

It must be kept in mind, however, that although these properties are important (and are, in several cases, the only properties to be taken in account when selecting a mortar) they are not the only important properties of a mortar. In the case of VIM or other processes in which refractory attack is important, one should look initially at the compatibility of the mortar with the conditions of the process. In our case, compatibility with high carbon activity or very low

oxygen activity metals under vacuum is essential. Only after this condition is met, can one proceed to test the ease of application and strength of a joint before firing. These properties in the case of VIM are not as important as the final quality of the material produced and the life of the lining. In other words, it may pay to use a cement that will not be as easy to trowell or to spread, and will not produce as strong a cold joint--in order to achieve longer lining life and better material quality.

In all steel tests with Coralbond, although the samples were well dried and prefired at 900^{o}C various degrees of boiling were observed, indicating a strong metal/refractory interaction. Fig. 19 shows the results for carbon consumption in Coralbond as a function of the square root of time, together with those for Tasil-X (mullite cement). The very good straight-line fit shows that in both cases the reaction is controlled by diffusion, probably of SiO and CO_2 (and maybe of P_2O_5) in the pores of the refractory as proposed by Mass and Abratis (73) for the reduction of mullite by Fe-C melts. It is interesting to note that both Coralbond and Tasil-X present the same decomposition rate in the tests performed.

When the interface Coralbond/metal is observed (Fig. 20), one notices the characteristic silica depletion and also the total decomposition of the bond. It is interesting to note that the bond decomposes (and the phosphorous content drops) at a constant distance from the working face (Fig. 21)

while the silica boundary is not as linear. This probably suggests that the phosphate bond decomposes by thermal and pressure effects, with the volatilization of P_2O_5, the straight interface indicating the isotherm corresponding to the decomposition temperature.

It is also clear again in this case that the metal penetrates into the porosity left by the reduced components (SiO_2 and P_2O_5), and that the altered layer has a much lower density than the bulk of the refractory. Evidence of the cement as source of non-metallic inclusions (with or without entrapped metal) is presented in Fig. 22.

It is clear from these observations that the combination of silica/phosphate bond makes Coralbond less than desirable, as far as chemical stability is concerned, for use in VIM furnaces.

3.1.6 Summary of Steel Tests

The very negative effect of silica with or without other oxides or as a 'lower activity' form in a compound has been observed. Although unexpected, the results with the mullite cement seemed to be superior to those of the 10% SiO_2/Al_2O_3 cement--Taylor 320. This type of behaviour was also observed in wettability studies performed by Sveshkov et al. (74). The reason for this behaviour perhaps can be found in the fact that the phases present in the higher alumina cement are not those predicted by equilibrium considerations, since after firing its behaviour was improved. In any event, both cements proved unsuitable for the application in question and

no further investigation was undertaken.

The possibility of using fluorides as fluxes, instead of silica, was shown, since they do not reduce the stability of the basic alumina cement employed in the tests and do promote bonding to the bricks.

The physical characteristics of the refractories are indeed important with respect to the extent of the metal ceramic reaction, although this factor alone could not prevent the corrosion reaction.

In several cases the corrosion of one of the refractory constituents was observed to cause the formation of inclusions in the metal which may or may not be completely dissolved during the remaining part of the heat depending on the stage of formation and size and composition, etc.

3.2 Tests Using X-750 Superalloy

Since it soon became apparent that the interactions between X-750 (and probably any other low-C superalloy) and the refractories under vacuum were not enough to cause any easily detectable variation in any of the alloying elements, it was decided instead to concentrate attention on the actual alterations at the metal/refractory interface. In addition, the variation of the oxygen content of the alloy, caused either by the dissolution of refractory oxides or by entrapment of refractory inclusions was to be studied.

Due to the relatively high percentage of aluminum titanium and chromium in this alloy, all of which have highly negative interaction coefficients with oxygen in Ni alloys ($\varepsilon_O^{Al} = -210$, $\varepsilon_O^{Cr} = -38.6$, $\varepsilon_O^{Ti} = -70$ at 1873^oK (75)) one should expect a relatively high oxygen content in this alloy in equilibrium with, for example, alumina. This is clearly shown in Fig. 23, where the oxygen content in equilibrium with alumina is shown, for a Ni-Al alloy, as a function of percentage of aluminum. One can readily see that the usual 10ppm oxygen range of values achieved in the production of superalloys are rather displaced from equilibrium and can only be obtained due to the melting practice of initial deoxidation with carbon followed by addition of reactive elements and tapping. It is clear that the longer the holding time after the addition of the more reactive elements (as Ti and Al) the closer the system will approach equilibrium with the most stable mixture of oxides.

It must be stressed that in this case there is a quite pronounced deviation from the simple deoxidation equilibria observed when small amounts of deoxidant are present (aluminum deoxidation of steel, for instance). In those cases, the aluminum concentration is small, and in the expression for the activity coefficient of oxygen, fo

$$\log fo = e_o^o wt\%O + \sum_{i=1}^{n} e_o^i \, wt\%i$$

the term corresponding to $e_o^{Al} wt\%Al$ is also small. The difference between the Henrian activity and the weight percentage of oxygen can be neglected, as shown in Fig. 23 up to approximately 0.08% Al in Nickel. In this range of compositions, one can use a relationship of the type

$$wt\%O^{\,3} \; wt\%Al^{\,2} = \kappa a_{Al_2O_3}$$

or

$$3 \log wt\%O + 2 \log wt\%Al = \kappa' \log a_{Al_2O_3}$$

and show that log wt%O is a linear function of log wt%Al .

As the aluminum content of the alloy increases, however, the term $e_o^{Al} wt\%Al$, cannot be neglected any more and h_o departs from wt%O, according to the relationship

$$h_o = f_o wt\%O \; .$$

While the relationship $h_o^3 h_{Al}^2 = \kappa$ is still valid for a fixed alumina activity, as shown by the extension of the activity straight line in Fig. 23, the weight percentages are not linearly related any more, due to the interaction of the

two solutes in the alloy, which causes departure from the simple Henrian behaviour.

Assuming that the only significant interaction effect is that caused by aluminum on oxygen, the weight percentages of the two elements can be related by the following expression

$$h_O^3 h_{Al}^2 = \kappa a_{Al_2O_3}$$

$$3\log h_O + 2\log h_{Al} = \kappa'$$

$$2\log wt\%Al + 3(\log fo + \log wt\%O) = \kappa'$$

$$2\log wt\%Al + 3e_O^{Al} wt\%Al + 3\log wt\%O = \kappa' \qquad (1)$$

Equation (1) shows that log wt%O is not a linear function of log wt%Al , and can only be assumed to be so when the term $3e_O^{Al} wt\%Al$ is negligible, which only happens for small concentrations of aluminum.

It is then obvious why the refractory/metal interface becomes important in the system, since it will control the thermodynamics of the process (by the compound formed, and hence exposed to the metal) and the kinetics of the process, (by its physical characteristics). The oxygen content of the alloy will indicate the approach of the system to equilibrium, and, if a constant time is taken as a basis for comparison, the most satisfactory refractory from this standpoint.

Table 7 shows the oxygen value found in samples of X-750 held for 15 minutes at 1500^{o}C in crucibles of different refractory materials. It is evident that the refractories

composed of $MgO \cdot Al_2O_3$ spinel and either Al_2O_3 or MgO (Magnel and 85% Al_2O_3/14% MgF_2/1% MgO (SP2)) present the lowest oxygen values amongst the samples followed by Taylor 341 (Alumina bonded by 4.5% P_2O_5), Peribond (MgO with SiO_2), Alundum 1139, the calcium fluoride-alumina cement (CAF) and last, Coralbond.

From these data it is clear that the most advisable refractory for holding Inconel X-750 would be one containing a high percentage of spinel and as little as possible low-stability oxides, the ideal combination being Magnel/SP2. Taylor 341 performed well with an oxygen content not much higher than that of the spinel based materials. On the other hand, Coralbond reached 60 ppm oxygen in 15 minutes (from 7 ppm initial oxygen). Since its main chemical difference from Taylor 341 is in the silica content and the slightly higher P_2O_5, it can be concluded that the presence of these oxides makes Coralbond the least suitable cement for melting superalloys. In a real furnace those high oxygen values will never be observed, of course, due to the much more favourable surface/volume ratio; however, as far as cement attack is concerned the results will be the same or even more pronounced, due to the almost constant low oxygen potential in the metal, and consequent high driving-force for the dissolution. It can also be noticed that the variation in silica activity has, in this instance, some effect on the stability, since Peribond presented a significantly lower oxygen value than Coralbond, for comparable silica contents. It is unfortunate that in superalloy melting, the initial stage of a heat involves

carbon deoxidation and hence severe attack even to low silica activity compounds such as those probably present in Peribond.

Observing the metal/refractory interface of the Magnel sample one can rationalize the processes occurring when X-750 is melted in this material. Since the Magnel brick is composed of large periclase grains bonded by smaller magnesia and spinel grains, the working face of a crucible drilled in a brick with a diamond drill will have both MgO and $MgO \cdot Al_2O_3$ areas exposed to the metal.

Fig. 24 shows a cross section of the interface of a sample after use, while Fig. 25 depicts this interface when detached from the metal. The observed gap between the metal and the brick in Fig. 24 is due to shrinkage during cooling and, on the right hand side, one can observe a periclase grain. The pieces of oxide adhering to the metal at this point in the interface are of an oxide rich in Mg and Al, probably spinel. The mechanism for the formation of this layer would be precipitation from the melt, described in a 1% Al,Ni alloy by the following processes:

1) Dissolution of silica from the binding phase of the periclase grain, due to the very low oxygen potential in the melt and low silica stability:

$$SiO_2 = \underline{Si} + 2\underline{O}$$

This process will contribute with oxygen for the precipitation of the most stable oxides.

2) Dissolution of MgO due to the very low oxygen activity coefficient in the melt after the addition of the reactive elements as shown in Fig. 26 for 1% Al in the melt:

$$MgO = \underline{Mg} + \underline{O}$$

3) Formation of spinel over the MgO grains either directly precipitated from the melt,

$$\underline{Mg} + 2\underline{Al} + 4\underline{O} = MgO \cdot Al_2O_3 \qquad (3a)$$

according to the equilibrium fixed by line 3A in Fig. 26 on formation of spinel in equilibrium with MgO, by precipitation and reaction of Al_2O_3,

$$2\underline{Al} + 3\underline{O} + MgO = MgO \cdot Al_2O_3 \qquad (3b)$$

shown by line 3B in Fig. 26. It is clear that the process described by equation (3b) should be the most favourable from a thermodynamic viewpoint, since line 3B will always be reached before any other in Fig. 26 as the oxygen content of the melt increases. This is due to the very low magnesium contents to be expected at this stage of the melting process. Should Mg in amounts over 100 ppm be added in a latter step of the process, MgO may become the most stable oxide, due to the very strong interaction of Mg with O in Nickel alloys.

The fact that enough oxygen should be available locally from process (1) and the thermodynamic advantage of process (3b) over (3a), favour reaction (3b) as the one probably responsible for the formation of the spinel layer.

One must also be aware of possible kinetic differences between the precipitation of alumina or that of spinel, which

involve more species and of the intersolubilities of these various oxides which may not be negligible at the temperatures in question.

These reactions would have the effect of producing an essentially all-spinel lining (or brick) with relatively low oxygen equilibrium concentration which would be favourable for the holding of very low oxygen activity metals. This is also a good evidence of the suitability of all spinel linings for VIM.

Based on this rationale it is easy to understand the excellent stability shown by the cement SP2. Since the firing of the MgF_2/Al_2O_3 mixture produces a complete sheath of $MgO \cdot Al_2O_3$ around the alumina grains, it is clear that this cement will behave almost as pure spinel, and hence achieve the best values for residual oxygen with X-750 alloy.

When one compares the large difference between the values for Taylor 341, Alundum 1139 and Coralbond, the observation of the interface again plays an important role in elucidating the causes for their different behaviour. In this case, since all cements are high in alumina, and both Mg and MgO are essentially absent, there is no chance for spinel precipitation. One must then look for the next most stable oxide mixture. In the case in question, this proved to be a mixture of chromium oxides with the oxides of the refractory and some traces of oxides of other alloying elements (such as Ti). Alundum 1139, for instance, presented a pink layer, about 2mm deep, behind the interface, rich in chromium. This agrees with the observations of Spendelow (40) when melting Hastelloy

235 in alumina crucibles. The layer formed in Taylor 341 was greenish, thin and very dense, almost impervious, as shown in Fig. 27. This layer, composed mainly of alumina and chromium oxide in somewhat higher concentration than in the case of Alundum 1139 (and containing also some P and Ti) probably limits the extent of the reaction, allowing a lower oxygen potential phase to surround the metal as a real 'crucible' of higher stability with respect to the melt than the parent crucible. In the case of Alundum 1139, however, its more open structure precludes the formation of a dense layer and the chromium oxide can diffuse into the refractory, while the metal, at all stages, 'sees', essentially, Al_2O_3, and hence seeks a higher oxygen equilibrium concentration. In the case of Coralbond, even though the interfacial layer formed is dense and impervious it contains a rather large amount of silica (and also P). The superalloy in question contains a minimum percentage of silicon and this element is a mediocre deoxidant even when alone in Nickel alloys ($a_{SiO_2}/h_{si}h_o^2$ = 6.18 (10^5) as compared to $a_{Al_2O_3}/h_{Al}^2 h_0^3 = 4.5(10^{13})(3)$). As discussed before, since the activity coefficient of SiO_2 in SiO_2/Al_2O_3 mixtures is close to unity, one should expect this silica to act as a continuous source of oxygen to the metal.

CHAPTER 4

OBSERVATIONS OF INDUSTRIAL SAMPLES

In order to relate the experimental results with the actual VIM practices and to verify the validity of some of the observations made in the theoretical review, some samples from materials used in or produced by VIM furnaces were examined. These consist of a sample of slag produced in VIM de-S treatment, samples of macro-inclusions in nickel base superalloys; and a Magnel brick used in a furnace melting steels and nickel-base superalloys, and a rammed VIM lining which failed prematurely.

4.1 Sample of Slag Used in VIM de-S Treatment

In order to desulphurize Ni-base alloys, it is a known practice to make calcium oxide additions to the charge. Although in most heats there is no problem, in some cases a violent slagging occurs due to refractory attack. The sample analysed is from one of those heats.

Figs. 28 and 29 show the characteristic microstructure of the slag, in the SEM. The matrix is composed essentially of calcium aluminates, with some other oxides, as shown by the MgKα and AlKα photographs in Fig. 29, several small mixed-oxide sulphide inclusions and large MgO grains.

The first observation to be made is related to the significant sulphur content of the slag, confirming the adequacy of this treatment as a de-S treatment. However, the large magnesia grains clearly originate from the refractory used, which was a spinel-bonded magnesia rammed lining. It is clear then that, apart from desulphurizing the lime addition also fluxes the binding phase of the lining producing the calcium aluminates which constitute the bulk of the slag. The fact that the fluxing occurs in some heats can be possibly attributed to the cumulative effect of various treatments, until sufficient calcium oxide has been absorbed to produce the low melting mixtures of MgO, spinel and calcium aluminates. These, combined with the absorption of oxides of elements such as Zr and Ti from the skull, have a very high fluxing ability in this system.

It is interesting to compare these observations with the comments by Ward et al. (55), when employing a lime desulphurization treatment in either Magnesia Spinel or pure Magnesia linings. He observed definite swelling in the former after the treatments while no alteration occurred in the Magnesia linings, probably due to the absence of alumina.

4.2 Magnel Brick

A sample of Magnel brick from the working lining of a large VIM furnace was examined, both macro- and microscopically.

4.2.1 Macroscopic Observation

Metal fining was found in the Coralbond joints, which was the reason why the lining was removed. Since there is still quite a substantial thickness of brick available, this represents a considerable waste of material and bricklaying effort. This confirms the observations that the worst problem in VIM brick linings is at the working face joints.

One also observed (Fig. 30) a considerable penetration of metal into the Magnel brick itself. In order to study the mechanism of this process, microscopic observations were made of the region close to the working face.

4.2.2 Microscopic Observation

Fig. 31 shows some entrapped metal in the refractory, which actually contains inclusions (spinel, alumina and calcium aluminates). This shows that although the mortar joints are the weakest link in the system, one can also expect the bricks to contribute to the inclusion content of the melt. The presence of calcium aluminates was found to be rather intriguing, since Magnel is supposed to have a very low CaO content (Table 6). In addition, as Figs.32 and 33 show, the metal seems to find its way into the refractory particularly via these aluminates. This occurs by what appears to be melting and dissolu-

tion (Fig. 32), or possibly by fluxing with TiO_2 or ZrO_2 (Fig. 33).

The calcium aluminates occur as an intergranular phase in the periclase grains close to the working face of the brick. When one observes the periclase grains in unused Magnel brick, Fig. 34, one sees the typical structure of high purity periclase, in which the MgO grains are both direct bonded and bonded by a calcium silicate intergranular phase. There has been considerable work done on the desirable composition of this silicate phase, both with respect to the CaO/SiO_2 ratio (76) and to the impurity content (77). The CaO/SiO_2 ratio will control, in the system $CaO/SiO_2/MgO$, the amount and the temperature at which liquid will be formed. It is known that ratios greater than about 2 or very low should be used, if no liquid is to be present at 1600^oC. In the case of Magnel, it seems that this ratio is around $\frac{3}{2}$ which is recommended for Electric furnace and Open-Hearth applications (77). The content of impurities (other oxides) has a marked effect on the dihedral angle of the liquid phase, Alumina and TiO_2 being amongst those causing pronounced lowering in this angle, hence promoting liquid penetration into the grain boundaries and refractory disruption.

When Magnel is used for steel or superalloy melting under vacuum, two main processes occur. Reduction or dissolution of silica and formation of alumina at the working face. These two processes can lead to an increase in the amount of intergranular liquid phase or to the lowering of the liquid

formation temperature. Indeed, Fig. 35, shows a periclase grain, 15 mm away from the metal/refractory interface where, besides the larger amount of intergranular compound, one notices a change in its composition with a decrease in silica and an increase in alumina content. As one gets closer to the interface, there is virtually no silica left and the intergranular liquids are basically of the system $CaO/Al_2O_3/MgO$, probably with small fluxing additions of other oxides, for instance TiO_2.

One can also observe, in some instances (Fig. 36), the presence of a layer of calcium aluminates in contact with the metal, probably drained intergranular liquid. This will, of course, be a possible source of calcium aluminate inclusions in the melt.

Although the attack on the brick is obviously small (at least compared to that on the joints) this shows that even if a more superior cement were developed, the refractories would still contribute inclusions, although they would have a much longer useful life. It also draws attention to the importance of the <u>total</u> analysis of the refractory, both chemical and physical, since the concentration of CaO and SiO_2 in an intergranular phase makes the brick less resistant than it could be if, say, fused MgO grains, of the same bulk composition were used.

Fig. 37 shows a layer of spinel over a periclase grain at the working face, supporting the experimental observations presented earlier and the theory that spinel should be the

most stable oxide phase in contact with Nickel-based super-alloy containing high percentages of aluminum in a Magnel crucible.

4.3 Inclusions in Ni-Based Superalloy

Although it is well known that vacuum induction melting produces cleaner material than air melting (5, 51), particularly in the case of superalloys containing reactive elements, this is mainly due to the elimination of the atmosphere from the system, preventing the excessive formation of oxides and nitrides. One must be aware, however, of the fact that 'exogenous' inclusions from refractories can still be produced by mechanisms such as erosion, and chemical attack as discussed in the previous chapter, and that these products will, in most cases, be oxides. It is now well established that stable nitrides and carbonitrides (such as Ti(CN)) are hardly affected by the usual treatment in VIM or VAR and hence, once formed, will most likely remain in the alloy.

It becomes then of paramount importance to control the factors that will promote the formation of those inclusions, such as ferro-chromium alloy with high nitrogen content, ferroalloys with high oxide content, etc. Besides, one must be ready to recognize that there will be some inclusion formation from the refractories, since all observations show that no present VIM refractory can be considered totally inert under the processing condition.

In order to illustrate these comments, some samples of Ni-based superalloy from a VIM furnace were examined.

Fig. 38 shows calcium aluminate inclusion stringers in a partially forged VIM-VAR superalloy. When one examines these inclusions in more detail they show small entrapped

metal particles and are surrounded by smaller titanium carbo-nitrides (Fig. 39). This would indicate that they were partially molten at some stage of the processing and that they tend to cluster during melting and remelting, probably due to favourable surface energy considerations. In Fig. 40 one sees a spinel inclusion, found in another sample from the same material. Although it is not our purpose to discuss in depth the genesis or these inclusions, it seems rather clear that their oxide core should be related to refractory materials employed in the VIM furnace, if not for their size (too large to be deoxidation products nucleated in the melt), for their composition (since there is no intentional calcium or CaO addition in this case and the only magnesium added is in the form of a small addition of Ni-Mg alloy for workability improvements). It is easier to believe that those inclusions were formed from interactions of the metal with the bricks, since the interactions observed previously could explain the formation of large spinel or calcium aluminate inclusions without difficulty. These inclusions would only have to cluster in the melt whether floating or not and find their way into the tundish and later into the ingot.

It is also clear that in the present state of refractory technology and practice, the formation of these inclusions cannot easily be avoided. One is left then with the option of removing them, by adequate pouring temperature control, tundish design and holding time, and perhaps also pouring through a slag.

4.4 Piece of Rammed Lining

As discussed before, industrially, the alternative to brick/cement lining is a rammed lining. In this case, a carefully sized mixture of alumina, periclase and silica, roughly in a 60%MgO/40%Al_2O_3 composition was used to melt the superalloy Nimonic 901.

4.4.1 Macroscopic Observation

The failed lining shows metal incrustation and penetration on the working face and metal fins along cracks (Fig. 41) these cracks being the reason why the lining was removed from service.

4.4.2 Microscopic Observation

Fig. 42 shows the structure of the rammed lining 6cm away from the metal/refractory interface. It shows a sintered matrix essentially composed of spinel, surrounding large periclase grains. These periclase grains, resemble very much the large MgO grains found in the slag sample previously presented (4.1), in agreement with the theory forwarded for their origin. The most interesting characteristic of the matrix is that the sintering is quite inhomogeneous, i.e., some regions are densely bonded, while others are porous and probably loosely bonded. One also observes a very high SiO_2/CaO ratio indicating the possible presence of forsterite.

The metal/refractory interface shown in Fig. 43 presents a layer of Ti/Al oxides. This layer, as in the case of Magnel bricks, contributes macro inclusions to the melt when

eroded (Fig.44). Close to this layer, there is complete depletion of silica in the refractory, the intergranular volumes being filled by metal in a region very close to the Ti/Al oxide layer and by Ti/Ce oxide mixtures further into the lining (Fig.45).

This can be rationalized in the following manner. Silica dissolves in the low oxygen activity alloy, bringing the oxygen content locally into the range of oxide precipitation. In the case of Nimonic 901, both the high Ti content (as compared to X-750) and the high Fe content (which increases the effectiveness of Ti as a deoxidant and decreases that of Cr) favours the precipitation of a mixture of Ti/Al oxides instead of Cr/Al or Mg/Al oxide mixtures as observed in the previous cases. Since there is very little MgO exposed to the melt, the Mg available for spinel precipitation would be readily exhausted. Titanium oxides are excellent fluxes in this system and should diffuse readily into the liquid matrix, decreasing the dihedral angle, increasing the amount of liquid phase and hence enhancing the attack process by separating the grains of refractory. Although it is not known, it is quite possible that a heat from this lining would contain a slag very similar to the one caused by CaO addition as discussed before, with the CaO substituted by titanium oxide.

The metal fin/refractory crack interface shows very little evidence of reaction. This indicates that the crack should have occurred due to thermal stresses caused by inhomogeneous expansion of the lining, and that the metal simply wets the refractory and penetrates into the crack.

One also notices no alteration in the fused MgO grains (Fig. 46) which are evidently more stable than the sintered periclase grains of Magnel.

The presence of cerium is probably due to a de-S treatment with REM, as described by Cremisio (63) and others. This is a very effective technique and its use has been discussed previously, the only practical limitation to its application being the REM residuals and carry-over problems.

Rothman (65) reported a significant carry-over of Ce into the first heat in a crucible after the REM treatment was performed. Although he attributed this only to the skull, Cremisio (63) suggested that the refractories could play a role in the reversion of Ce into the subsequent heats, making its recovery uncertain. It is also noteworthy that Cremisio when Ce desulphurizing Nimonic 901 reported the "development of an innocuous 'oxide-like' cover on heats containing cerium" which would certainly confirm our observations on the presence of Ce in the liquid phase of the refractory, enhancing its mechanical break-up.

CHAPTER 5

CONCLUSIONS AND RECOMMENDATIONS

5a. The tests performed with superalloys do not simulate the initial part of the heat, in which the raw materials (less the reactive elements) are molten and carbon deoxidized. In this stage, however, the attack mechanism will be essentially the same as that of the steel tests, with the obvious differences that the amount of carbon used as deoxidant in a superalloy is much lower than that present in AISI 1095 steel, and that the processing temperatures are substantially lower for Ni-superalloys than for most steels.

Hence, the fact that melting of steel is usually observed to be more aggressive to the refractories than melting of Nickel-based superalloys can be related to the higher operating temperature and the absence of attack products at the steel/refractory interface at any time.

5b. The extremely low stability of silica in the presence of carbon in metals under vacuum or in contact with low oxygen-low silicon superalloys makes it a very poor choice as a component in any refractory for VIM applications. Unfortunately, besides its presence as an impurity in many ores used for refractory fabrication, its excellent properties for refractory production make it difficult to exclude it totally from the design of a refractory. The low stability of silica also frustrates most attempts to combine it in a lower

activity form--such as mullite--to reduce its attack by reactive elements. From these conclusions it is clear that when one selects a cement (or any refractory that will be in contact with the metal) for a VIM furnace, special attention should be given to its silica content, if the best results are to be achieved.

Although the controlling step in the corrosion of silica containing cements seems to be its transport (difusion) to the reaction interface, it is also clear, from the physical observation of the altered portion of the medium-high silica cements (5-10% SiO_2 in this context) that there is hardly any hope that steel 'wash-heats' may actually accomplish any washing, in the sense of conditioning the lining by the production of a silica-depleted, more stable layer. The removal of the binding phase results in a very fragile and porous layer, strongly adhering to the metal, that would not function properly as a lining during the charging of the next heat.

One might recommend then, that if firing heats are to be used, they should be of very low reactivity, and preferably of a Nickel-base alloy, should this be compatible with the temperatures needed for firing.

5c. The use of fluorides to promote the bonding of cement grains and their reaction with the refractory bricks did not, in any of the tests, compromise the basic grain stability. Best results are obtained by selecting fluorides of elements which form oxides that react with the basic oxide of the mortar or the brick. In some cases as shown in the

tests of CaF_2/Al_2O_3 and MgF_2/Al_2O_3 cements, the same stability of the basic alumina was observed when in contact with steel and improved stability was shown when in contact with a superalloy. The fact that the fluoride-containing mixtures react with Magnel bricks enhances their cementing properties. It is felt that the use of the $Al_2O_3/MgF_2/MgO$ composition developed in this work with a more reactive and better sized alumina powder and controlled additions of lignin sulphite to satisfy the bricklaying needs would present a definite improvement in the chemical stability of the VIM furnace linings. Also, an analogous composition, using a basic MgO grain and AlF_3 should present very promising results. As a corollary, considerable improvement can probably be achieved by substituting fluorides (AlF_3 or MgF_2) for silica in ramming mixtures such as the 60% $MgO/40\%Al_2O_3$ previously described.

5d. The physical characteristics of the refractory can have a definite influence on the kinetics of attack, as shown by the tests with fired and unfired Taylor 320 cement. This suggests that in all cases, firing to a temperature as high as possible should be attempted, before bringing a new lining or tundish in service. This will also have favourable effects on thoroughly drying the refractories. One should not expect, however, dramatic improvements in the case of materials of recognized low stability.

5e. Since the presence of comparatively high percentages of aluminum (or other elements with high affinity for oxygen) substantially lowers the activity coefficient of oxygen in a superalloy melt, the oxygen content in these alloys will be governed by the following factors:

1. Phases (and compounds) present at the metal/refractory interface
2. Time of holding in the crucible
3. Physical characteristics of the interface.

The first factor will control the equilibrium oxygen content of the alloy, by fixing the oxide activities, while the other two will determine the kinetics of the oxide dissolution process.

It follows then, that the best selection of a refractory for VIM (for both steels and superalloys) will be a mixture of oxides with as high as possible a stability with respect to carbon, high melting point and good mechanical properties. Also, aluminum is usually present in high enough quantities in superalloys to be the element that will control the oxygen potential. It is therefore desirable to have as low alumina activity as possible in the refractory in order to drive the equilibrium

$$2\underline{Al} + 3\underline{O} = Al_2O_3 \quad \text{(in the refractory)}$$

as much as possible to the right. Magnesium aluminate spinel conforms almost perfectly to this description--apart, of course, from the mechanical characteristics point of view, which is very much a function of manufacturing technique. Indeed, the best results with superalloys were obtained with refractories with high percentages of spinel.

The importance of mechanical characteristics is made apparent by comparison of the residual oxygen values obtained with Taylor 341 and Alundum 1139 in the superalloy tests.

Although the former contains some more lower stability oxides, the fact that a dense complex $(Al_xCr_yTi_z)O_w$ layer is formed, allows the achievement of very good results. In the case of Coralbond, however, the considerably higher content of lower stability oxides, especially silica, hinders the possibility of achieving a low oxygen content.

5f. The use of slags or lime additions to the melt in VIM will, in almost any case, promote erosion and degeneration of the lining, producing inclusions in the melt. In addition, even the bricks presently used in VIM, when kept in contact with the alloys in question will introduce inclusions into the melt.

In order to achieve de-S, it seems that either new techniques will be introduced and accepted by the users--as Rare Earth treatments--or that less orthodox treatments, with lime mixtures such as the one described by Volkov (61) will have to be used. It is evident that the use of lime refractories would be ideal under vacuum melting conditions, since their main metallurgical limitation--inability to resist FeO fluxing--is removed under vacuum. However, the hydration problems have yet to be circumvented and it seems that some time will pass before they will be used in any industrial VIM furnace on a regular basis. It is especially interesting to note that the use of calcium fluoride may present many advantages in the production of lime refractories, acting as a sintering and binding agent and improving the hydration resistance, as noticed by Schlegel (78).

Even though the chemical upgrading of the presently used refractory bricks would be possible--by the use of lower ($CaO + SiO_2$)periclase or fused MgO grains instead of the presently used periclase, for instance--one would still be likely to find eroded grains and inclusions in the metal.

It seems then that, as far as inclusions are concerned, the main emphasis should be placed on pouring facilities, i.e., the correct selection of pouring temperatures, tundish design and construction, time in the ladle. The possibility of pouring through a low-melting fused slag should also be studied.

BIBLIOGRAPHY

BIBLIOGRAPHY

(1) Bonar, K.M., Cunningham, J.L. and Walther F.H., Cer. Bull., 46, No.7, (1967), 683

(2) "BOF Steelmaking", vol.2, Pehlke, R.D. et al. (eds.), TMS-AIME, New York, 1975

(3) Sigworth, G.K., et al., Trans. Met. Soc. of C.I.M., Annual Volume, (1977), 104

(4) Yavoyskiy, V.I., et al., Rus. Metall., No.2. (1974), 10

(5) Winkler, O., Metallurgical Reviews, 5, No.17, (1960), 1

(6) Bennett, G.H.J., Protheroe, H.T., and Ward, R.G., J.I.S.I., 195, (1960), 174

(7) Moore, J.H., Metal Progress, 64, No.4, (1953), 103

(8) Öberg, K.E., et al., Jernkont. Ann., 155, No.6, (1971), 251

(9) Machlin, E.S., Trans.Met.Soc. AIME, 218, (1960), 314

(10) Schaffer, P.S., in "Trans.Vac.Met.Conf. 1960", Bunshah, R.F. (ed.), Interscience Publ., New York, (1960), 151.

(11) Turillon, P., Mem.Sci.Rev.Metall., 57, No. 9, (1960), 649

(12) Darken, L.S., in "Basic Open Hearth Steelmaking", Derge, G. (ed.), TMS-AIME, New York, 3rd Edition, (1964), 608

(13) Kraus, T., in "Trans.Vac.Met.Conf. 1963", Bunshah, R.F. (ed.), AVS, Boston, (1964), 50.

(14) Kinsman, G.J.M, Hazeldean, G.S.F., and Davies, M.W., J.I.S.I., 207, (1969), 1463.

(15) Beteridge, W. and Heslop, J., "The Nimonic Alloys", Crane Russak & Co., New York, 2nd Edition, (1974).

(16) Ritter, J.E. and Burton, M.S., Trans.Met.Soc. AIME, 239, (1967), 21.

(17) Armstrong, W.M., Chacklader, A.C.D. and Clarke, J.F., J.Amer.Cer.Soc., 45, No. 3, (1962), 115

(18) Champion, J.A., Keene, B.J. and Allen S., J. of Mater. Sci., 8, (1973), 423

(19) Sutton, W.H., in "Proc. of the Fifth Int. Symp. on Electroslag and Other Special Melting Technologies", Part II, Bhat, G.K. and Simkovich, A. (eds.), ASM-AVS, Pittsburgh, (1974), 648.

(20) Snape, E., Ph.D. Thesis, University of Leeds (1965).

(21) Gupta, R.D., Mathur, N.N. and Rao, M.R.K., Steel Furnace Monthly, 9, No.2, (1974), 171

(22) Kamamura, M., et al., Tetsu-to-Hagané, 62, No.14, (1976), 1823

(23) Winkler, O., in "Vacuum Metallurgy", Winkler, O. and Bakish, R., (eds.), Elsevier Publ. Co., Amsterdam, (1971), 1.

(24) Graham, S.W., and Argent, B.B., J.I.S.I., 205 (1967), 1066.

(25) Hunter, C.W. and Tarby, S.K., in "Trans.Vac.Met.Conf. 1968", Barrow, R.B. and Simkovich, A. (eds.), AVS, New York, (1968), 355.

(26) Decker, R.F., Rowe, J.P. and Freeman, J.W., Trans.Met. Soc. AIME, 212, (1958), 686

(27) Turillon, P., Mem.Sci.Rev.Metall., 57, No.9, (1960), 658

(28) Simkovich, A., in "Trans.Vac.Met.Conf.1967", Foster, E.L., (ed.). AVS, New York, (1967), 361

(29) Renkey, A.L. and McWalter, H.G., J. of Metals, 17, (1965), 678

(30) Schlatter, R. and Simkovich, A., in "Trans.Vac.Met. Conf.1966", Orehoski, M.A. and Bunshah, R.F., (eds.), AVS, Boston, (1966), 338.

(31) Schlatter, R., in "Trans.Vac.Met.Conf. 1968", Barrow, R.B., and Simkovich, A., (eds.), AVS, New York, (1968), 333.

(32) McIntire, H.O., Foundry Trade J., 103, No.2143, (1957), 543.

(33) Leinbach, Jr., R.C. and Hamjian, H.J., J. of Metals, 18, (1966), 219.

(34) Pagiev, S.S., Belous, V.V. and Nam, B.P., Sov.J.of Non-Ferrous Met., 11, No. 7, (1970), 62.

(35) Strushchenko, P.V., et al., Steel in the USSR, 7, (1977), 221.

(36) Khudozhnik, O.A. and Krapivner, L.L., Sov.J. of Non-Ferrous Met., 11, No.1, (1970), 73.

(37) Gard, M., Josso, E. and Migaud, B., Met.Constr.Mec., 100, No.3, (1968), 165

(38) Cameron Iron Works, private communication

(39) Yamanishi, H. and Ishikawa, E., Tetsu-to-Hagané, 63, No. 13, (1977), 2134

(40) Spendelow, Jr., H.R., Servi, I.S. and Fritzlen, G.A., in "1954 Vac.Met.Symp.", The Electrochemical Society, Boston, (1955), 24.

(41) Baraclough, K.C. and Thompson, C., in "Measurement and Control in the Melt Shop--The Proc. of SIMAC 72 Conf.", Sheffield, (1973), 2/1.

(42) Dyrkacz, W.W., J. of Metals, 9, (1957), 1513

(43) Hudson, B.P., in "Trans.Vac.Met.Conf. 1963", Bunshah, R.F., (ed.), AVS, Boston, (1964), 103.

(44) Child, H.C. and Harris, G.T., J.I.S.I., 190, (1958), 414

(45) Richardson, B.F., in "Quality Requirements of Superduty Steels", vol.3, Lindsay, R.W. (ed.), Interscience Publ., New York, (1959), 285

(46) Ward, R.G., in "Aspects of Modern Ferrous Metallurgy", Kirkaldy, J.S.,(ed.), Univ. of Toronto Press, Toronto, (1964), 215.

(47) Bonchack, J., private communication

(48) Langworthy, D.E., in "Vacuum Metallurgy", (Proc.Vac. Met.Conf. 1977), Krutenat, R.C. (ed.), Science Press, Princeton, (1977), 1.

(49) Kawai, S., Tetsu-to-Hagané, 63, No. 13, (1977), 1975

(50) Magoteaux, O.R., Ind.Heat., 36, No. 9, (1969), 1794, 1796, 1806

(51) Child, H.C. and Oldfield, G.E., in "Vacuum Metallurgy", Winkler, O. and Bakish R., (eds.), Elsevier Publ. Co., Amsterdam, (1971), 517.

(52) Chester, J.H., Trans.Bri.Cer.Soc., 48 (1949), 263

(53) Schlatter, R., private communication

(54) Floridis, T.P., Trans.Met.Soc. AIME, 215, (1959), 870

(55) Ward, R.G., and Hall, R., J.I.S.I., 195, (1960), 75

(56) Coate, D.W., in "Proc. of the Third Int. Symp. on Electroslag and Other Special Melting Technologies", Part III, Bhat, G.K. and Simkovich, A., (eds.), ASM-AVS, Pittsburgh, (1971), 31

(57) Tezuka, H., et al., in "Proc. Fourth Int. Conf. on Vac. Met.", I.S.I.J., Tokyo, (1974), 142

(58) Afanasyev, Yu.M., et al., Rus. Metall., No.3, (1963), 41

(59) Polyakov, A.Yu., et al., Akad.Nauk. SSSR, Izv. Met.i Gornoe Delo, No.3, (1964), 37

(60) Linchevskiy, B.V., ibid., No. 2, (1963), 25

(61) Volkov, S.Ye., et al., Rus. Metall., No.4, (1964), 24

(62) Schlatter, R., et al., U.S. Pat. 3,853,540; Dec.10, 1974.

(63) Cremisio, R.S., Cannon, J.G. and Elliot, C.F., in "Proc. of the Third Int. Symp. on Electroslag and Other Special Melting Technologies", Part III, Bhat, G.K. and Simkovich, A. (eds.), ASM-AVS, Pittsburgh, (1971), 1

(64) Bailey, R.E., Shiring, R.R. and Anderson, R.J., in "Superalloys: Metallurgy and Manufacture, Proc. of the Third Int. Symp., 1976", Kear, B.H., et al. (eds.), Claitor Publ. Co., Baton Rouge, (1976), 109

(65) Rothman, M.F., in "Vacuum Metallurgy", (Proc.Vac.Met. Conf. 1977), Krutenat, R.C. (ed.), Science Press, Princeton, (1977), 49

(66) Ashley, W.E., private communication

(67) Armstrong, W.M., Chacklader, A.C.D. and Rose, D.J., Trans. Met. Soc. AIME, 227, (1963), 1109

(68) Rosenqvist, T., "Principles of Extractive Metallurgy", McGraw-Hill, New York, (1974)

(69) Butt, Yu.M., Timashev, V.V. and Sulimenko, L.M., Izv. Akad. Nauk. SSSR., Neorg. Mat., 5, No.6, (1969), 1116

(70) Pirogov, A.A., et al. Refractories (Ogneupory) No.1, (1970), 39

(71) O'Hara, M.H., Duga, J.J. and Sheets, Jr., H.D., Cer. Bull., 51, No. 7, (1972), 590

(72) Khoroshavin, L.B., Dolgikh, G.V. and V.M. Ustyantsev, Refractories (Ogneupory), No.8, (1970), 509

(73) Mass, V.H. and Abratis, H., Archiv für das Eisenhüttenwesen, 40, (1969), 153

(74) Sveshkov, Yu.V., Kalmikov, V.A. and Ageyev, P.Ya., Rus. Metall., No.4, (1972), 29

(75) Kulikov, I.S., "Deoxidation of Metals", Metallurgya, Moscow, (1975)

(76) Kappmeyer, K.K. and Hubble, D.H., in "High Temperature Oxides", part I, Alper, A.M., (ed.), Academic Press, New York, (1970), 2.

(77) White, J., ibid, 77

(78) Schlegel, E., East Ger. Patent 59,500, Jun 25, 1966

FIGURES

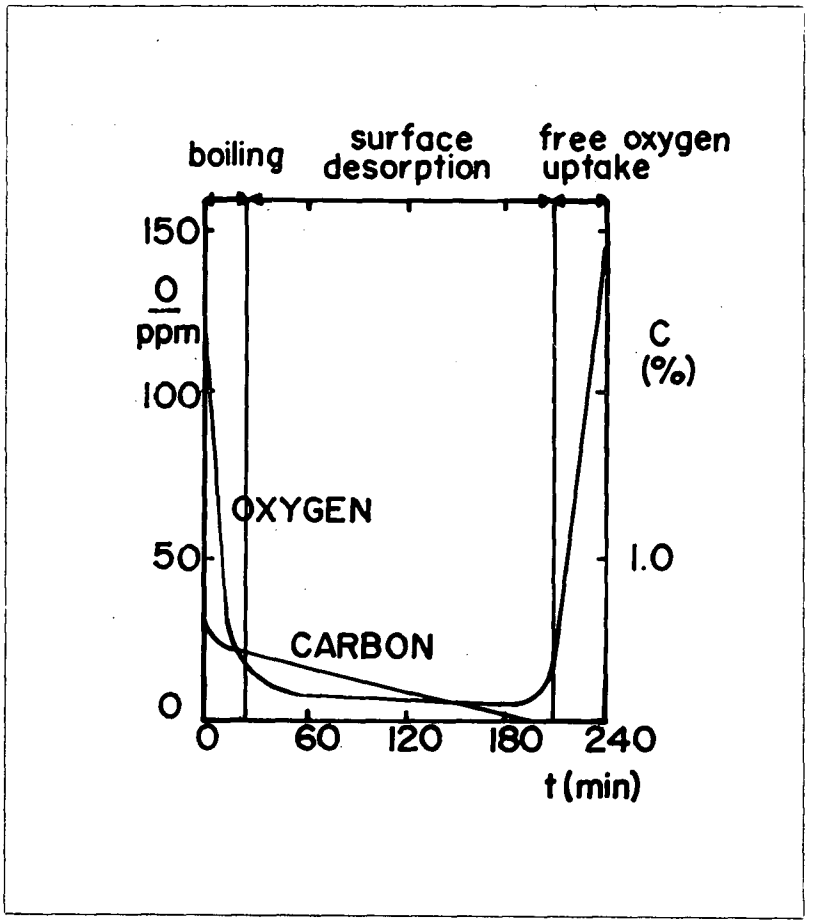

Fig. 1 Theoretical deoxidation diagram (8).

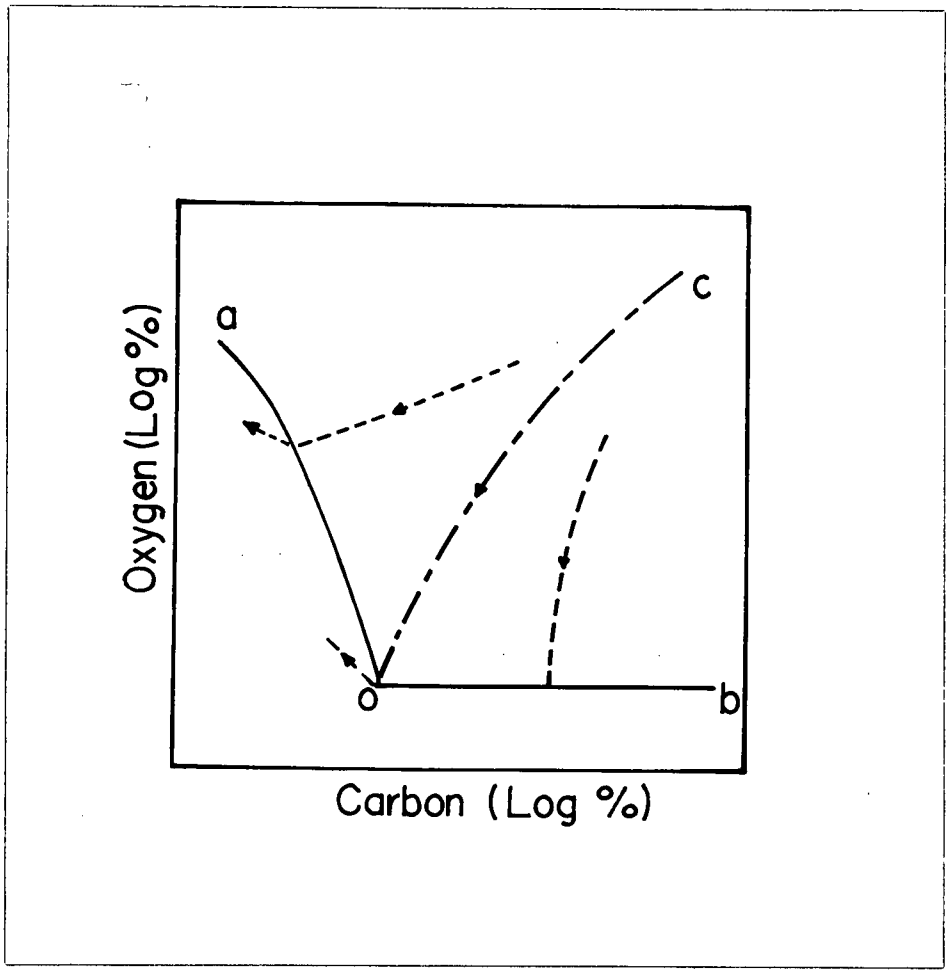

Fig. 2 Deoxidation Curves (11)

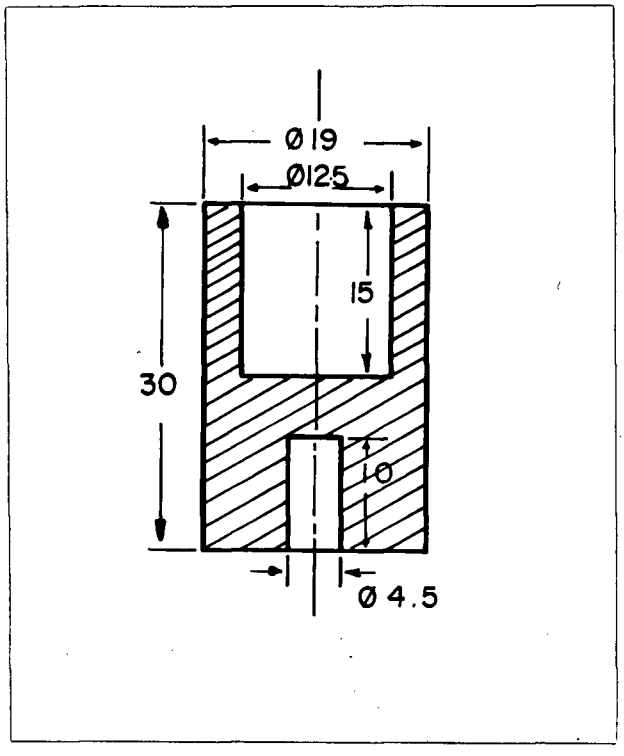

Fig. 3 Dimensions of the crucibles used in the tests (mm).

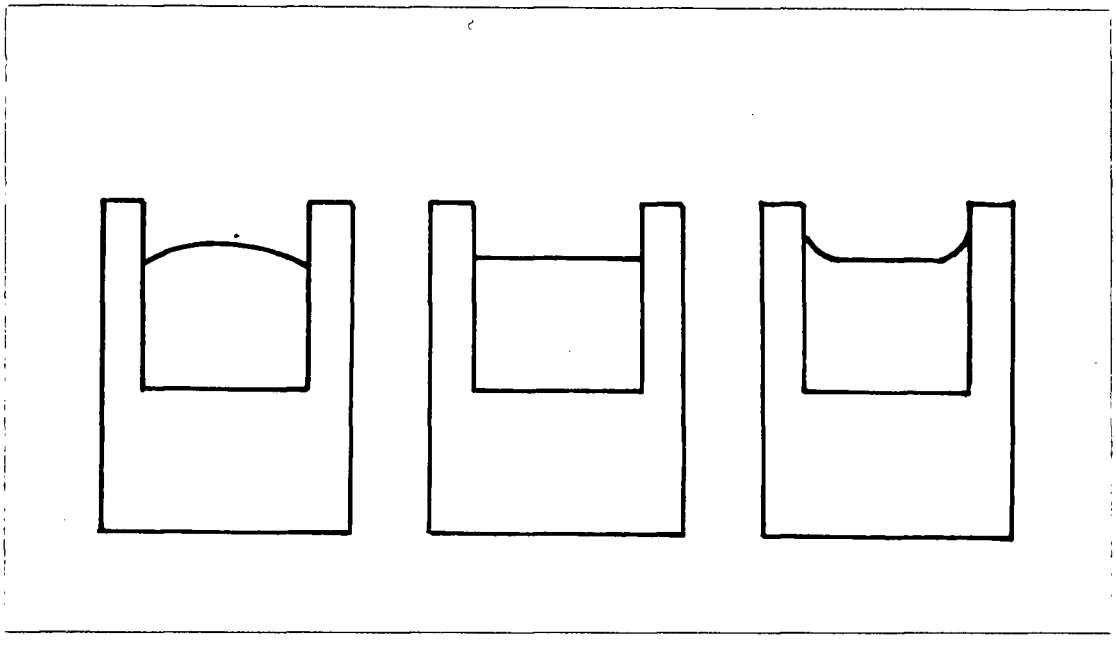

Fig. 4 Different wetting behaviours

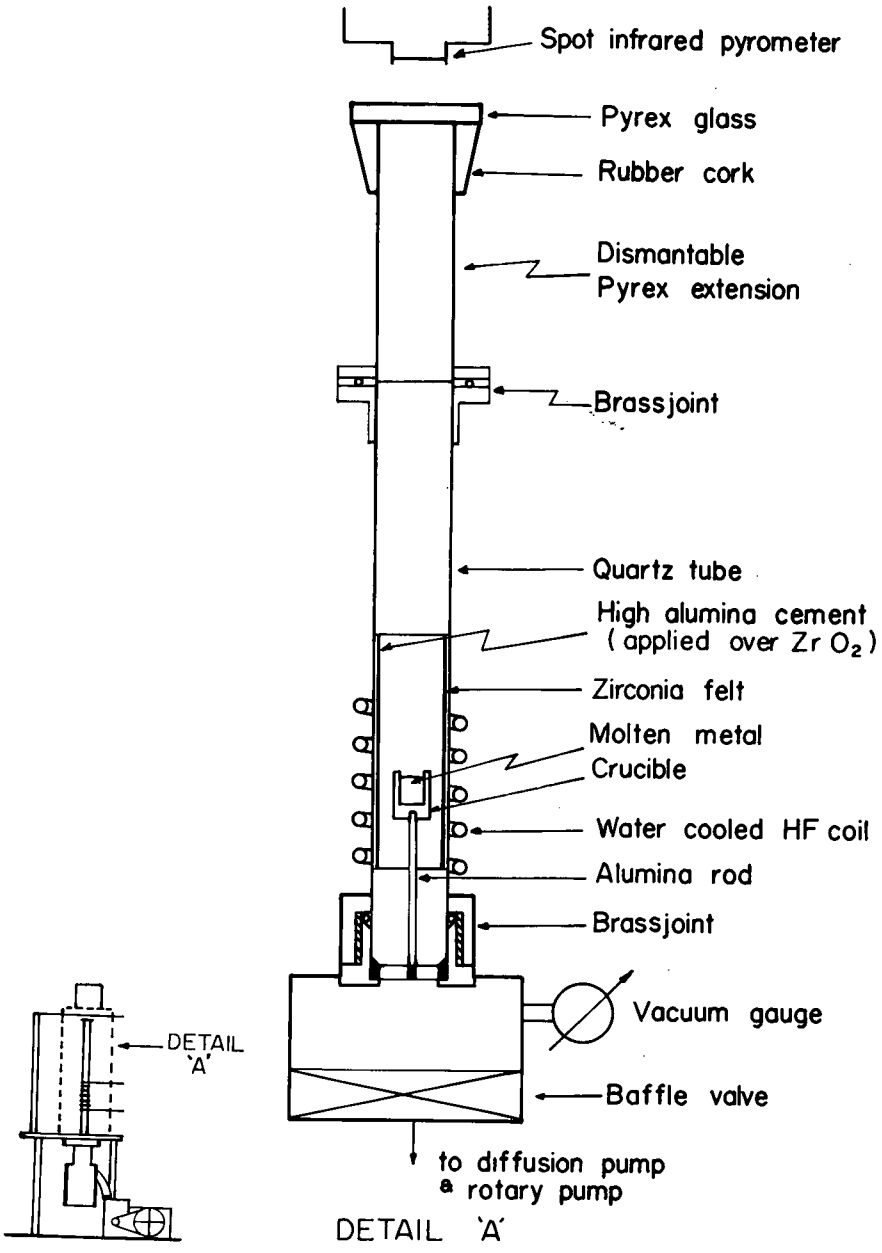

Fig. 5 Experimental Apparatus

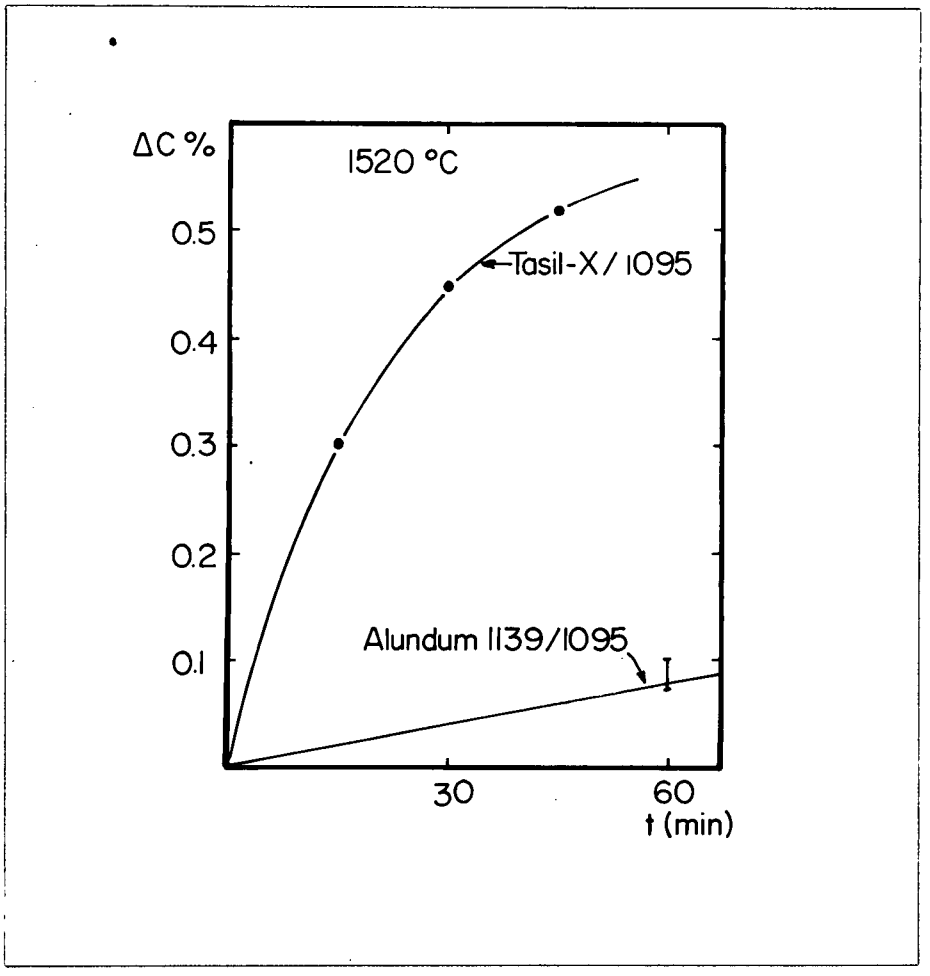

Fig. 6 Variation in carbon content of AISI 1095 steel melted in Tasil-X crucibles

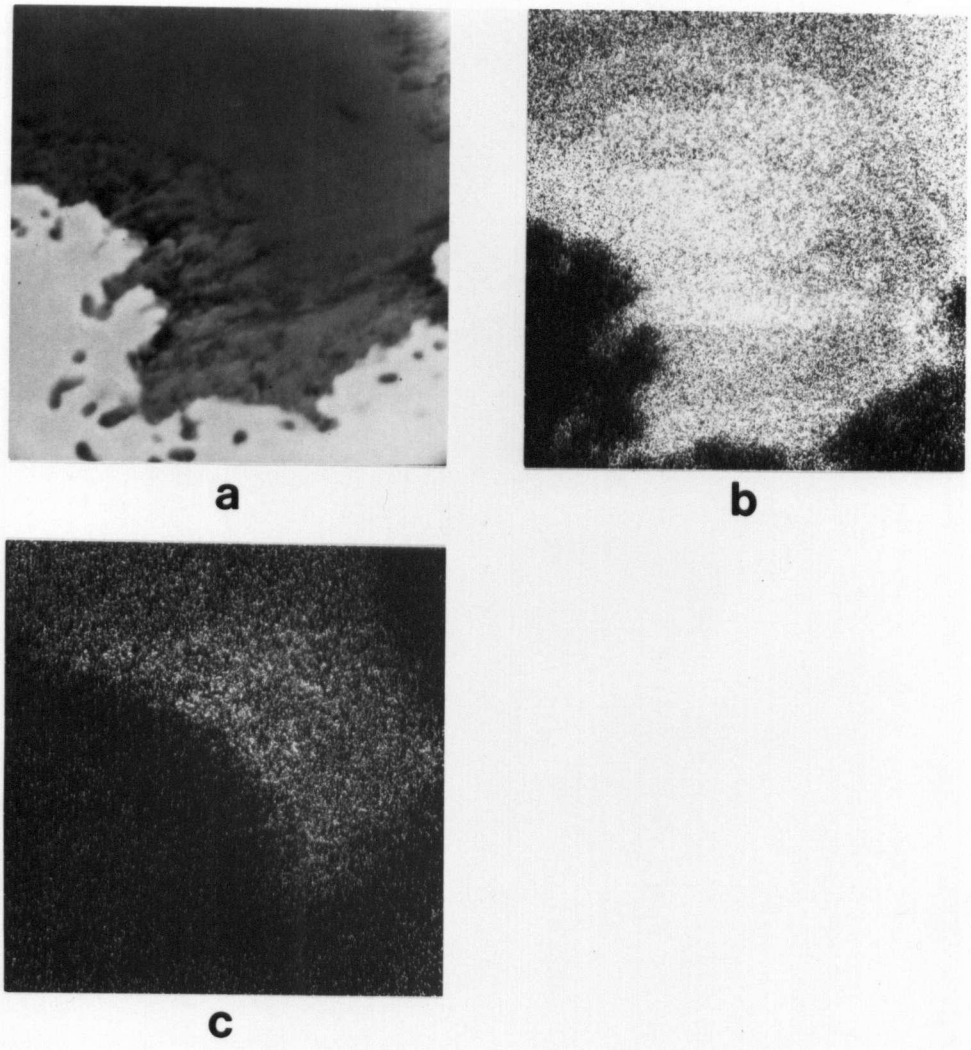

Fig. 7 Interface AISI 1095/Tasil-X. X2400

a) Secondary Electrons
b) Aluminum X-Ray map
c) Silicon X-Ray map

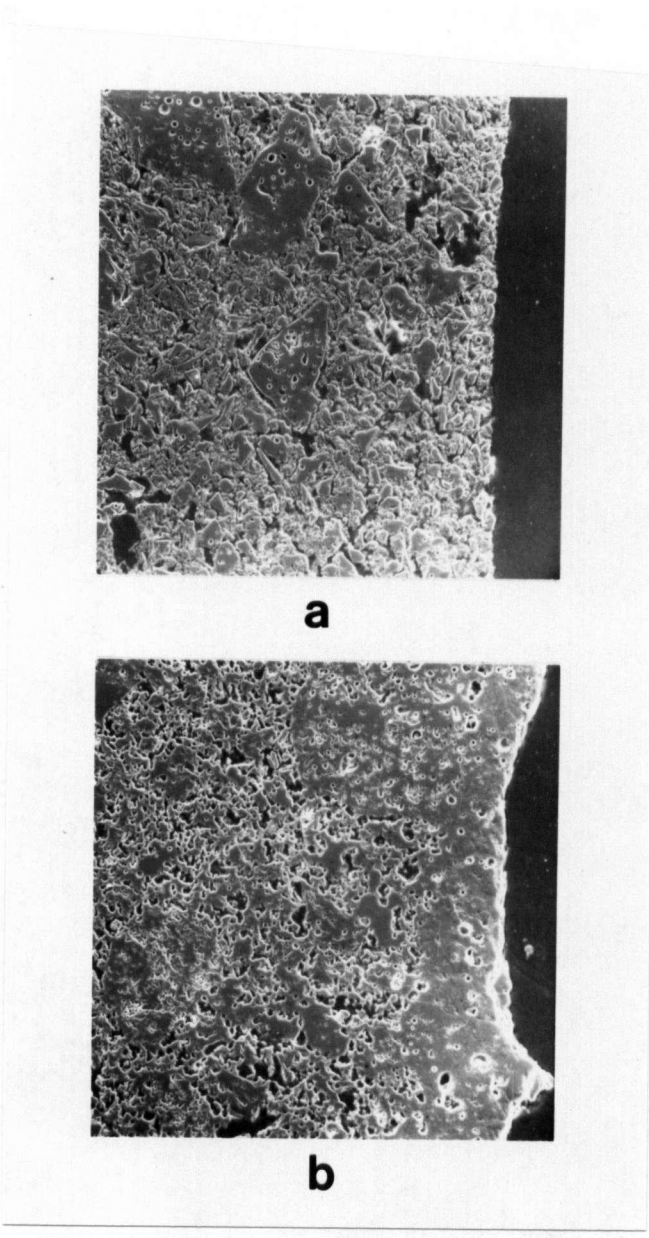

Fig. 8 Microstructure of Taylor 320. X120, Secondary Electrons

a) Dried at 600°C
b) Fired at 1000°C

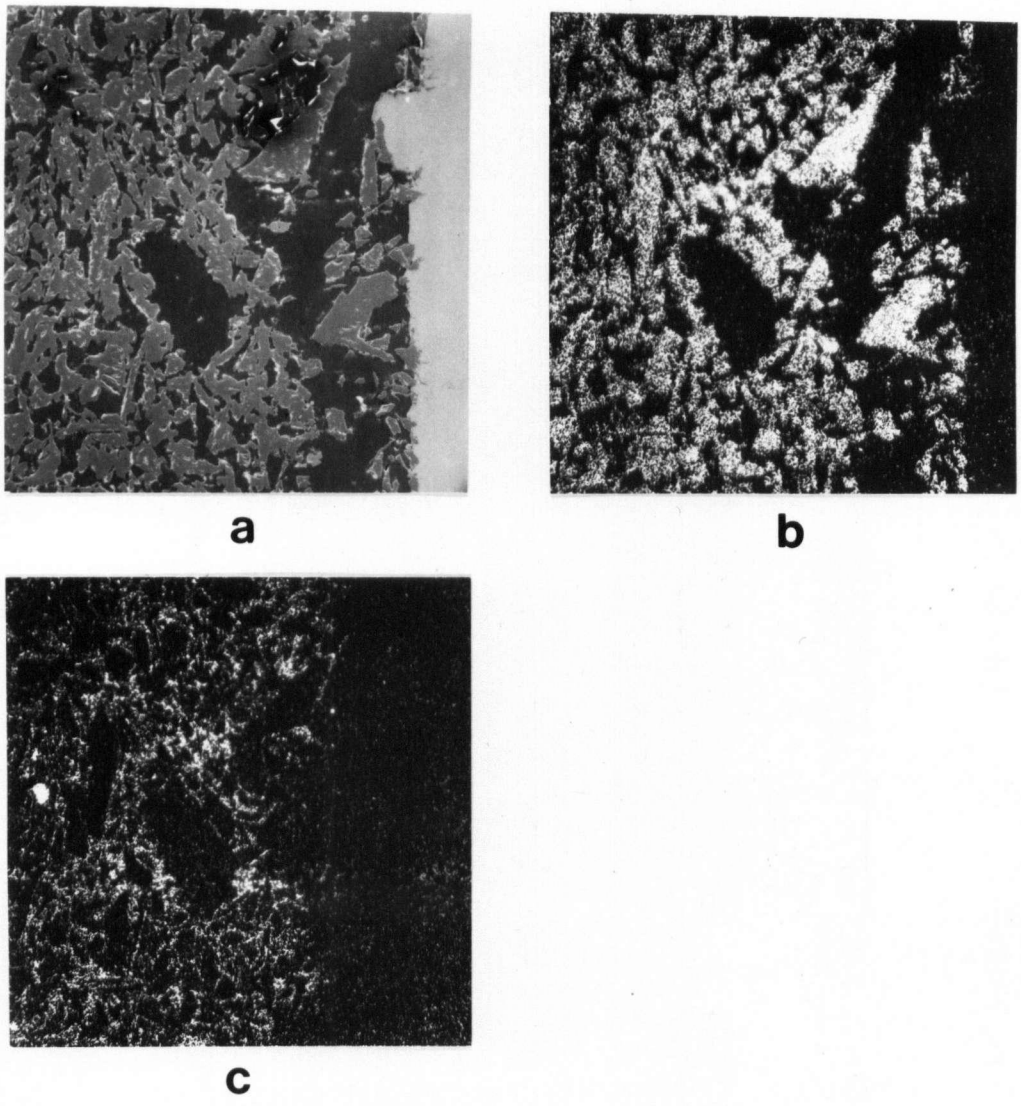

Fig. 9 Interface AISI 1095/Alundum 1162. Melt time 5 min. x48

a) Secondary Electrons
b) Aluminum X-Ray map
c) Silicon X-Ray map

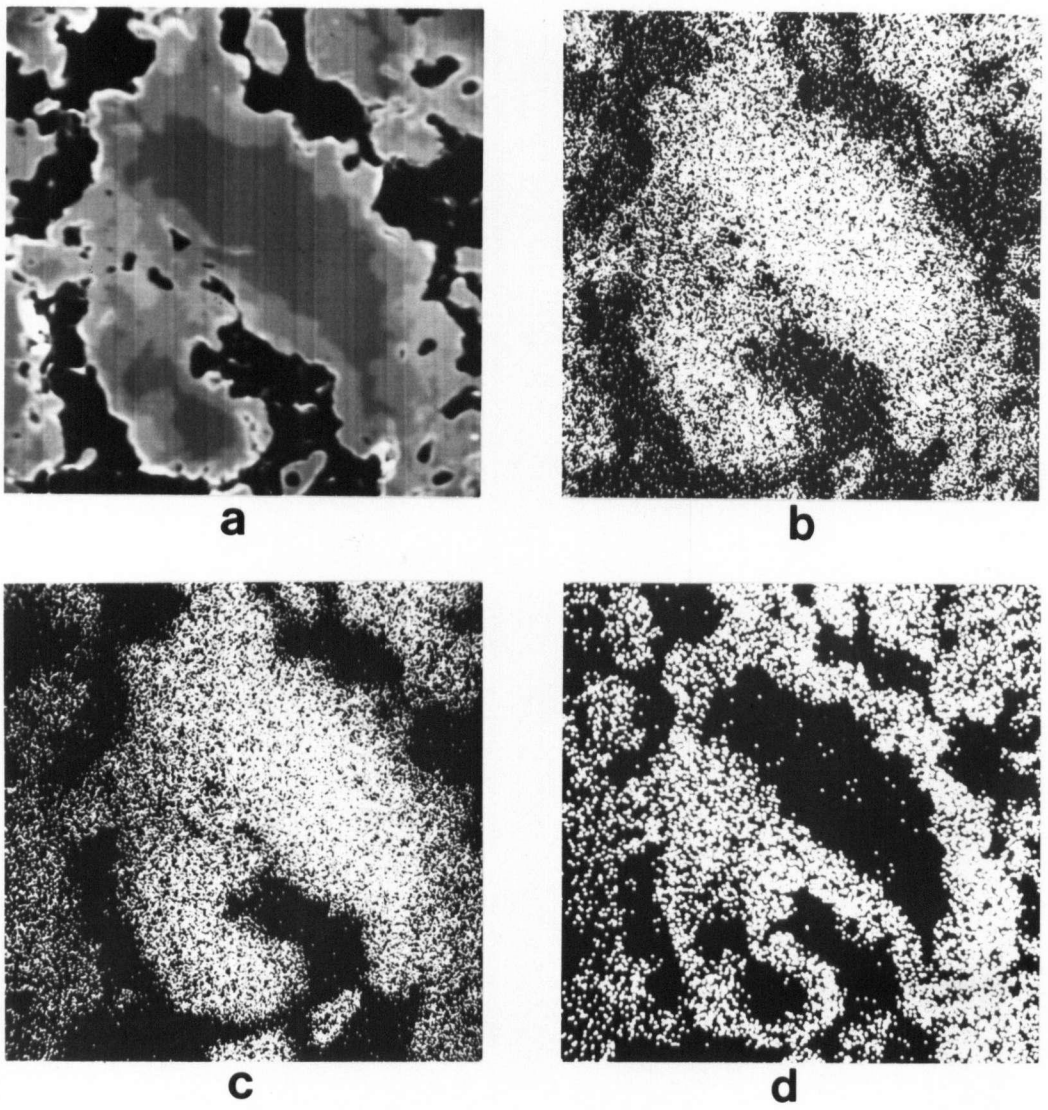

Fig. 10 Typical microstructure of a cement made from Al_2O_3 and CaF_2 (CAF). X300.

a) Backscattered Electrons
b) Oxygen X-Ray map
c) Aluminum X-Ray map
d) Calcium X-Ray map

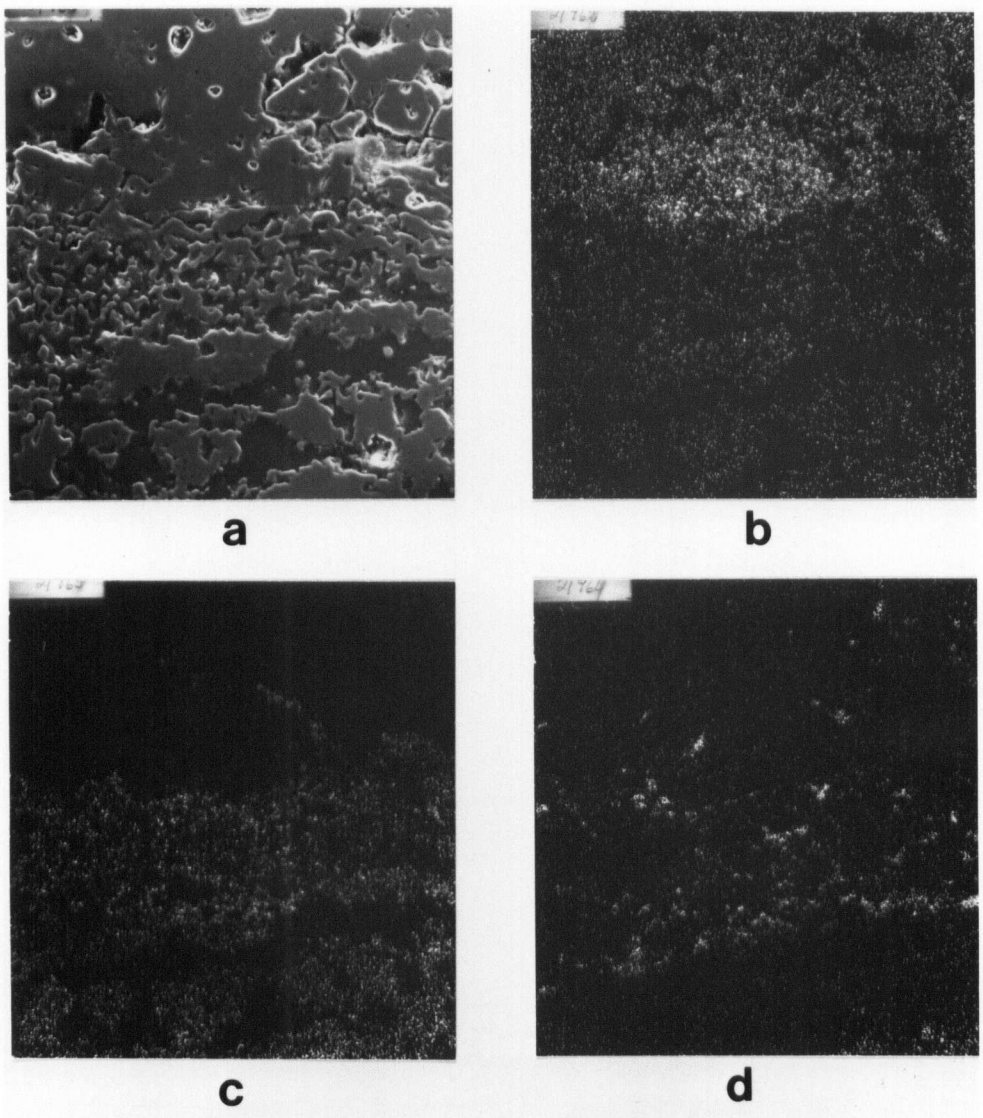

Fig. 11 Adherence test. Interface Magnel/CAF. X240

a) Secondary Electrons
b) Magnesium X-Ray map
c) Aluminum X-Ray map
d) Calcium X-Ray map

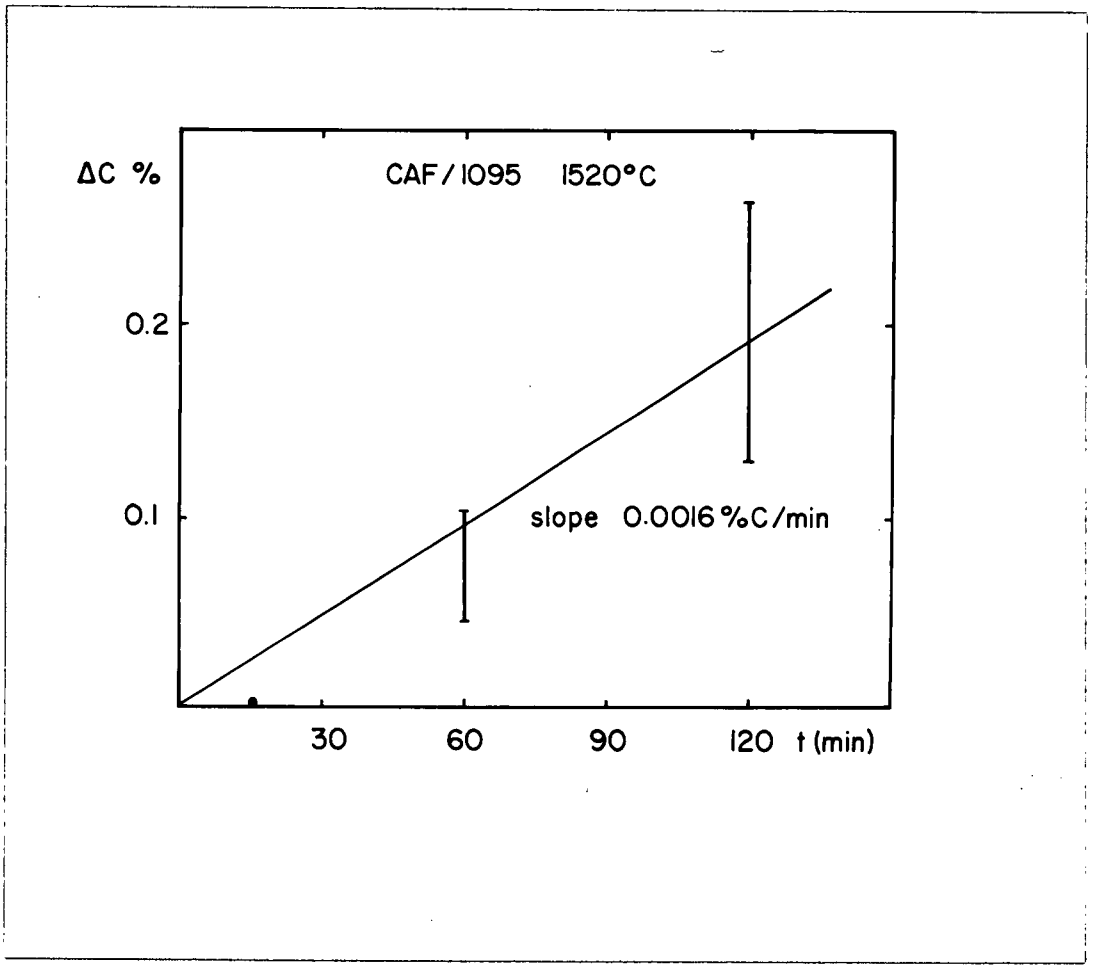

Fig. 12 Variation in carbon content of AISI 1095 steel melted in CAF crucibles

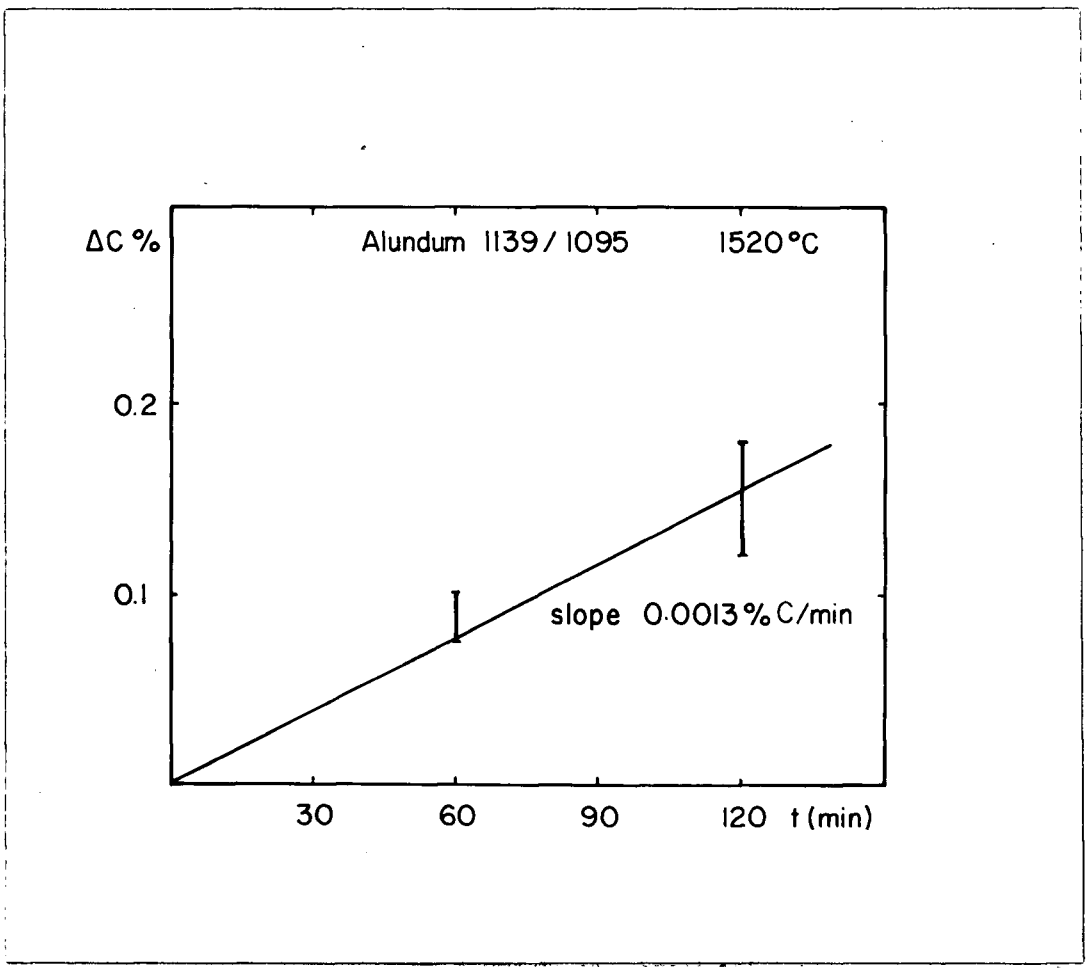

Fig. 13 Variation in carbon content of AISI 1095 steel melted in Alundum 1139 crucibles

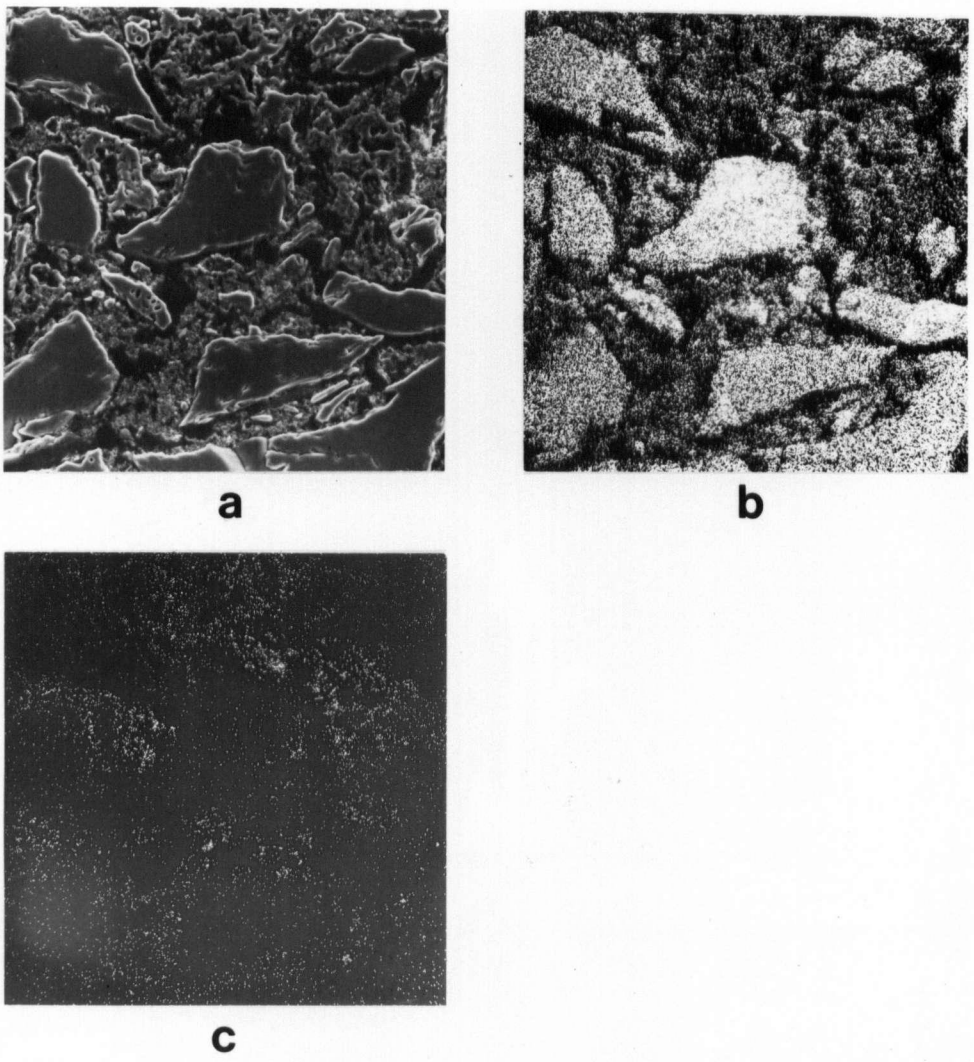

Fig.14 Typical microstructure of a cement made from Al_2O_3 and MgF_2 (SP2). X240

a) Secondary Electrons
b) Aluminum X-Ray map
c) Magnesium X-Ray map

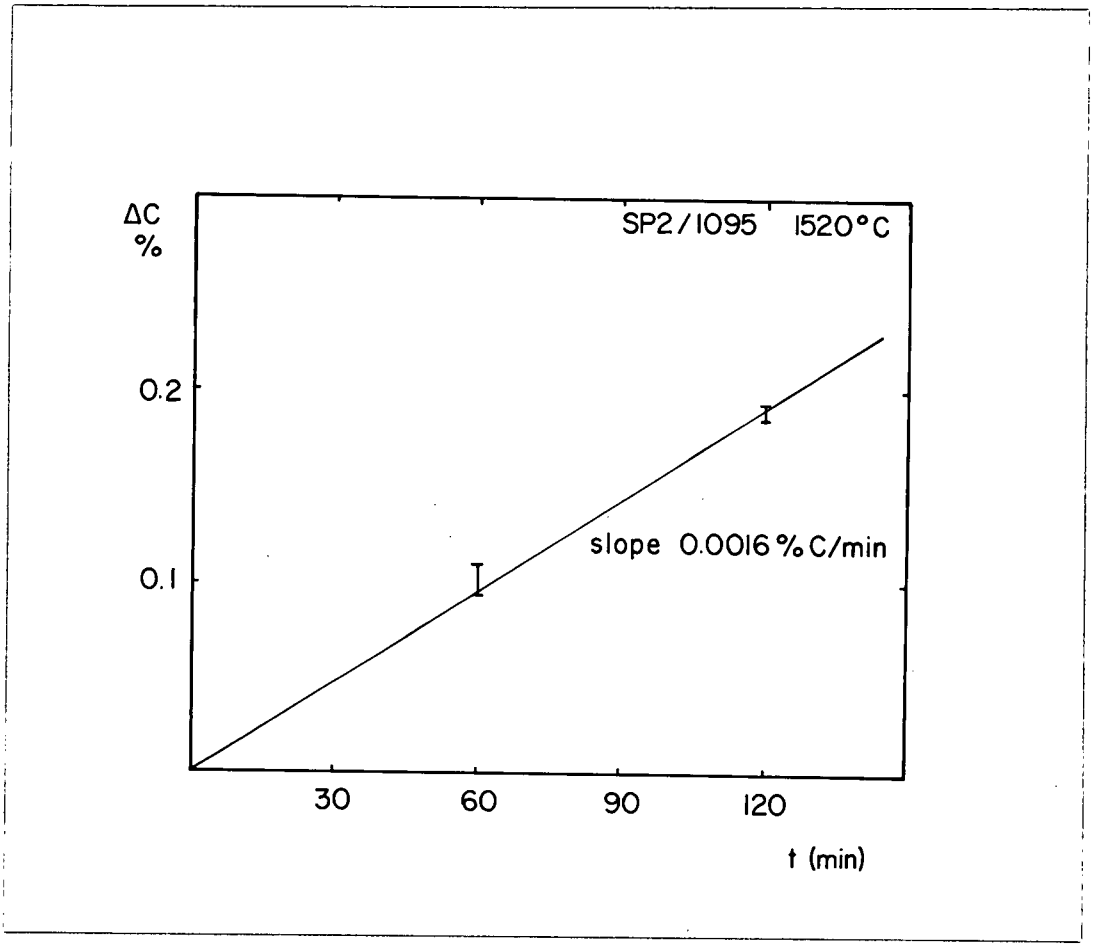

Fig. 15 Variation in carbon content of AISI 1095 steel melted in SP2 crucibles

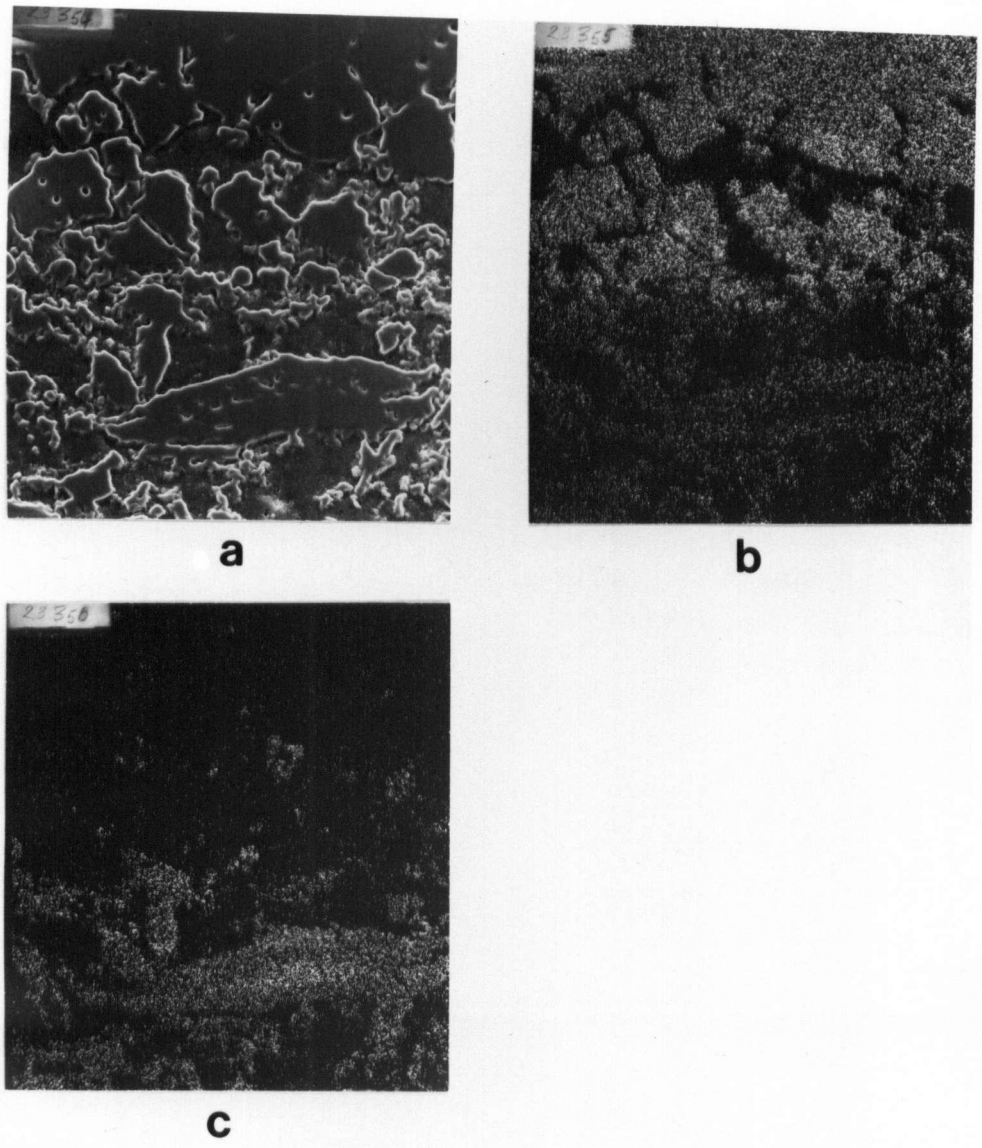

Fig. 16 Adherence test. Interface Magnel/SP2 X240

a) Secondary Electrons
b) Magnesium X-Ray map
c) Aluminum X-Ray map

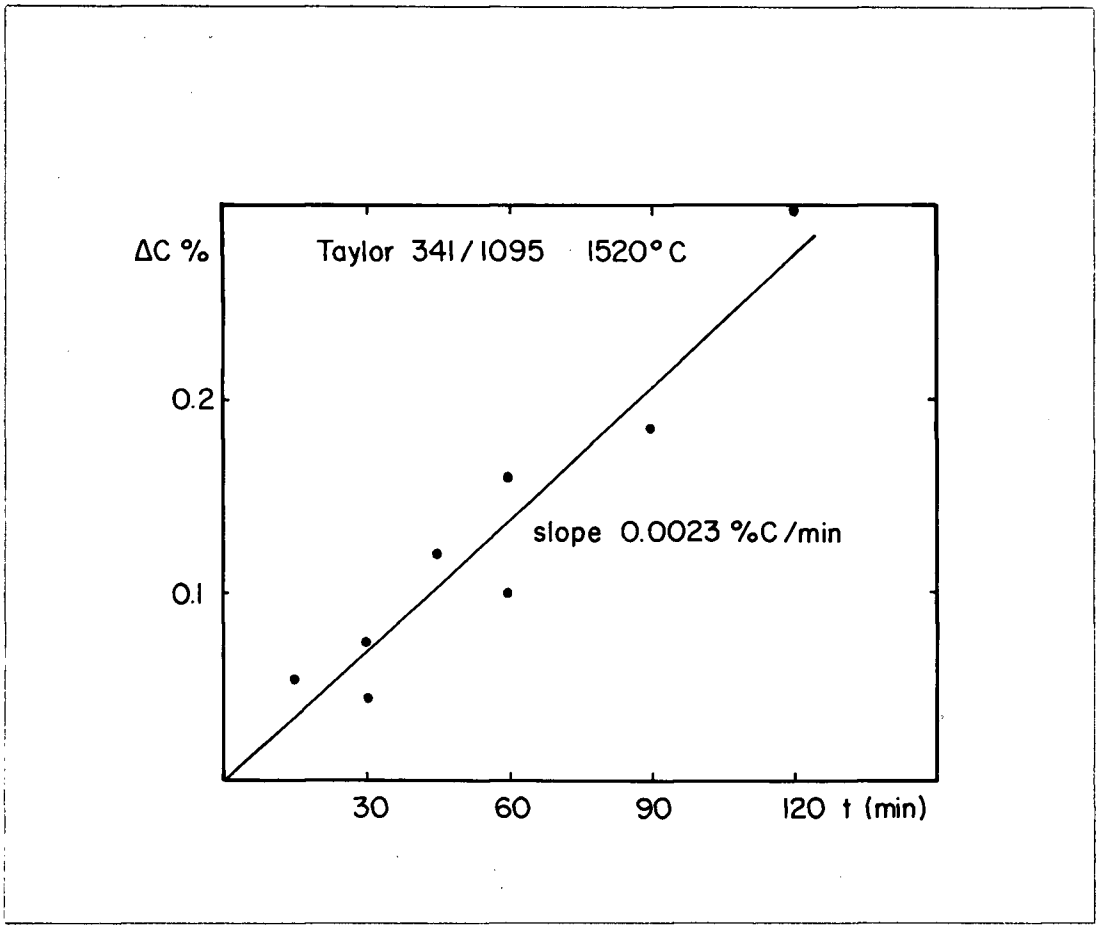

Fig. 17 Variation in carbon content of AISI 1095 steel melted in Taylor 341 crucibles

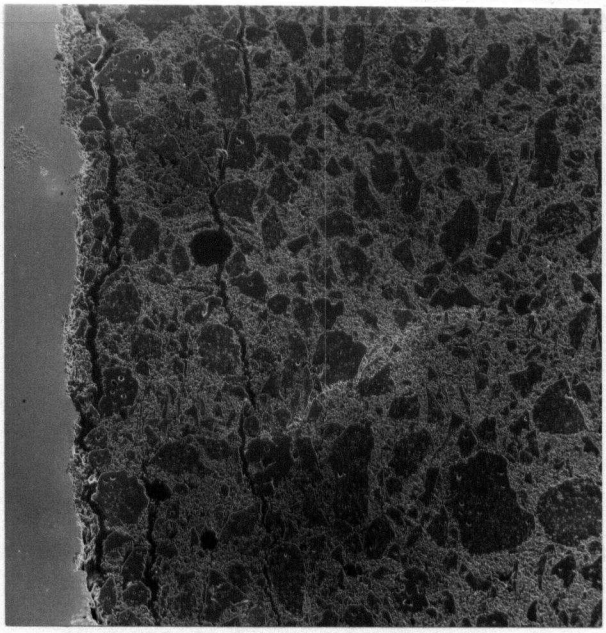

Fig. 18 Interface AISI 1095/Taylor 341. Melt time 15 min. X 40, Secondary Electrons

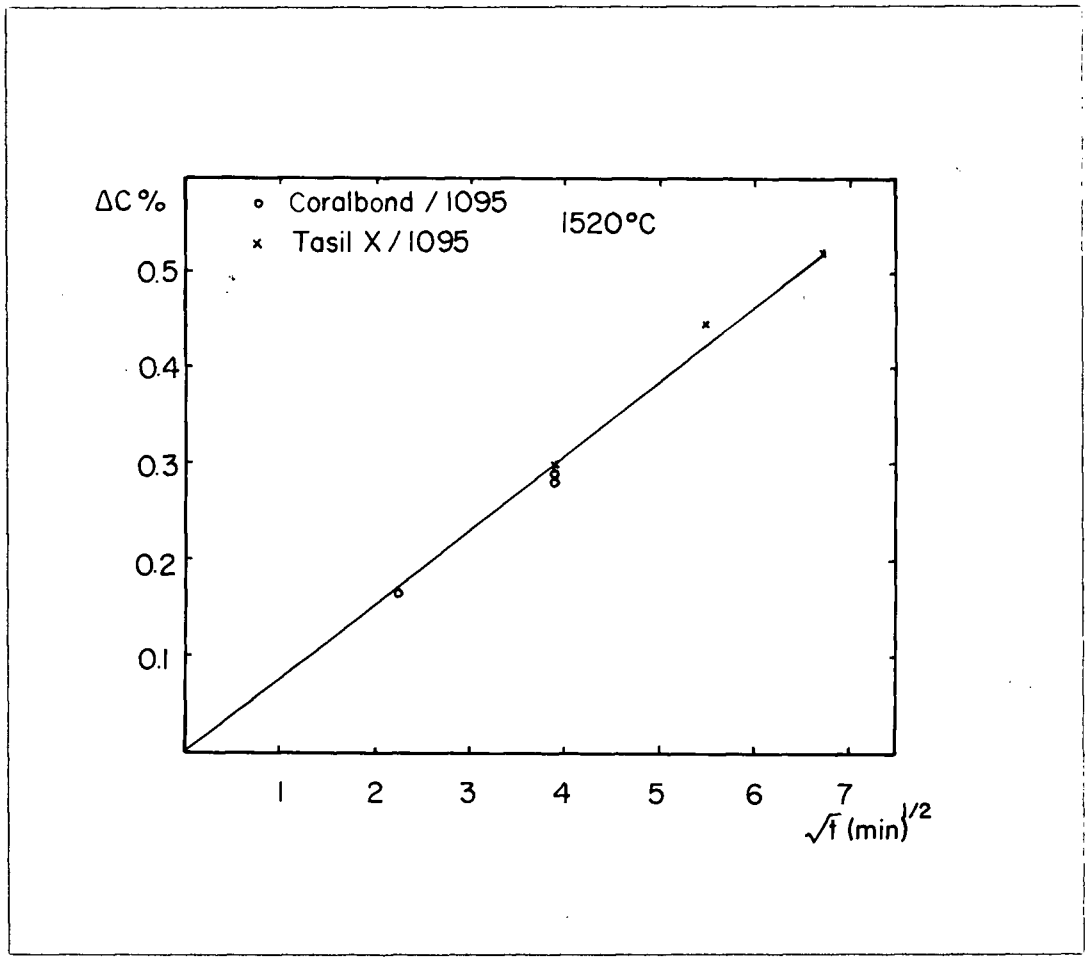

Fig. 19 Variation in carbon content of AISI 1095 steel melted in Coralbond or Tasil-X crucible, as a function of $t^{1/2}$

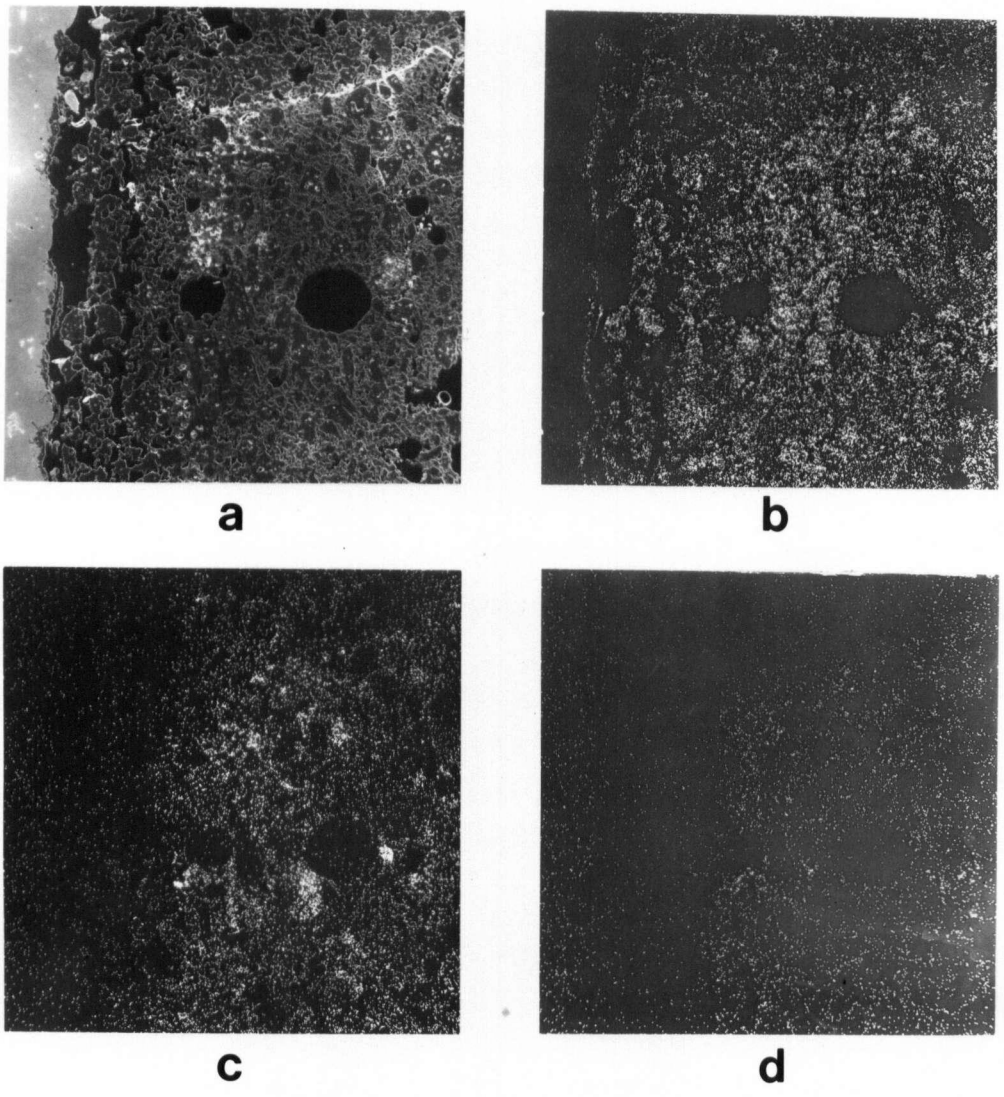

Fig. 20 Interface AISI 1095/Coralbond. Melt time 15 min. X24

a) Secondary Electrons
b) Aluminum X-Ray map
c) Silicon X-Ray map
d) Phosphorous X-Ray map

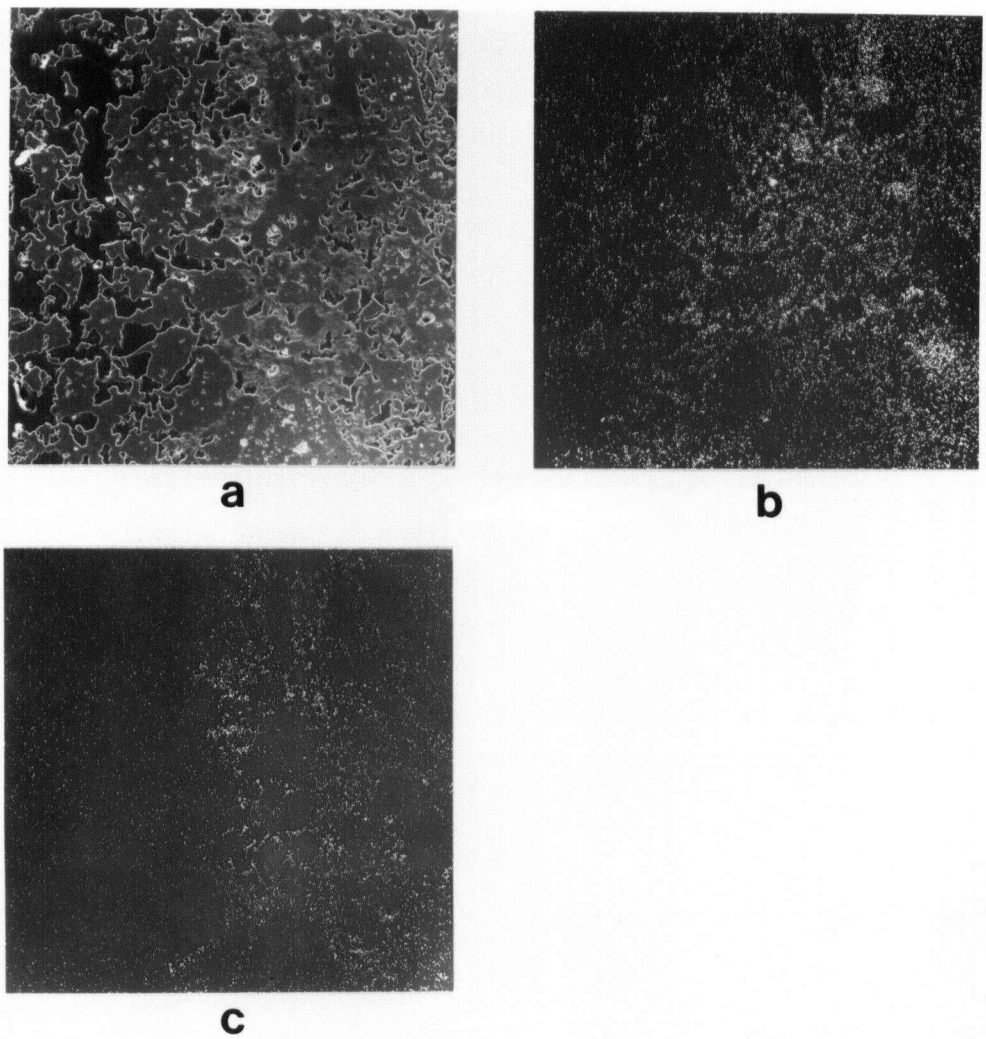

Fig. 21 Detail of altered Coralbond (Fig.20). X60

a) Secondary Electrons
b) Silicon X-Ray map
c) Phosphorous X-Ray map

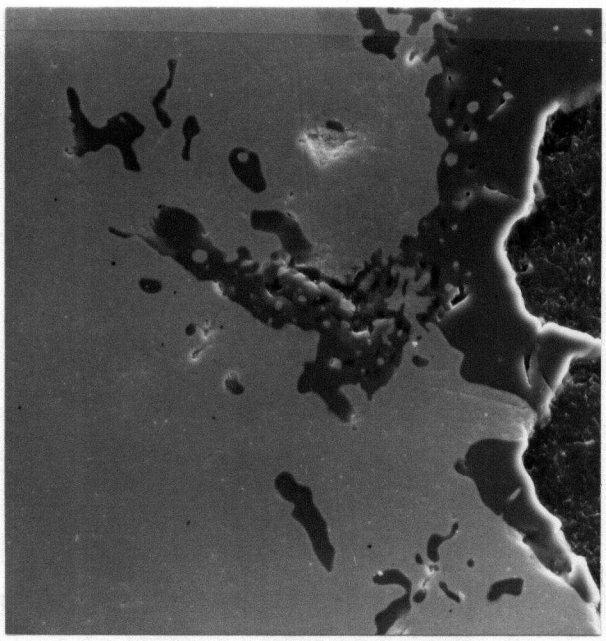

Fig. 22 Alumina inclusions from Coralbond. Interface AISI 1095/Coralbond. X1000, Secondary Electrons

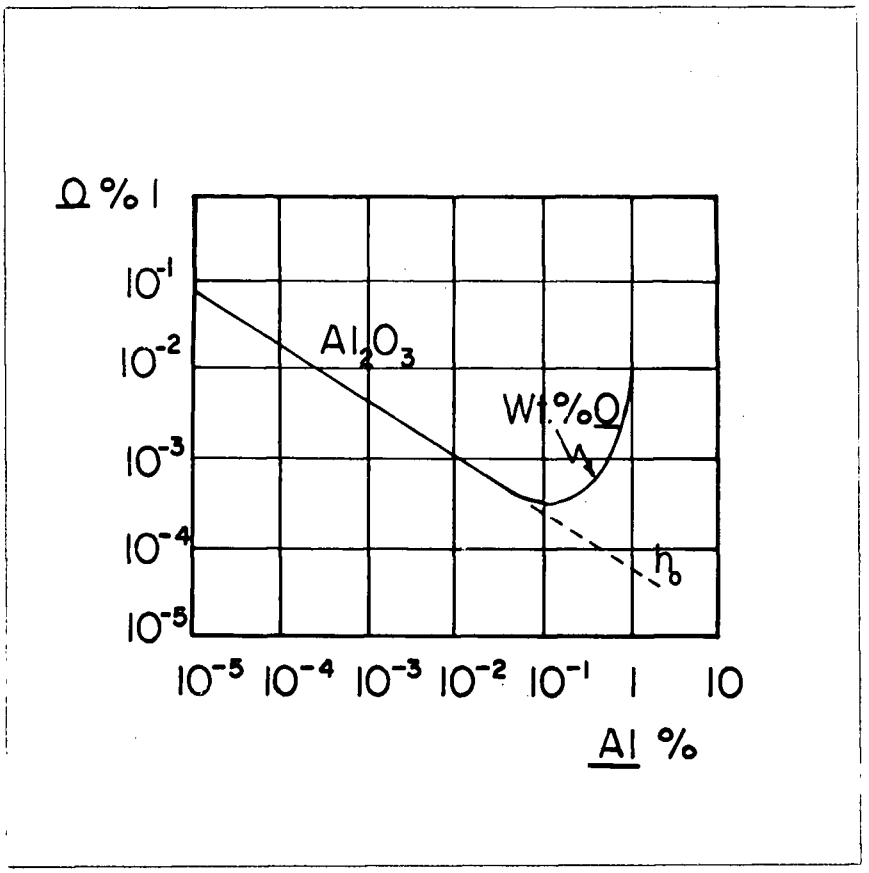

Fig. 23 Equilibrium $Al_2O_3 = 2\underline{Al} + 3\underline{O}$, in Nickel

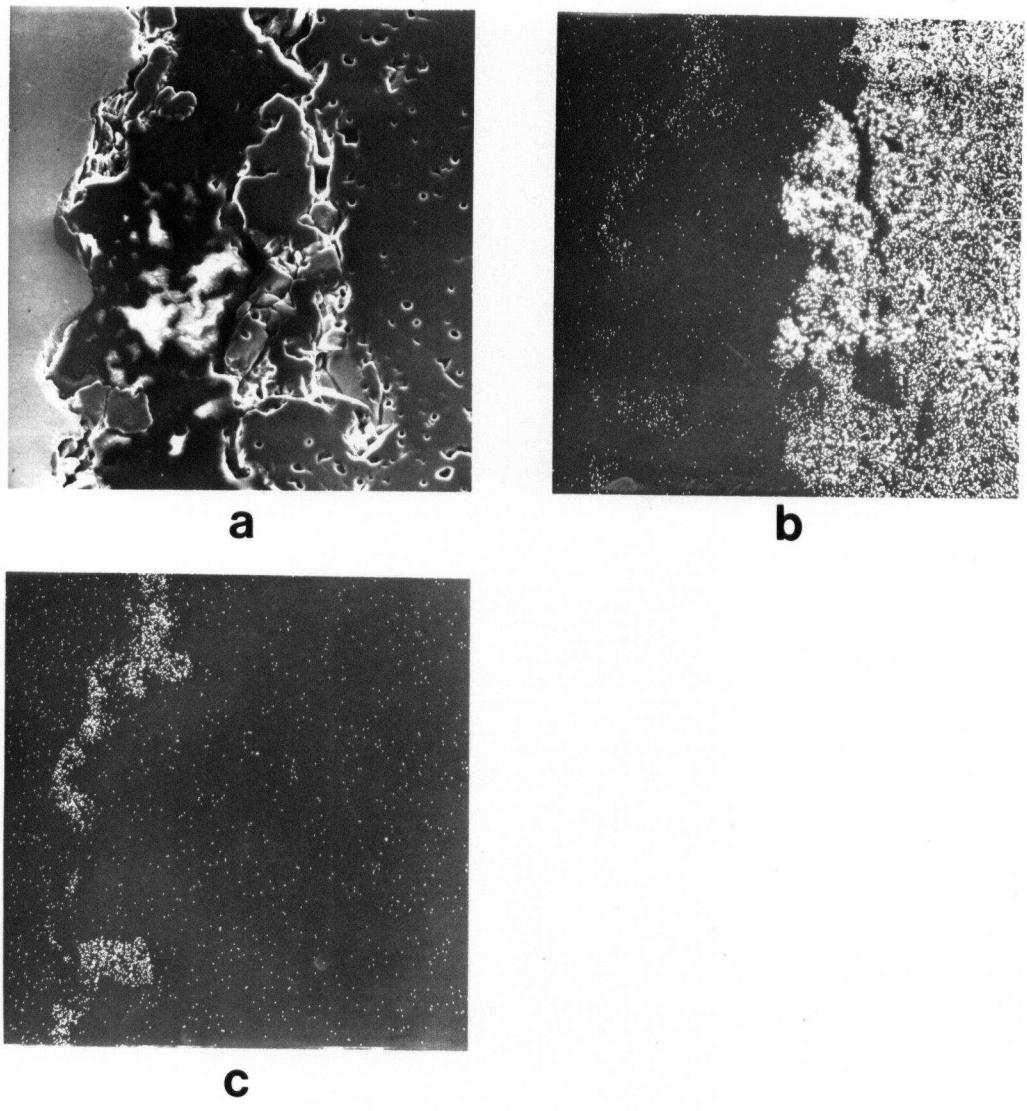

Fig. 24 Interface X-750/Magnel. Melt time 15 min. X240

a) Secondary Electrons
b) Magnesium X-Ray map
c) Aluminum X-Ray map

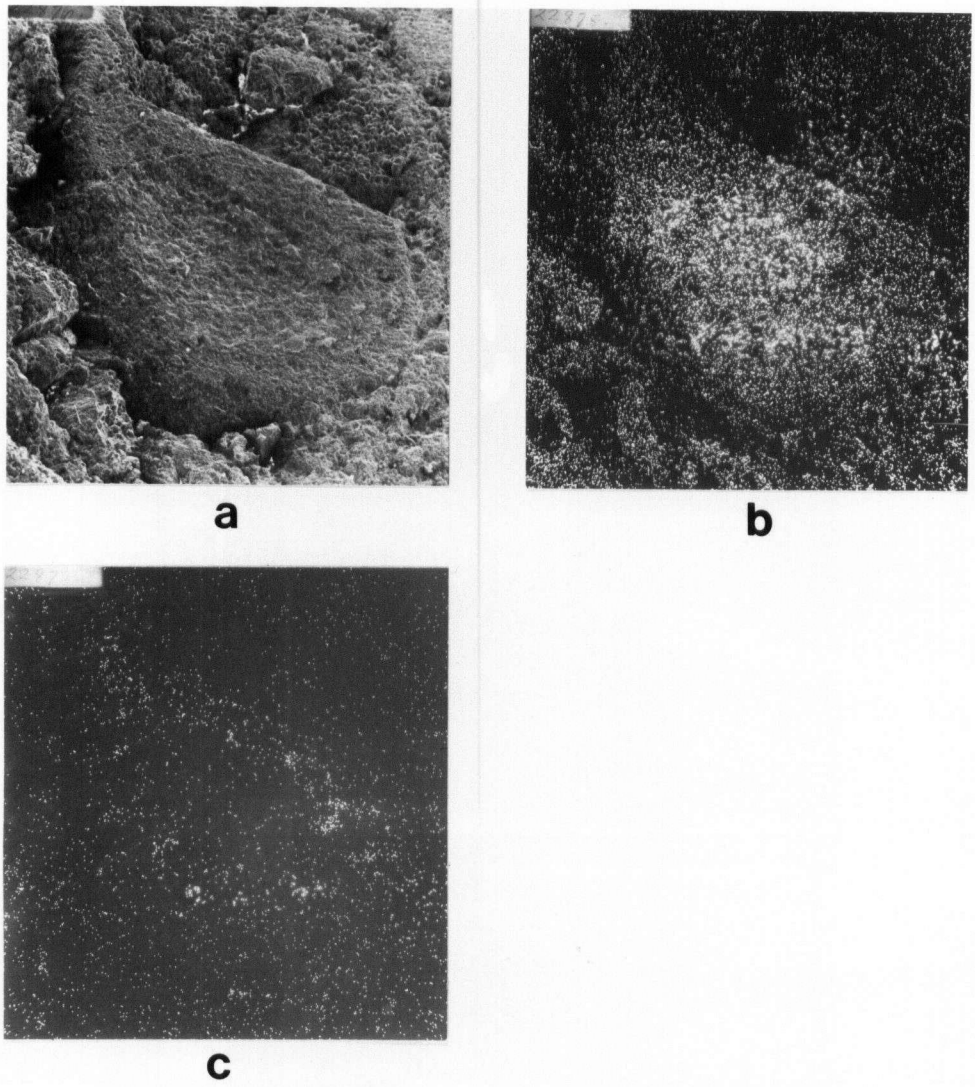

Fig. 25 Interface X-750/Magnel, metal removed. X17

a) Secondary Electrons
b) Magnesium X-Ray map
c) Aluminum X-Ray map

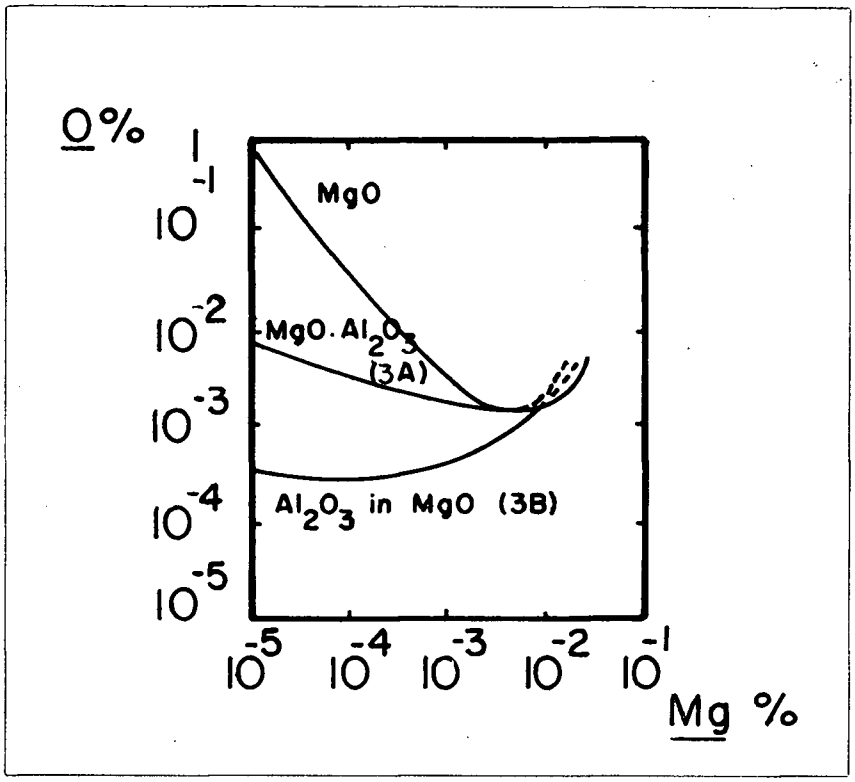

Fig. 26 Deoxidation equilibria in a Ni-1%Al Alloy

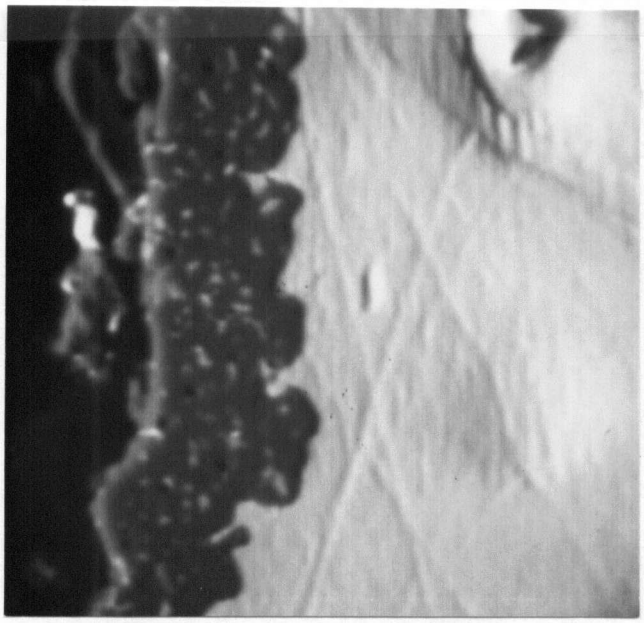

Fig. 27 Dense layer formed at interface X-750/Taylor 341
X1000, Backscattered Electrons

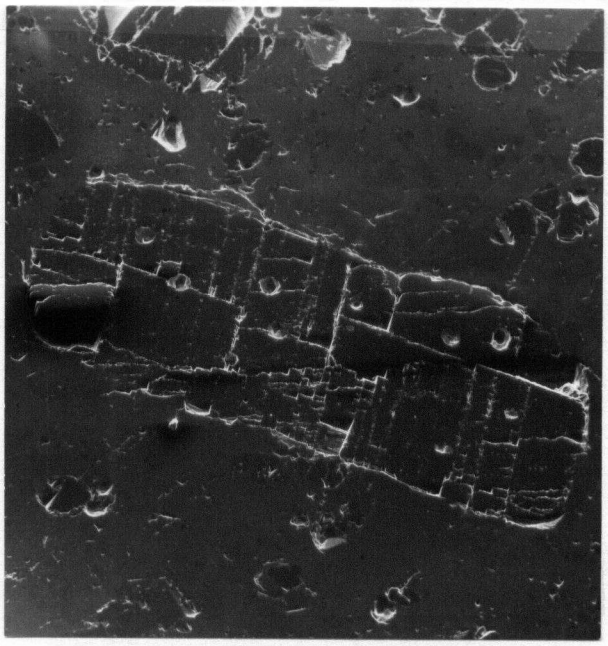

Fig. 28 Microstructure of slag from desulphurization treatment. X60, Secondary Electrons

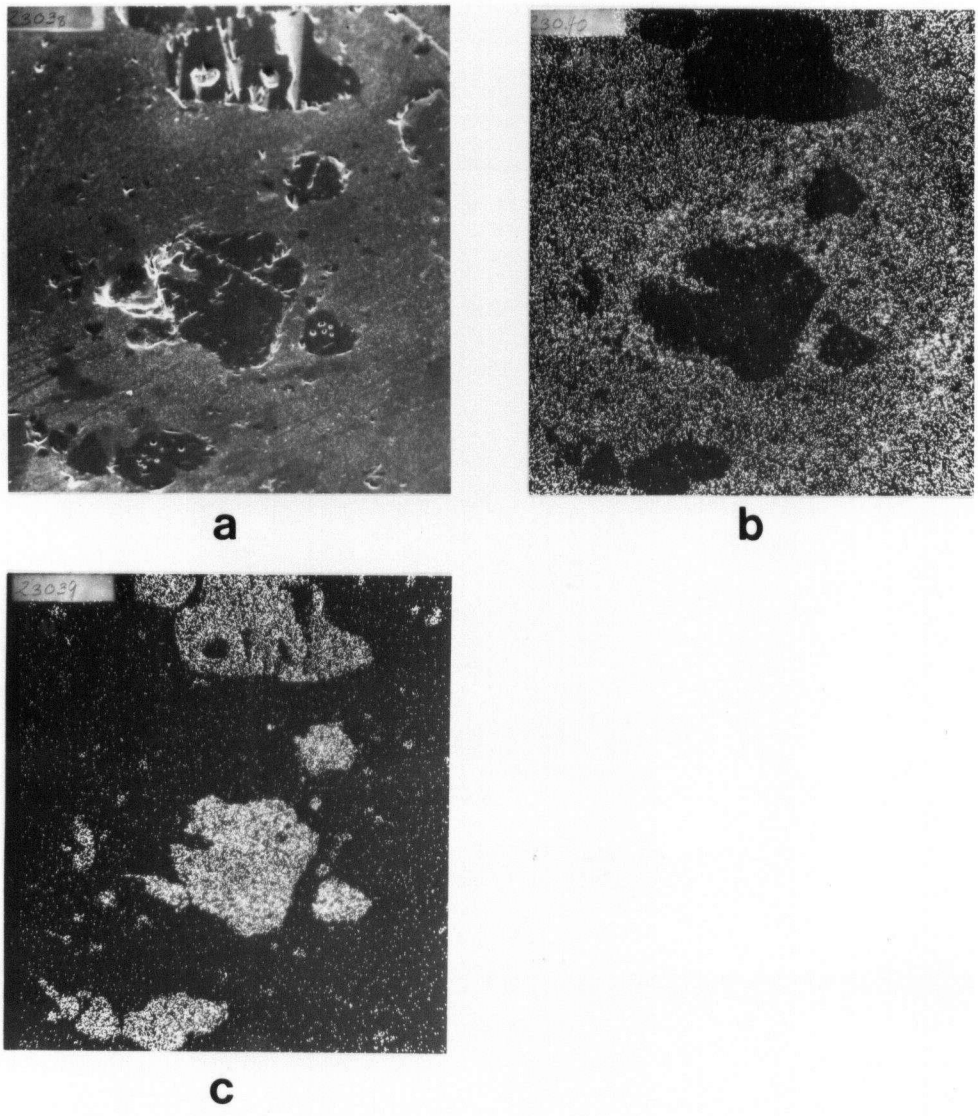

Fig. 29 Microstructure of slag from desulphurization treatment. X120

a) Secondary Electrons
b) Magnesium X-Ray map
c) Aluminum X-Ray map

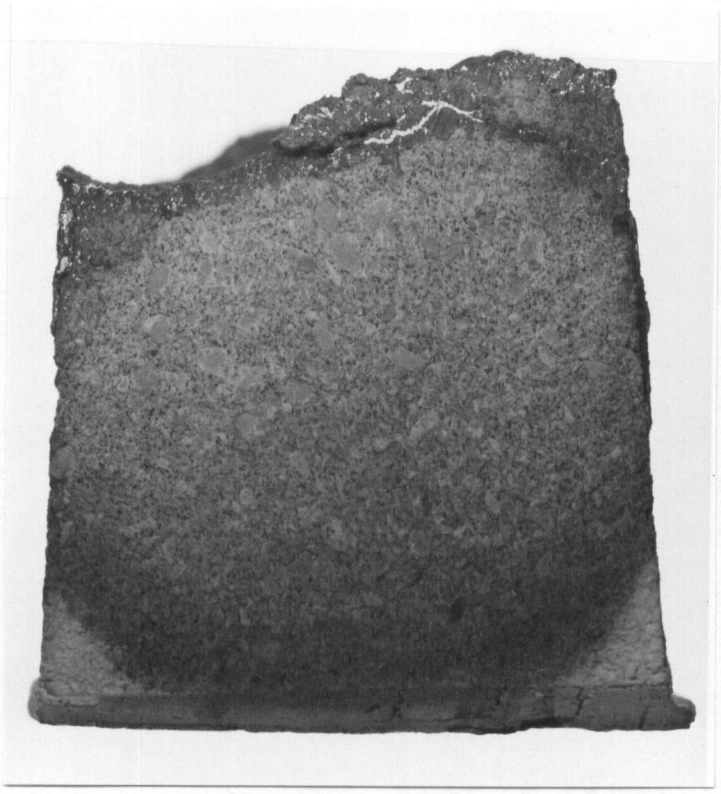

Fig. 30 Used Magnel brick, X1

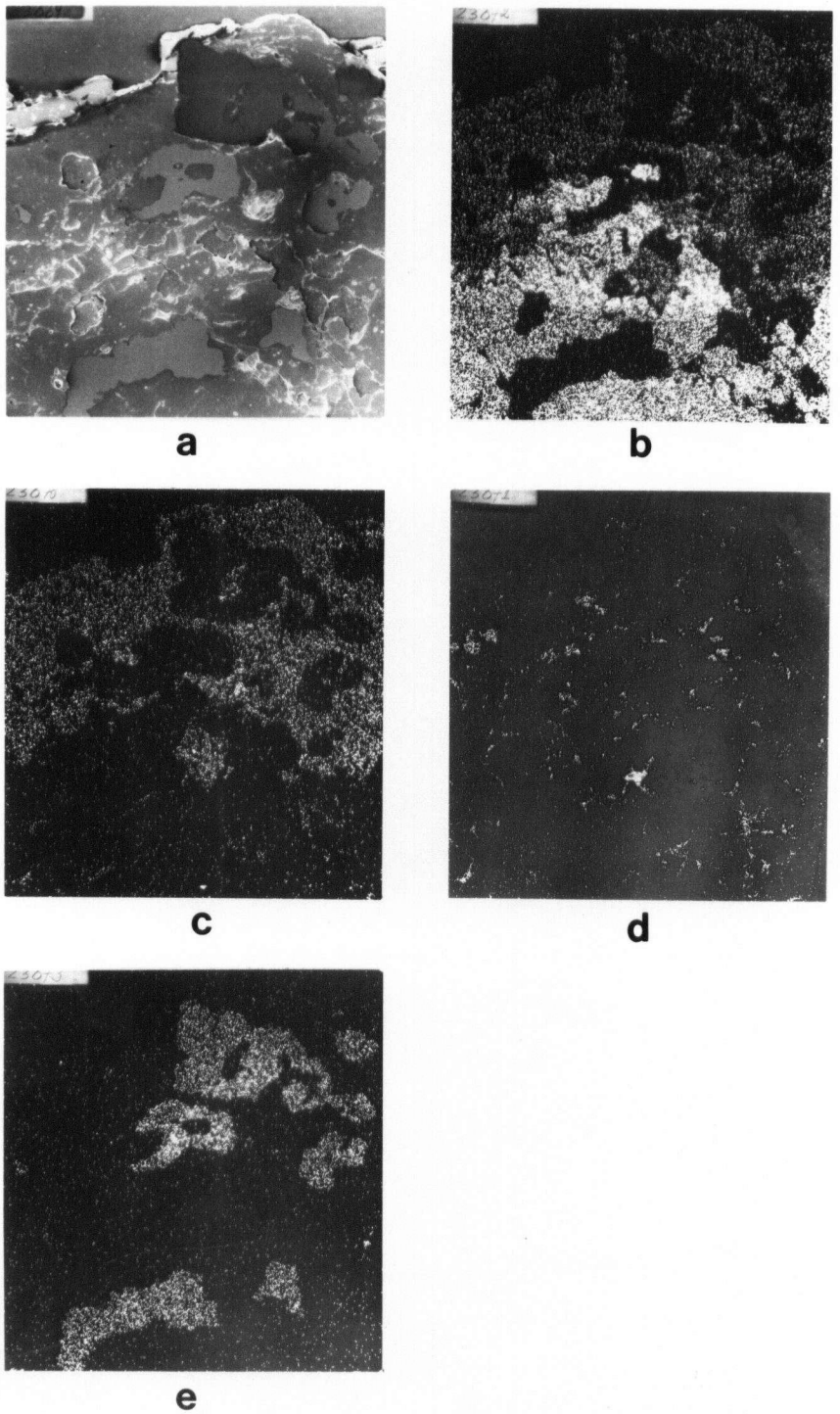

Fig. 31 Cross section of working face of Magnel brick (Fig. 30). X60

a) Secondary Electrons
b) Magnesium X-Ray map
c) Aluminum X-Ray map
d) Calcium X-Ray map
e) Nickel X-Ray map

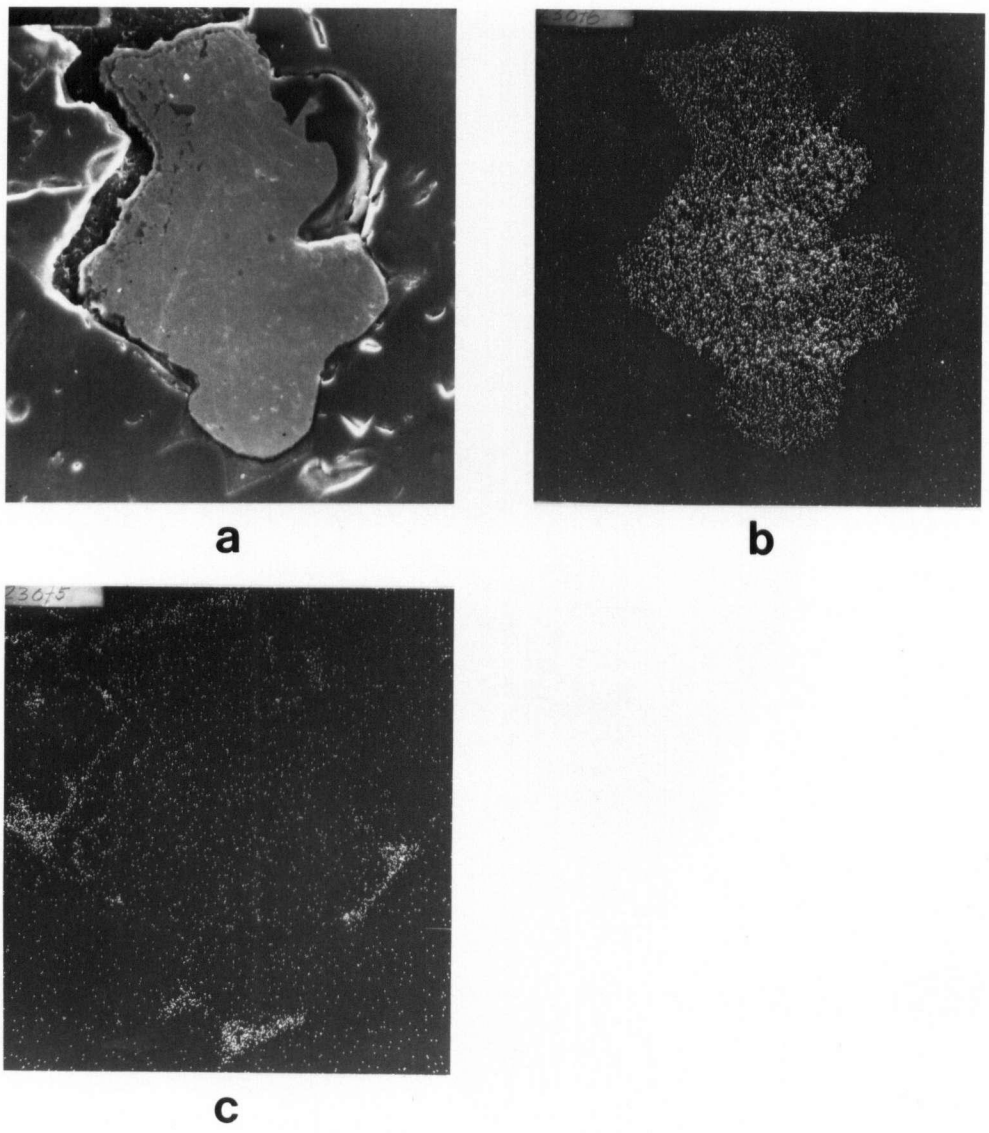

Fig. 32 Metal penetration in Magnel brick via Calcium-Aluminates. X480

a) Secondary Electrons
b) Nickel X-Ray map
c) Calcium X-Ray map

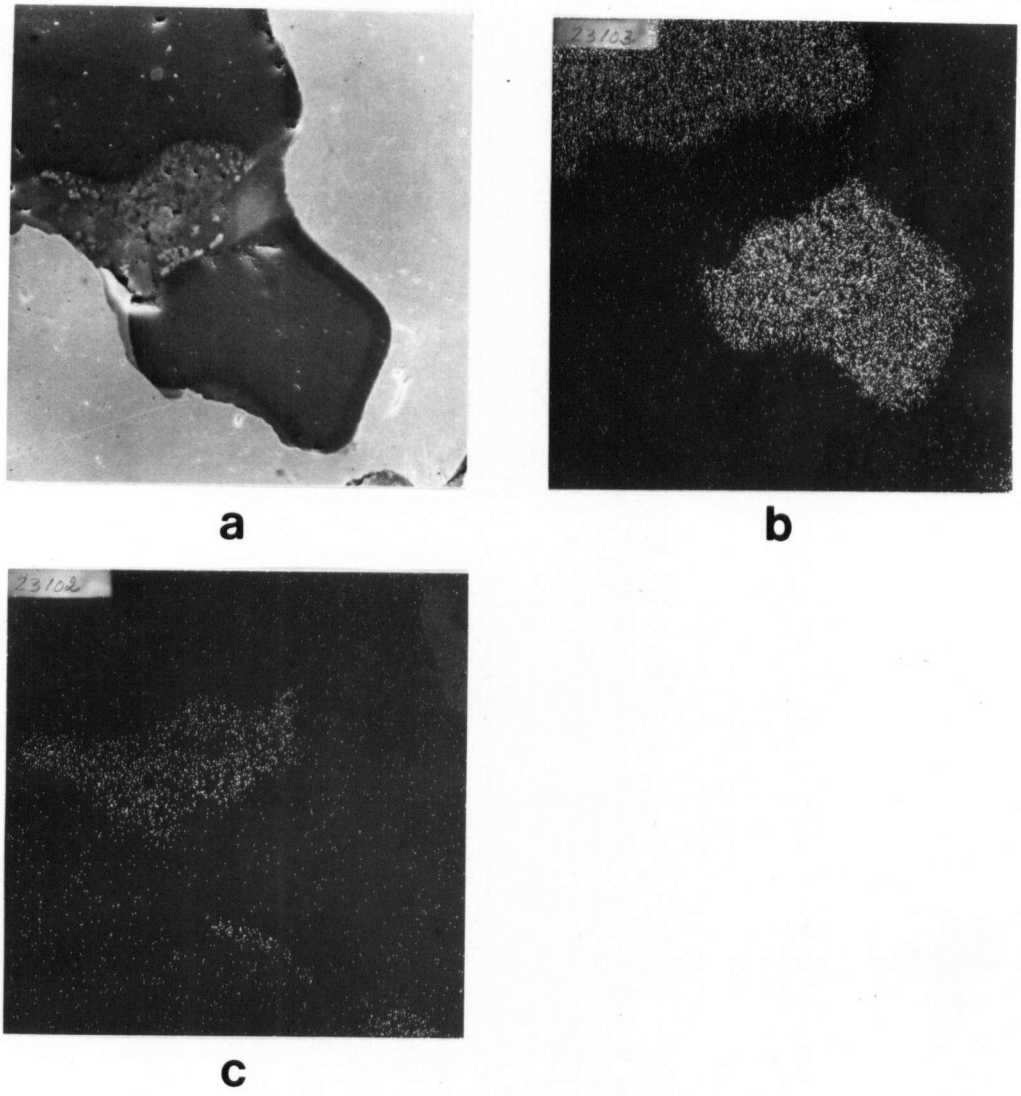

Fig. 33 Metal penetration in Magnel brick--Calcium-Aluminate containing Titanium and Zirconium. X600

a) Secondary Electrons
b) Magnesium X-Ray map
c) Aluminum X-Ray map

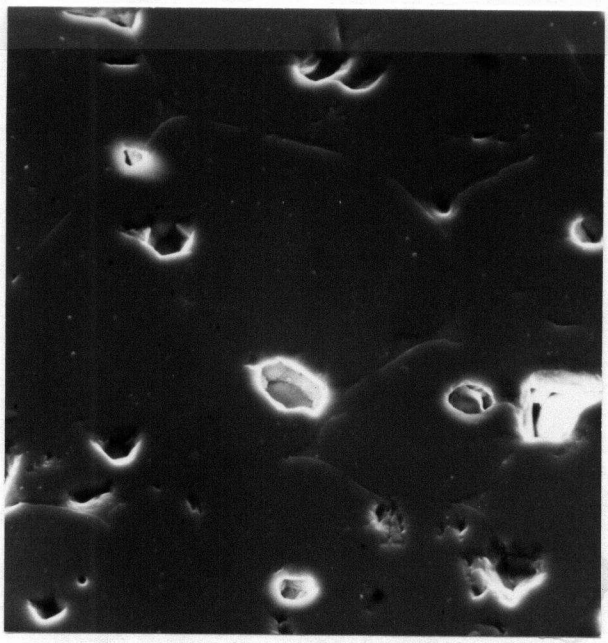

Fig. 34 Detail of a Periclase grain in Unused Magnel brick. X1000, Secondary Electrons

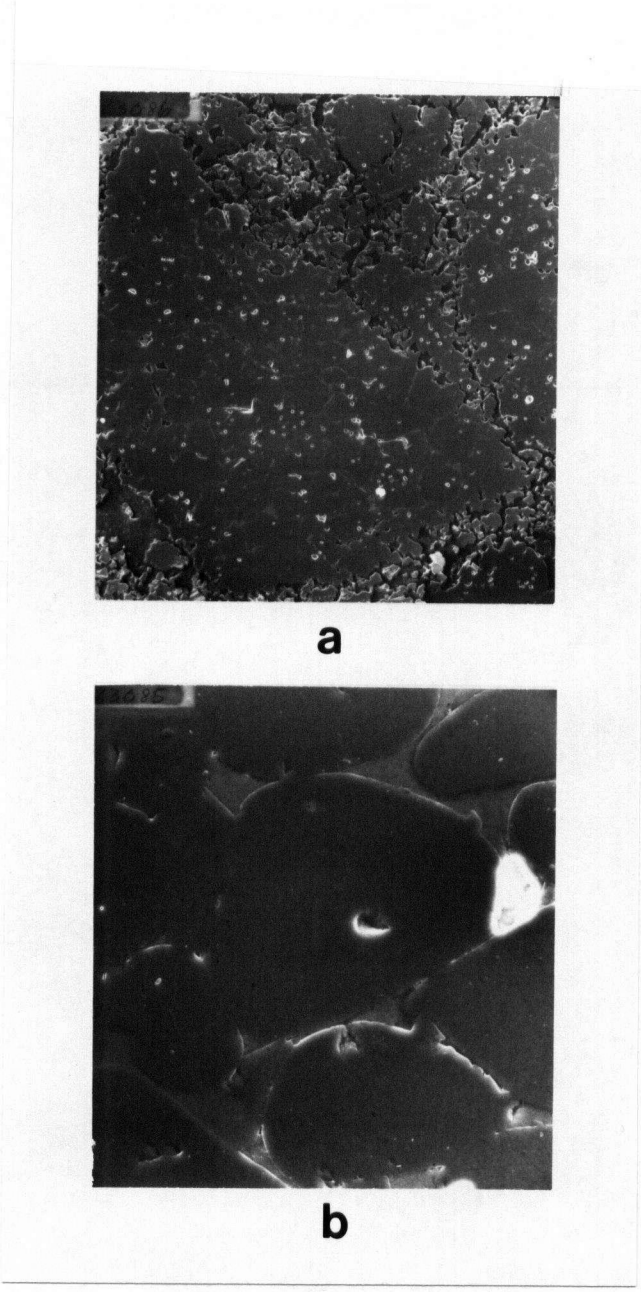

Fig. 35 Periclase grain in Used Magnel brick, 15mm from working face. Secondary electrons.

a) X60
b) X600

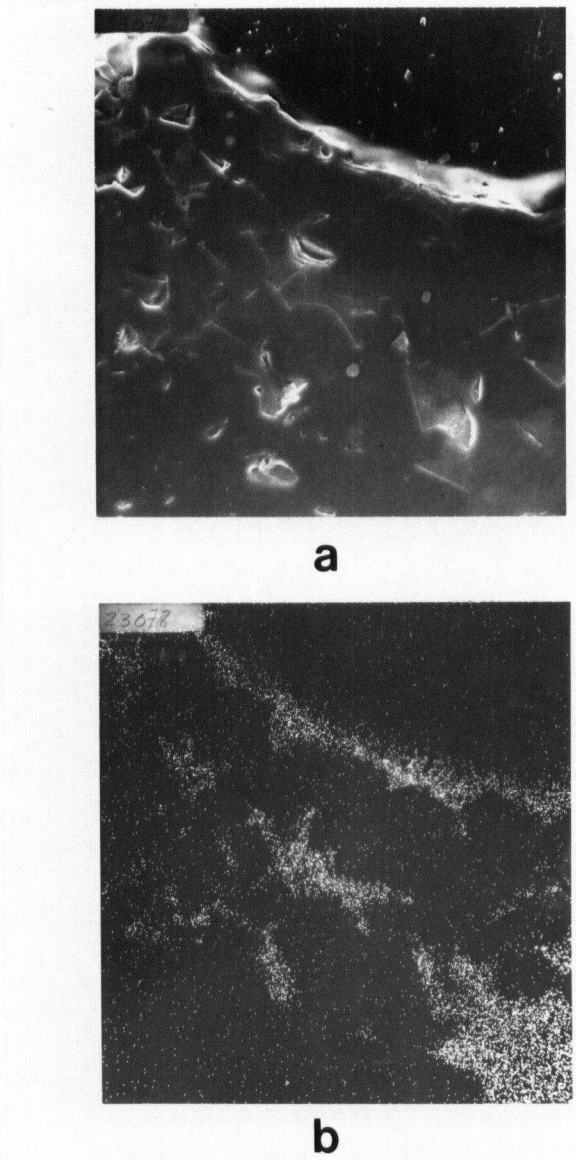

Fig. 36 Calcium-aluminates on the working face of Magnel X480

a) Secondary Electrons
b) Calcium X-Ray map

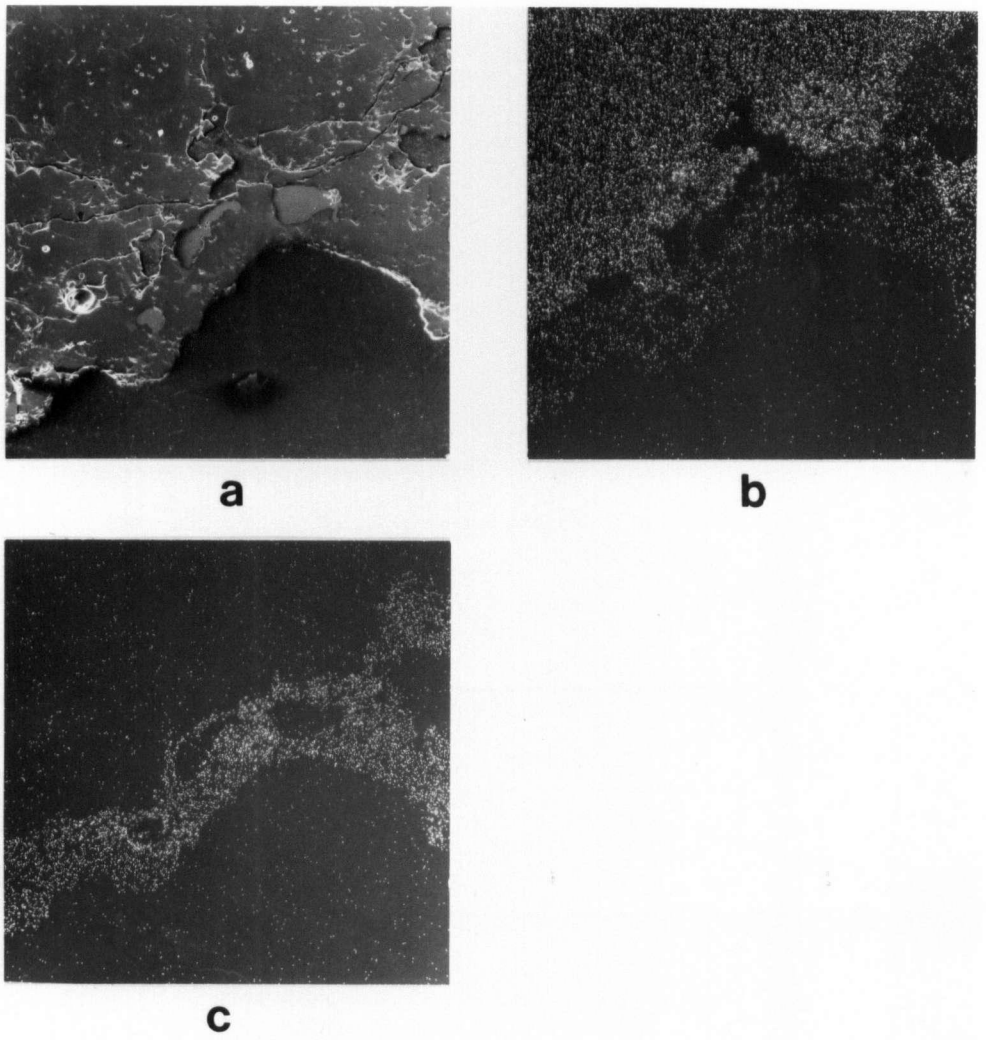

Fig. 37 Spinel layer on the working face of Magnel X60

a) Secondary Electrons
b) Magnesium X-Ray map
c) Aluminum X-Ray map

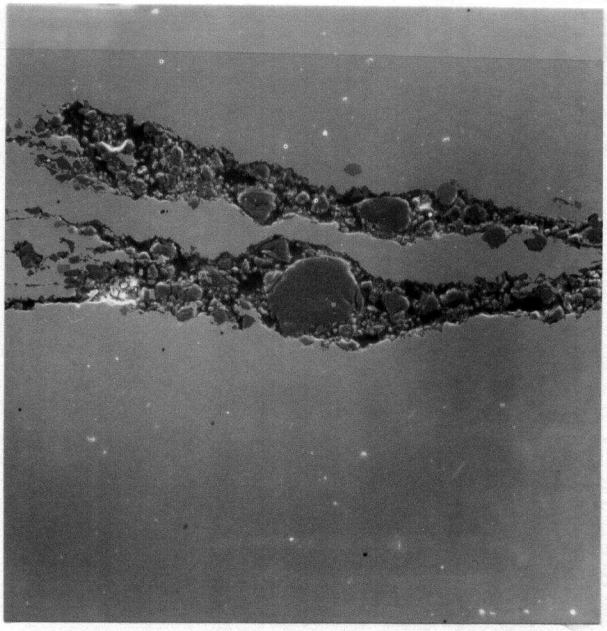

Fig. 38 Macroinclusions in partially forged Nickel-based Superalloy. X200, Secondary Electrons

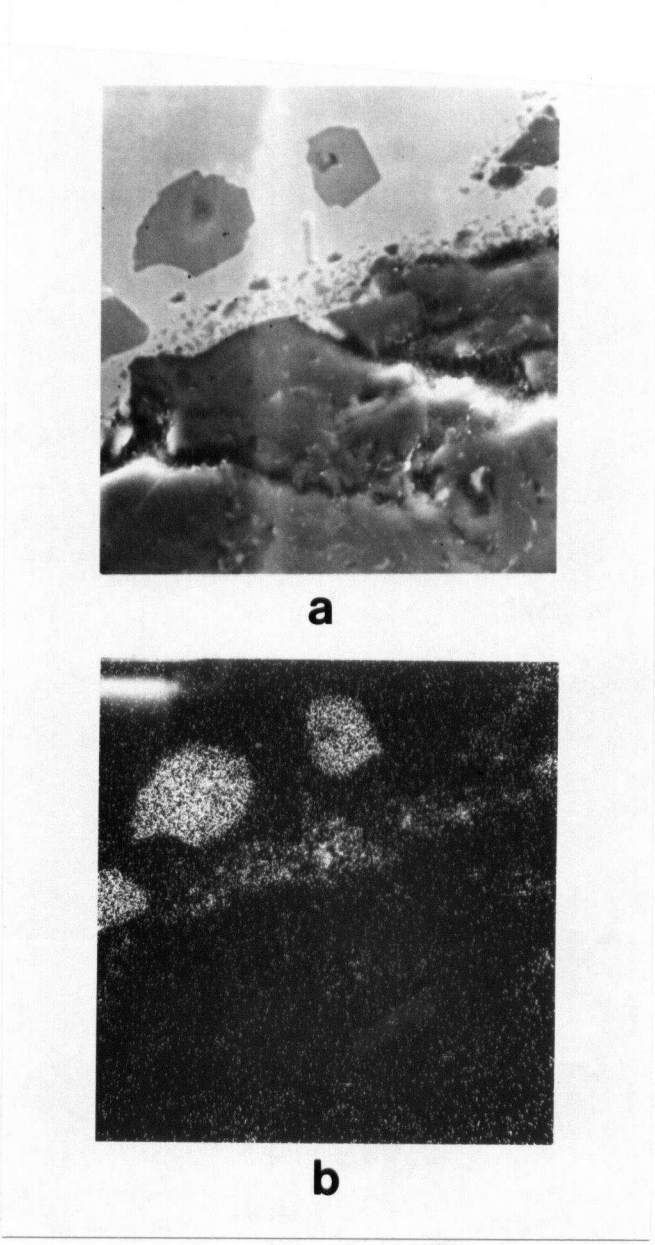

Fig. 39 Microstructure of Calcium-aluminate inclusion (Fig.38). X1200.

a) Secondary electrons
b) Titanium X-Ray map

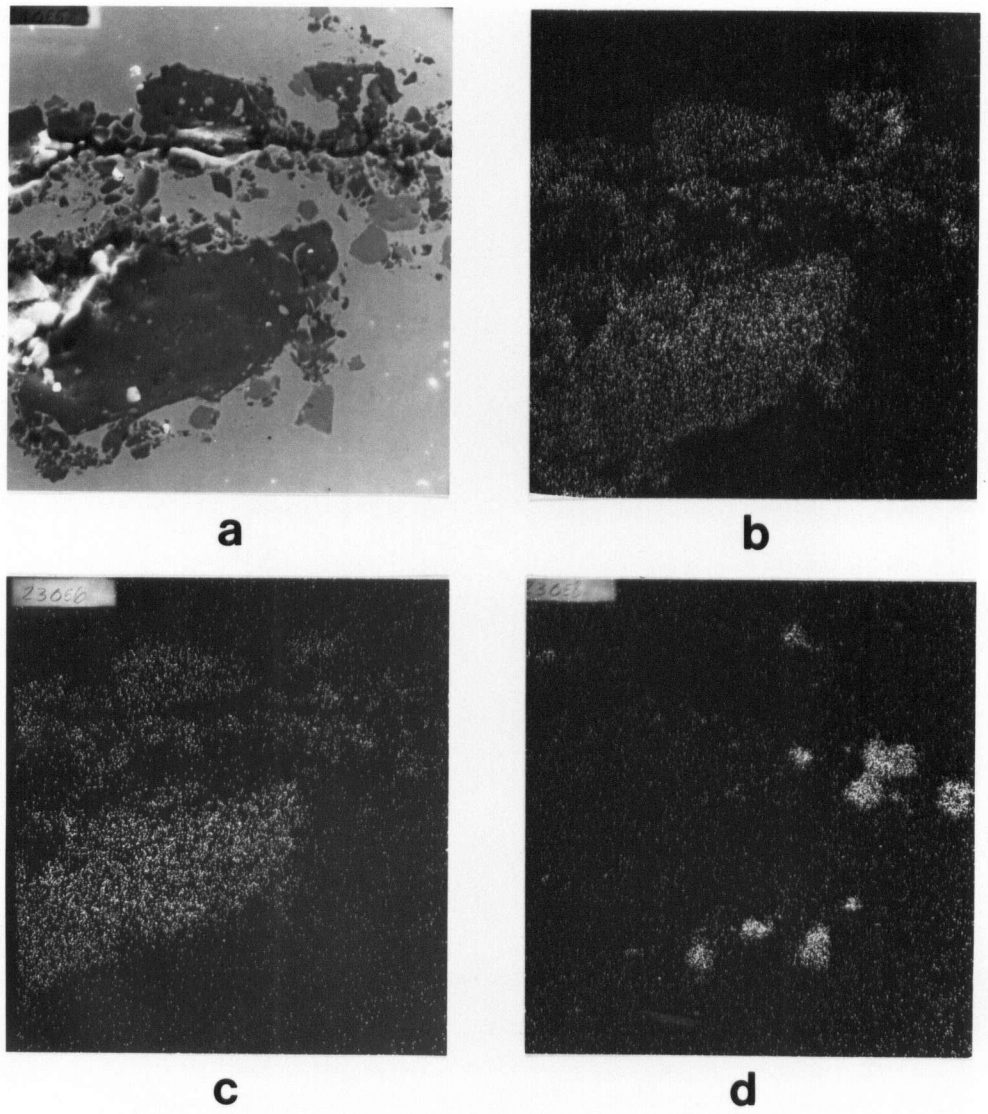

Fig. 40 Microstructure of spinel inclusion. X600

a) Secondary Electrons
b) Aluminum X-Ray map
c) Magnesium X-Ray map
d) Titanium X-Ray map

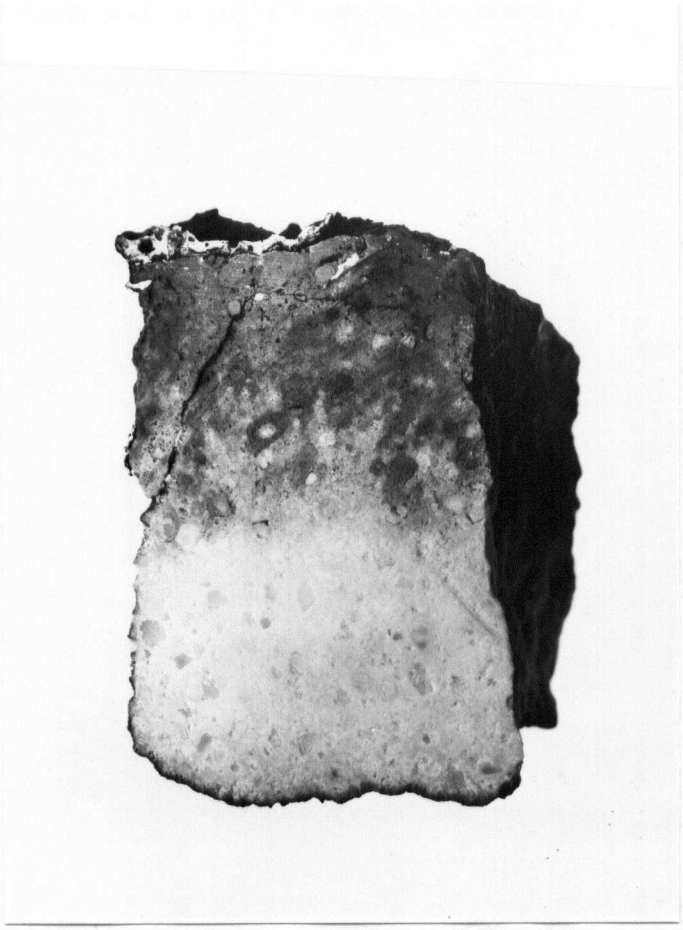

Fig. 41 Piece of used Rammed lining. X1

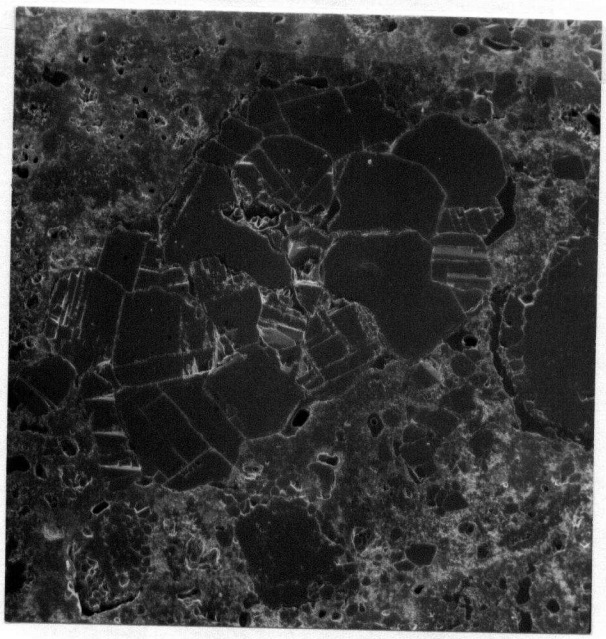

Fig. 42 Typical microstructure of the rammed lining 6cm from the working face. X20, Secondary electrons

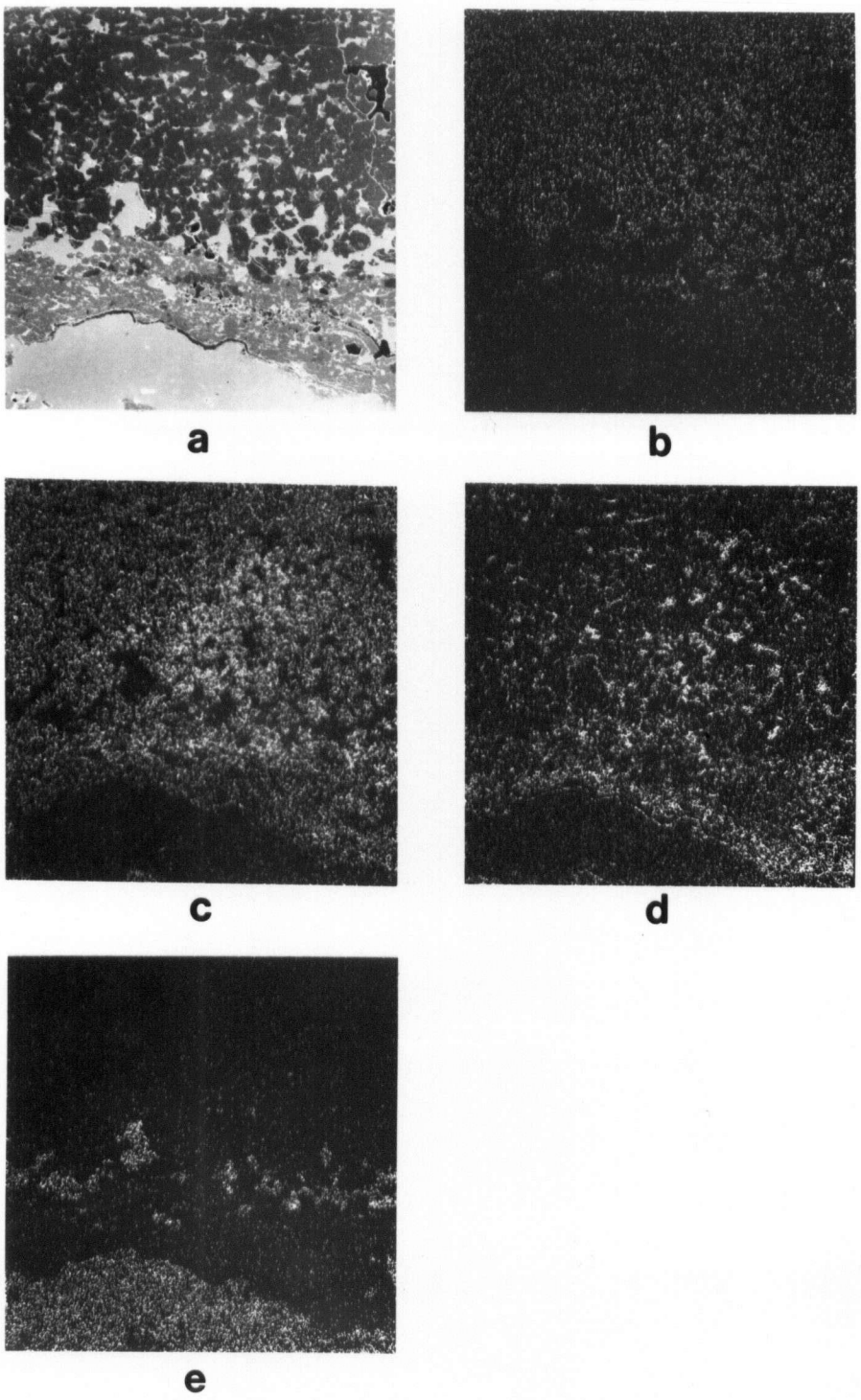

Fig. 43 Cross section of working face of rammed lining. X24

a) Secondary Electrons
b) Magnesium X-Ray map
c) Aluminum X-Ray map
d) Titanium X-Ray map
e) Nickel X-Ray map

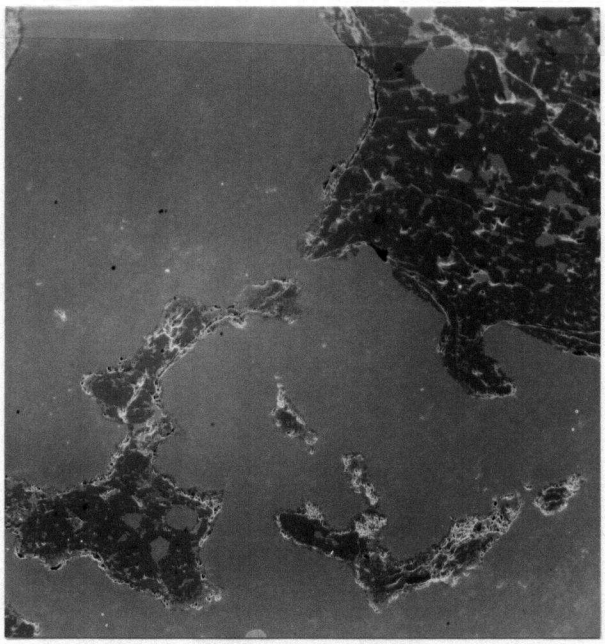

Fig. 44 Inclusions from rammed lining, Interface Nimonic 901/ rammed lining, X80, Secondary Electrons

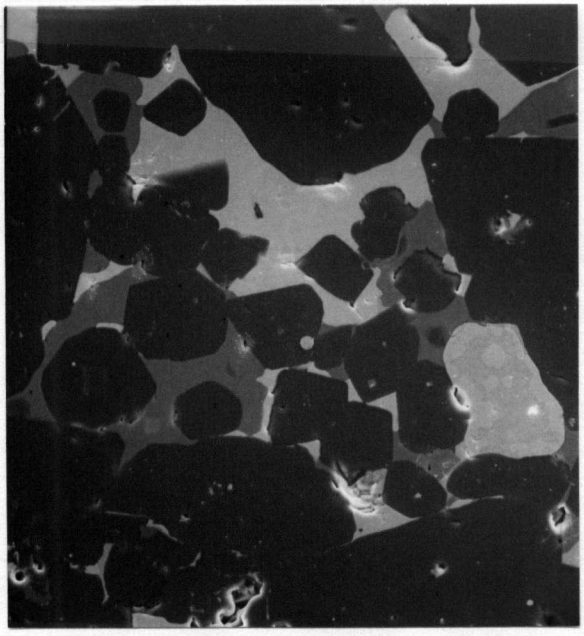

Fig. 45 Altered rammed lining (5mm from interface). Dark phase: spinel; gray phase: titanium rich; light phase: titanium and cerium rich. X400, Secondary Electrons

Fig. 46 Unaltered MgO grain close to working face of rammed lining. X40, Secondary Electrons.

TABLES

OXIDE	IN IRON	IN NICKEL
Al_2O_3 $(h_{Al}^2 \cdot h_o^3)$	4.3×10^{-14}	2.2×10^{-14}
Cr_2O_3 $(h_{Cr}^2 \cdot h_o^3)$	1.1×10^{-4}	1.5×10^{-8}
SiO_2 $(h_{si} \cdot h_o^2)$	2.2×10^{-5}	1.6×10^{-6}
TiO_2 $(h_{Ti}\ h_o^2)$	2.8×10^{-6}	2.5×10^{-8}
MgO $(h_{Mg}\ h_o)$	3.2×10^{-6}	3.1×10^{-7}

TABLE 1. Solubility products of oxides in iron (2) and Nickel (3)

OXIDE	STEEL COMPOSITION OR ASSUMPTIONS		PcO
MgO	%C = 0.4%	$P_{co} = P_{Mg}$	3.86 mm Hg
ZrO_2	%C = 0.4%	%Zr = 0.1%	4.11 mm Hg
Al_2O_3	%C = 0.4%	%Al = 0.1%	16.9 mm Hg
SiO_2	%C = 0.4%	%Si = 0.25%	1.95 atm
CaO	%C = 0.4%	$P_{co} = P_{Ca}$	0.68 mm Hg

TABLE 2. Pressures of CO in equilibrium with different oxides and steel melts at 1600°C (From Schaffer (10))

Alloy	Ni	C	Si	Fe	Mn	Cr	Ti	Al	Co	Mo	B	Zr
Inconel 718	52.5	max. 0.06	max. 0.35	bal.	max. 0.35	19.	0.9	max. 0.6	max. 1.0	3.0	max. 0.003	--
Inconel X-750	bal.	0.04	0.3	7.0	0.7	15.	2.5	0.9	0.5	0.3	--	0.03
Nimonic Pk50*	bal.	0.03	max. 0.15	max. 2.0	max. 0.1	19.5	3.0	1.4	13.5	4.2	0.007	max. 0.05
Nimonic 901	bal.	0.02 0.06	max. 0.4	bal.	max. 0.5	11.0 14.0	2.8 3.1	0.15 0.3	max. 1.0	5.0 6.5	0.01 0.02	--
Nimocast Pk24 (IN 100)	bal.	0.15 0.20	max. 0.2	max. 1.0	max. 0.2	8.0 11.0	4.5 5.0	5.0 6.0	13. 17.	2. 4.	0.01 0.02	0.03 0.09

*Similar to Waspalloy

TABLE 3. Nominal compositions of some Vacuum Melted Superalloys.

TABLE 4. Refractory Practices

MATERIAL (REFRACT.)	SIZE OF FURN.	TYPE OF LINING	PRODUCTS	LIFE AND/OR RESULTS	COMMENTS	REFERENCE
ZIRCONIA or ALUMINA SILICA (KORUNDAL XD) or MAGNESITE -CHROME (GUIDON)	5.2kg LAB. " "	PRE-FIRED TO TEMP. OF BRICK MAKING OPERATION	D-979 AISI 4340 AISI 52100	All showed substantial and comparable C losses both in 1st & 2nd heats. Oxygen content constant for each alloy.	Did not try Korundal XD with 52100. Some decrease in C composition after 1st heat	(28)
MAGNEL or KORUNDAL XD	27 ton PROD.	BRICK & MORTAR	LATROBE STEEL	25-45 heats	Backup lining: Korundal XD Working lining: Korundal XD Magnel	(29) (30) (31)
MAGNESIA + ALUMINA (2%SiO_2)	200kg	RAMMED SINTERED @1600°C	Ni-base superalloys Heat res. steels Austnitic steels	~43 heats	MgO depletion in the surface and formation of sulphur rich layer	(22)
ALUMINA -SILICA 95,60,42% Al_2O_3	12kg	PRE-FIRED	%0.2C	Decreasing Si pickup for decreasing SiO_2 in the crucible (and C cons.)		(24)

.../cont'd

TABLE 4. (Cont'd)

MATERIAL (REFRACT.)	SIZE OF FURN.	TYPE OF LINING	PRODUCTS	LIFE AND/OR RESULTS	COMMENTS	REFERENCE
MAGNESIA +ALUMINA (70/30)	7 ton	RAMMED WET/ GRAPHITE	Nickel alloys Steels (Carpenter Steel)	30 heats		(33)
MAGNESIA	12kg	PROBABLY PRE-FIRED	0.2% Steel		STEADY STATE $\underline{O}$ 5 ppm - $\overline{10}$ ppm	(6)
ZIRCONIA (5% CaO)	15kg	?	NiMo 1.5 Alloy	Zr + Si pickup		(34)
MAGNESIA	Also 100kg			Mg + Fe + Si pickup		
ALUMINA				Al + Si pickup		
FUSED LIME	20kg	RAMMED SINTERED @2000°C	Ni-Fe Alloys	44 heats or more 8 cycles to room temp.	Very effective $\underline{Si}$ de-Ox. and $\overline{de}$-S	(35)
MAGNESIA + ALUMINA 65/25 6%SiO_2 (NORTON RM 1170)	50/150 kg	RAMMED	Fe-C melts		Steady State $\underline{O}$ 12 ppm	(11)

.../cont'd

TABLE 4. Cont'd

MATERIAL (REFRACT.)	SIZE OF FURN.	TYPE OF LINING	PRODUCTS	LIFE AND/OR RESULTS	COMMENTS	REFERENCE
MAGNESIA + ALUMINA Termax B3 Termax MG 10 ~75/20 $5SiO_2$	350kg	RAMMED	Nickel Alloys (Mg/W) C deoxidation			(36)
SPINEL or MAGNESIA or ALUMINA	10kg	?	Fe=Ni Ni-Fe-Mo Ni	For Pure Iron best de-Ox in Alumina (3.6×10^{-5} $\underline{C} \times \underline{O}$) then Spinel and then Magnesia ($16 \times 10^{-5} \underline{C} \times \underline{O}$)		(37)
MAGNEL	60t	BRICK & MORTAR	Steels Superalloys (Cameron Iron)			(38)
MAGNESIA	1 ton	RAMMED (PROBABLY)	20% Mo-Ni Alloy Daido Steel			(39)
MAGNESIA	250kg		Hastelloy R-235			(40)
	5-10t	RAMMED	FIRTH-BROWN		Firing with template	(41)

...cont'd

TABLE 4. Cont'd

MATERIAL (REFRACT.)	SIZE OF FURN.	TYPE OF LINING	PRODUCTS	LIFE AND/OR RESULTS	COMMENTS	REFERENCE
MAGNESIA or MAGNESIA-ALUMINA or ALUMINA		RAMMED	Fe,Ni alloys	Spinel ~35 heats 250-1000kg Magnesia-half of the life of Spinel	Firing with template or graphite core--Stresses in MgO are large	(5)
ZIRCONIA or MAGNESIA	150-1000 kg	RAMMED (?)	Ni alloys, Steels (Special Metals, 1957)			(42)
MAGNESIA	6t	RAMMED			12 hour vacuum drying	(43)
MAGNESIA MAGNESIA ALUMINA (70/30)	300kg	RAMMED	Ni alloys Steels (Jessop & Sons)		Firing with graphite @ 2000°C is preferred since it allows the refractory to be checked before use.	(44)
MAGNESIA ALUMINA (70/30)	500kg	RAMMED	Steels (Kelsey-Hayes Co.)			(45)
MAGNESIA or MAGNESIA-ALUMINA (66/25)		RAMMED	Steels Ni-Alloys		Firing with template or graphite core. Magnesia bonded by $CaO + SiO_2$ Magnesia-Alumina by $CaO + SiO_2 + FeO$	(46)

.../cont'd

TABLE 4. Cont'd

MATERIAL (REFRACT.)	SIZE OF FURN.	TYPE OF LINING	PRODUCTS	LIFE AND/OR RESULTS	COMMENTS	REFERENCE
KORUNDAL XD CORALBOND		BRICK and MORTAR		7 heats of Ni-superalloy Severe erosion in the joints		(47)
MAGNEL CORALBOND		BRICK and MORTAR		Better results than with KORUNDAL XD CORALBOND		(47)
MAGNEL PERIBOND	10t	BRICK and MORTAR	Steels (Armco Research)	15-20 heats (Cyclic operation)	Failure occurs in the bottom-Top layer of bricks bulges up. Backup is KORUNDAL XD	(48)
SPINEL BRICK or MAGNESITE-CHROMITE BRICK or ALUMINA BRICK	10 to 30t	BRICK and MORTAR	Steels, Stainless Tool Superalloys	20-45 heats	MAG-CHROMITE brick has 65%MgO/13% CrO_3/8%Al_2O_3 Alumina brick has 10% SiO_2 Importance of mortar joints	(49)
ALUMINA or SPINEL	<2.5 t	RAMMED	Ni, Co, Fe, Alloys		Spinel is used up to 10t	(50)

.../cont'd

TABLE 4. Cont'd

MATERIAL (REFRACT.)	SIZE OF FURN.	TYPE OF LINING	PRODUCTS	LIFE AND/OR RESULTS	COMMENTS	REFERENCE
ALUMINA or SPINEL	>2.5t 10t 25t 60t	BRICK and MORTAR		Good	Cement Taylor 341* Back Lining MULLITE BRICK with $NaSiO_3$ bonded silimanite (TAYLOR 320)	(50)

MATERIAL	C	Mn	Si	Cr	Ti	Al	Fe	Ni+Co
Nickelvac X-750*	0.067	0.08	0.04	13.55	2.58	0.71	7.75	71.35
AISI 1095 (nominal)	0.96**	0.40	0.30	-	-	-	bal.	-

* Analysis by Teledyne-Allvac
**Analysed at UBC

TABLE 5. Composition of metals used in the tests

MATERIAL	MgO	Al_2O_3	SiO_2	P_2O_5	CaO	Fe_2O_3	Others
Magnel	89.8	8.3	0.7	-	0.9	0.3	-
Alundum 1139	-	99.	0.7		0.1	0.1	Na_2O-- 0.3
Alundum 1163	-	81.	12.		0.4	1.3	TiO_2-- 5.
Coralbond	0.1	79.3	6.7	9.1	0.1	1.5	TiO_2-- 3.1
Peribond	78.8	2.4	14.7	-	0.1	0.8	Alkalies--2.2
Taylor 320	0.02	87.	10.	-	0.10	0.10	Alkalies--2.30
Taylor 341	-	95.	0.02	4.5	-	0.03	
Tasil X	0.1	55.	40.	-	0.1	1.0	Alkalies--2.7

TABLE 6. Typical chemical analysis (%, according to suppliers) of refractory materials tested.

MATERIAL	OXYGEN CONTENT (PPM)
SP2	17
MAGNEL	22
TAYLOR 341	28
PERIBOND	37
CAF	41
ALUNDUM 1139	46
CORALBOND	60
X-750 as received	7

TABLE 7. Oxygen content of X-750 after 15 min. holding time at 1500°C in different refractory materials.